UNIVERSIDADE DE SÃO PAULO
ESCOLA DE ENGENHARIA DE LORENA

GABRIELA LEILA BERTO

Biochemical pre-treatments for isolation of cellulose nanofibrils

Lorena
2020

GABRIELA LEILA BERTO

Biochemical pre-treatments for isolation of cellulose nanofibrils

Thesis presented at Escola de Engenharia de Lorena of Universidade de São Paulo to obtain the degree of Doctoral of Science issued by the Programa de Graduação em Biotecnologia Industrial in the field of Biotecnologia Industrial.
Advisor: Prof. Dr. Valdeir Arantes

Corrected Version

Lorena
2020

GABRIELA LEILA BERTO

Pré-tratamentos bioquímicos para isolamento de celulose nanofibrilada

Tese apresentada à Escola de Engenharia de Lorena da Universidade de São Paulo para obtenção do título de Doutor em Ciências do Programa de Pós-Graduação de Biotecnologia Industrial na área de concentração Biotecnologia Industrial.

Orientador: Prof. Dr. Valdeir Arantes

Versão Corrigida

Lorena

2020

Ficha catalográfica elaborada pelo Sistema Automatizado
da Escola de Engenharia de Lorena,
com os dados fornecidos pelo(a) autor(a)

Berto, Gabriela Leila
Biochemical pre-treatments for isolation of cellulose nanofibrils / Gabriela Leila Berto; orientador Valdeir Arantes - Versão Corrigida. - Lorena, 2020.
138 p.

Tese (Doutorado em Ciências - Programa de Pós Graduação em Biotecnologia Industrial na Área de Biotecnologia Industrial) - Escola de Engenharia de Lorena da Universidade de São Paulo. 2020

1. Properties of nanocelluloses. 2. Endoglucanase. 3. Energy consumption.. 4. Hydrolytic enzymes. 5. Enzyme-cellulose interaction. I. Título. II. Arantes, Valdeir, orient.

This thesis is to my grandfather and
to all those who taught me love and kindness

ACKNOWLEDGMENTS

I would like to express my great appreciation to my advisor, Prof. Dr. Valdeir Arantes, who was the key person to the fully development of this thesis. Thank you for all the outstanding discussions, guidance and commitment with my work and the team!

I would like to express my gratitude to Prof. Dr. Orlando Rojas for warmly receiving me (in Finland) in his family/group. You are an amazing inspiration and it was an honor to learn from you and know your spirit of passion about science and personal relationships.

I am deeply thankful to Prof. Dr. Fernando Segato, firstly, regarding to the collaboration, providing the purified enzymes applied in this study. Secondly, and the most important, for being an incredible husband and life partner. I love you and you make my every day an amazing adventure.

I am very grateful to my work partners: Ms. Josman Velasco, for the collaboration in the enzyme preparations and his sincere interest about our work. Ms. Barbara Pereira, for conducting HPLC analyses. José Moreira for helping to install the refiner and for supplying coffee and great talks. To Prof. Dr. André Ferraz for the collaboration in the generation of optical microscopy images and for being a great friend. In addition, Dr. Bruno Mattos for all the support, discussion, time and friendship during the internship period at Aalto University. Bin Zhao, for helping to obtain the electronic microcopies images. Wenchao Xiang for always being kind, helping me to explore the QCM-D in high temperatures.

To my colleagues at the Biocatalysis and Bioproducts Laboratory for making the most pleasant day to day, especially when everything insisted to go wrong. I thank my colleagues from Synthetic and Molecular Biology Laboratory, Wood Science, Biochemistry I and Biobased Colloids and Materials.

I give an immeasurable thank to my mom, Rose, for the love, support, and especially for her patience with me. You are the person who always put me on the right track and I always will be deepest grateful for it! I Love you!

I would like to express my thankful to my family and to all my friends and colleagues. And my deepest appreciation is to all the teachers and professors who were part of my growing development. You are all amazing! I always will be in debit with all of you!

My special acknowledgment to all staff at the Biotechnology Department and USP-EEL campus.

I also would like to thank my sponsors, CAPES and FAPESP, for the financial support and for believing in the high-level science and education in our country.

“O otimista é um tolo. O pessimista, um chato.
Bom mesmo é ser um realista esperançoso”
Ariano Suassuna

RESUMO

BERTO, Gabriela Leila. **Pré tratamentos bioquímicos para isolamento de celulose nanofibrilada**. 2020. 138 p. Tese (Doutorado em Ciências) – Escola de Engenharia de Lorena, Universidade de São Paulo, Lorena, 2020.

Celulose nanofibrilada (CNF) é um material biodegradável que possui excelente propriedades mecânicas e reológicas, o que a torna adequada para inúmeras aplicações (ex. impresão 3D e composto para reforço). A obtenção da CNF é usualmente feita por desfibrilação mecânica, em sistemas de alta pressão (microfluidizador ou homogeneizador) ou ultra-refinadores de disco. Estes processos demandam elevado consumo energético, sendo essa uma barreira econômica da produção. Uma etapade pré-tratamento reduz o alto consumo energético, sendo a utilização de enzimas bastante promissor devido à sua seletividade e ao apelo ambiental do processo.. A enzima mais explorada é uma endoglucanase (EG) monocomponente comercial, combinada com etapas sequenciais de pré-refino mecânico. As condições de reação descritas até o momento são extremamente amplas (ex. tempo de reação e carga enzimática), resultando em diferententes benefícos ao processo e nas características do nanomaterial final. Este trabalho explorou o efeito e a seletividade de diferentes enzimas hidrolíticas aplicadas em uma única etapa de pré-tratamento para o isolamente de CNF. Para isso, considerou-se a capacidade de redução do consumo energético na etapa de desfibrilação em SuperMassColloider e também as propriedades das nanofibrilas isoladas. Primeiramente, investigou-se detalhadamente a cinética de operação do ultra-refindor de disco, o qual foi adequeado para isolar CNF e também celulose microfibrilada (CMF), sendo que CNF com excelentes propriedades foi obtida atingindo o consumo energético de 20 kWh/kg. Em seguida, a EGtipicamente utilizada no pré-tratamento foi investigada em diferentes condições hidrolíticas previstas por planejamento experimental. Na condição mais drástica de pré-tratamento enzimático o consumo energético decaiu em 50% e a reologia da suspensão foi alterada, gerando um material desejável para algumas aplicações. Buscando otimizar a condição de pre-tratamento que resultase no mínimo consumo de energia e na maximização da reologia , a condição extremamente branda predita reduziu o consumo em 25% e preservou as propriedades reologicas. Nessa mesma condição , 5 EGs provenientes de 4 diferentes famílias de glicosil hidrolase, com e sem o modulo de ligação ao carbohidrato, foram investigas quanto seus efeitos no isolamento de CNF e interação com a superfície da celulose. Com exceção da EG da família 7, todas as EGs testadas foram eficientes na redução do consumo energético e na preservação das propriedades reologicas e morfologicas das CNFs. De maneira geral, a especificidade das EGs pelas regiões menos organizadas não comprometeu a qualidade da fibra de celulose e das CNFs obtidas, além disso o efeito hidrolítico foi negligenciável, atingindo 100% de rendimento de sólidos. As diferenças observadas quanto ao consumo energético podem ser relacionadas com os diferentes comportamentos de ação das EGs na fibra celulose (ex. interação com a superfície da celulose e modificação do grau de polimerização). Compreendendo o efetio das EGs é possível utilizar EGs de diferentes famílias e variar e controlar as condições do pré-tratamento enzimático, possibilitando obter CNF com as propriedades desejáveis.

Palavras-chave: Propriedades das nanoceluloses. Consumo energético. Enzimas hidrolíticas. Interação enzima-celulose. Endoglucanase.

ABSTRACT

BERTO, Gabriela Leila. **Biochemical pre-treatments for isolation of cellulose nanofibrils**. 2020. 138 p. Thesis (Doctoral of Science) – Escola de Engenharia de Lorena, Universidade de São Paulo, Lorena, 2020.

Cellulose nanofibrillated (CNF) is a biodegradable material that has excellent mechanical and rheological characteristics, or becomes easier for applications (e.g. 3D printing and reinforcement compound). The use of CNF is usually made by mechanical defibrillation, in high pressure systems (microfluidizer or homogenizer) or ultra-disc refiners. These processes require high energy consumption, which is an economic barrier to production. A pretreatment stage reduces high energy consumption, and the use of enzymes is very promising due to their selectivity and the environmental appeal of the process. The most explored enzyme is a commercial monocomponent endoglucanase (EG), combined with sequential mechanical pre-refining steps. The reaction conditions described so far are extremely wide (e.g. reaction time and enzyme load), resulting in different benefits to the process and to the characteristics of the final nanomaterial. This work explored the effect and selectivity of different hydrolytic enzymes applied in a single pre-treatment step for CNF isolation. For this, the ability to reduce energy consumption in the defibrillation stage in SuperMassColloider was considered, as well as the properties of isolated nanofibrils. First, the kinetics of operation of the disc ultra-refiner were investigated in detail, which was adapted to isolate CNF and also microfibrillated cellulose (MFC), with CNF with excellent properties reaching the energy consumption of 20 kWh/kg. Then, the EG typically used in the pre-treatment was investigated under different hydrolytic conditions predicted by experimental design. In the harsher condition, the energy consumption dropped by 50% and the suspension rheology was changed, generating a suitable material for some applications. Seeking to optimize the pre-treatment condition that results in minimum energy consumption and maximization of rheology, the predicted extremely mild condition reduced the energy consumption by 25% and preserved rheological properties. In this same condition, 5 others EGs from 4 different glycosyl hydrolase families, with and without the carbohydrate binding module, were investigated for their effects on CNF isolation and interaction with the cellulose surface. With the exception of the EG of family 7, all the EGs tested were efficient in reducing energy consumption and in preserving the rheological and morphological properties of CNFs. In general, the specificity of EGs by less organized regions did not compromise the quality of the cellulose fiber and obtained CNFs, in addition the hydrolytic effect was negligible, reaching 100% of solids yield. The differences observed in terms of energy consumption can be related to the different action behaviors of EGs on cellulose fiber (e.g. interaction with the cellulose surface and modification of the degree of polymerization). Understanding the effect of EGs it is possible to use EGs from different families and vary and control the conditions of the enzymatic pre-treatment, making it possible to obtain CNF with the desirable properties.

Keywords: Properties of nanocelluloses. Energy consumption. Hydrolytic enzymes. Enzyme-cellulose interaction. Endoglucanase.

LIST OF FIGURES

LIST OF TABLES

LIST OF ABBREVIATIONS AND ACRONYMS

AA	Auxiliary activity
BEKP	Bleached Eucalyptus Kraft Pulp
CAZy	Carbohydrate-Active Enzymes
CBM	Carbohydrate-binding module
CDH	Cellobiose dehydrogenase
CI	Crystallinity index
CMC	Carboxymethyl Cellulose
CNC	Cellulose nanocrystals
CNF	Cellulose nanofibrils
CNM	Cellulose nanomaterial
cP	Centipoises
DP	Degree of polymerization
DTG	Derivative Thermo Degradation
EC	Enzyme Commission
EG	Endoglucanase
Dx10	Density number where 10% of particles are smaller than displayed value
Dx50	Density number where 50% of particles are smaller than displayed value
Dx90	Density number where 90% of particles are small than displayed value
EGU/g	Endoglucanase activity unit per gram of biomass
EX	Endoxylanase
g	Gram
GH	Glycosyl hydrolase
GPa	Gigapascal
FEG-SEM	Field Emission Gun - Scanning Electron Microscopy
HPLC	High Pressure Liquid Chromatograph
°C	Degree centigrade
ID	Identification number
Kg	kilogram
kDa	kiloDaltons
kWh	kilowatt hour
L	Liter
LPMO	Lytic polysaccharide monoxygenase
MFC	Microfibrilled cellulose

MPa	Megapascal
MWh	Megawatt hour
NC	Nanocellulose
µg	Microgram
µL	Microliter
µm	Micrometer
µmol	Micromol
mmol	Millimolar
mg	Milligram
mL	Milliliter
nm	Nanometer
PASC	Phosphoric acid swollen cellulose
PEI	Polythylenimine
pH	Hydrogen potential
QCM-D	Quartz Crystal Microbalance - Dissipation
TEMPO	(2,2,6,6-Tetramethylpiperidin-1-yl)oxyl
TGA	Thermo Gravimetric Analysi
USA	United States of America
SSA	specific surface area
SDS-PAGE	Sodium Dodecyl Sulfate Polyacrylamide Gel Electrophoresis
SWO	swollenin
USP	Universidade de São Paulo
UV	ultraviolet light

SUMMARY

1. INTRODUCTION

The renewable polymer cellulose is the most abundant and worldwide available biomaterial. It is found in high concentration in the vegetal cell walls (40- 50%) (Henriksson and Lennholm, 2009). The hierarchical structure of the cellulose fibrils is responsible for its outstanding properties, such as high crystallinity, flexibility and mechanical strength. The investigation and application of the cellulosic fibrils into nanometric scale has being more intensively explored over the last two decades (Dufresne, 2013). The so called nanocelluloses, besides preserving the original cellulose properties, has improved the elastic modulus, dispersibility and optical properties specially because of their small dimension and great surface area (Klemm et al., 2011).

In the case of cellulose nanofibrils (CNF), the properties of this biomaterial make it very attractive for reinforcement, barrier and coating applications. CNF has great surface area, high aspect ratio and high level of available hydroxyl groups, resulting in lightweight products, with high mechanical strength and low oxygen permeability (Lavoine et al., 2012). These characteristics allow CNF to be applied in several industrial sectors, as food, textile, automobile and packaging.

The typical production of CNF is carried out by intensive defibrillation using mechanical processes (Qing et al., 2013). The most used equipments are the high pressure systems (e.g. homogenizer and microfluidizer) and the ultra-grinder (e.g. SuperMassColloider) (Kalia et al., 2014). Although each equipment has different operating systems and the defibrillation occurs as a result of different forces, their all share the similar principles: apply a shear force to promote the defibrillation, isolating cellulosic fragments with smaller diameter. The applied shear force must be extremely high to isolate fibrils with diameter within the nanoscale. For that reason, it is necessary to pass the cellulosic suspension through the system several times, resulting in a remarkable energy consumption (Spence et al., 2011). In the high-pressure systems, beyond the high energy consumption, clogging and blocking issues are also common due to the large size of cellulosic fiber that flows through the tiny chambers and cannels (Henriksson et al., 2007; Pääkko et al., 2007).

There are methodologies described to optimize the process and reduce the energy for the defibrillation process. The oxidative pre-treatment mediated by TEMPO (2,2,6,6-TetraMethylPiperidine-1-Oxyl) is very efficient to reduce the number of passes in high-pressure systems (Saito et al., 2009). However, TEMPO is a toxic reagent, has a high cost and, currently, there is no recycling cycle, thus its application in a large scale is still a

challenge (Kalia et al., 2014). Another pretreatment approach is the use of hydrolytic enzymes, that has also been shown to reduce the energy consumption (Henriksson et al., 2007; Pääkko et al., 2007). The enzymatic pretreatment is a bioprocess, without application of hazardous chemicals or the production of undesirable products and requires mild reaction conditions. However, there are some open questions regarding enzymatic pre-treatment, especially concerning the sequence of steps, since typically, the enzymatic pretreatment is combined with mechanical refining, in sequential steps. Also, there is a large variation of enzyme loading and reaction time, resulting in different effects at the finals properties of CNFs and at the process efficiency. Moreover, it is still unclear which is/are the appropriate type or combination of enzymes specifically for CNF isolation.

In this context, the main objective of this study is to investigate the properties of specific groups of cellulases and hemicellulases to aid in the defibrillation of bleached Eucalyptus Kraft pulp to isolate CNF at lower energy consumption using a disc ultra-refiner and without compromising key properties (such as, rheology and morphological aspect). Aiming to achieve a high reduction of the required energy while preserving the properties, the condition of the enzymatic pre-treatment was firstly optimized using a commercial endoglucanase enzyme. Then, endoglucanases from four distinguished families (GH5, GH6, GH7, and GH12), with or without a carbohydrate binding module (CBM), were investigated concerning their catalytic action on cellulosic fiber and for beneficial effect on the isolation of CNF.

2. OBJECTIVE

2.1. GERAL OBJECTIVE

This thesis presents a comprehensive study regarding the dynamics of CNF production by disc ultra-refiner (SuperMassColloider) using hydrolytic enzymes, with high affinity for the less organized regions of the cellulose, aiming to reduce energy demand and preserve morphology and rheological properties. The effect of these enzymes on cellulose and the benefit of one-step enzymatic pretreatment for efficient CNF production have been demonstrated.

2.2. SPECIFIC OBJECTIVES

- To produce a reference material and investigated the modifications of BEKP through the disc ultra-refiner process (e.g. morphology, crystallinity, thermal stability, transmittance);
- To determine the optimal condition for the enzymatic pre-treatment in a single step applying a commercial endoglucanase monocomponent;
- To develop a library of potential hydrolytic enzymes to be applied for the isolation of CNF;
- To investigate the effect of different endoglucanases regarding their selectivity and catalytic mode of action for isolation of CNF;
- To identify enzymes to be applied in the pre-treatment, considering the energy consumption and CNF properties;
- To characterize the solid fractions after enzymatic pre-treatment and evaluate the interaction of the different enzymes and the cellulosic substrate;

3. THESIS STRUCTURE

The literature review and experimental results reported in this thesis are divided in chapters for a better understanding of the developed stages. The chapters are subdivided into abstract, brief introduction, materials and methods, results and discussion, and conclusion.

Chapter 1 is a literature overview regarding CNF and MFC production routes, the current state of art in industrial scale and the challenge of an efficient production by green pathway applying biocatalysts, especially cellulases with high affinity to cellulose substrates.

Chapter 2 reports the kinetic of the disc ultra-refining of BEKP in SuperMassColloider. The energy consumption and changes in morphology and properties of the cellulose fibrils was monitored throughout the process. This section is intended to relate the expenditure of energy during the ultra-refining to the quality of the materials generated during the process.

Chapter 3 investigates the effect of the enzymatic pre-treatment conditions using a monocomponent endoglucanase on the energy required for defibrillation and on the properties of nanofibrils isolated by disc ultra-refiner. A statistical design of experiment was applied to optimize the process in terms of energy consumption and quality of nanofibrils and the mechanic of interaction of EG with cellulose superficial was further elucidated.

Chapter 4 is related to the investigation of EGs from different families and from different microorganisms, applied in the pre-treatment at the optimal condition for isolation of CNF. Herein, it was explored the effect of these different EGs on cellulosic substrate and the role play of them to improvement of mechanical isolation of CNF.

CHAPTER 1 - LITERATURE REVIEW

Part of the text of this chapter was used in a review article ("Disclosure of enzyme-produced nanocelluloses production, characteristics, technoeconomics and opportunities") recently accepted for publication at Cellulose (ISSN 0969-0239).

1.1 CELLULOSIC FIBERS AND NANOCELLULOSES

Cellulose chains are composed by D-anhydroglucopyranose residues joined by β-1,4 glycosidic bonds (Fengel and Wegener, 1989). Although the molecular structure of cellulose is simple, its supramolecular structure is extremely complex (Fig. 1.1A). The free hydroxyls on cellulose surface arrange themselves in intra and intermolecular hydrogen bonds and further interaction by van der Waals to assemble the nanofibrils, with highly organized (crystalline) and less organized (amorphous) regions (Henriksson and Lennholm, 2009). The nanofibrils interact with themselves and form the microfibrils, which in turn interact and form the cellulose macrofibers (fibrils) (Fig. 1.1B) (Tejado et al., 2012).

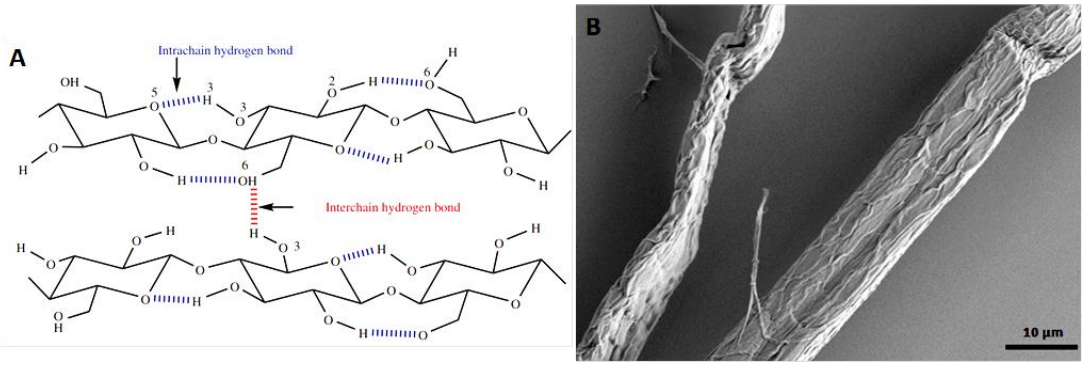

Fig. 1.1 (A) Representation of glycosidic bonds joining glucose residues and inter and intra hydrogen bonds (Chen et al., 2018); (B) Scanning electron microscopy (SEM) image of eucalyptus macrofibers isolated by Kraft pulping and a sequence of bleaching steps (author source).

In addition to cellulose, the plant cell wall is also composed by hemicelluloses and lignin. Hemicellulose is an amorphous polysaccharide, consisting of several sugars (e.g. xylose, mannose, glucose) and that interacts with cellulose forming a matrix of polysaccharides. Lignin is a macromolecule, also amorphous, consisting of phenolic and aliphatic structures and likewise, assembles with the polysaccharides completing the complex and recalcitrant matrix of plant cell walls. Although the contents of these three components can range among different plant specimens, and even among different plant cells, generally, cellulose represents the largest fraction. However, regardless of plant material, the isolation of

cellulose fibers requires chemical processes (pulping processes) to break down the recalcitrance and complex network (Sixta, 2006).

Typically, hardwood (e.g. eucalyptus) or softwood (e.g. pine) are used in pulping processes. As these woods have chemical and structural differences, the characteristics of the resulting wood-based pulps are also different from each other, and the length of the fibers is the most prominent difference, resulting in pulps and papers with different properties (Sixta, 2006).

There are several chemical processes (e.g. steam explosion, organosolv, dilute acid, ionic liquid) to isolate cellulose fibers, but the most widespread and industrially consolidated process is the Kraft pulping (Van Heiningen, 2006). In this process, wood chips are impregnated and cooked in the presence of sodium sulfate liquor and, approximately, 90% of lignin is removed. The pulp yield ranges from 45-55% (w/w). The pulp proceeds to successive bleaching stages, removing a considerable fraction of the residual lignin and also some of the hemicelluloses (Sixta, 2006). Commonly, bleached eucalyptus kraft pulp (BEKP) is composed of approximately 85% (w/w) cellulose and 15% (w/w) hemicelluloses. Using this wood-based fiber, it is possible to isolate fragments with small dimensions, the so called nanocelluloses (NC) with high crystallinity and outstanding mechanical and rheological properties (Klemm et al., 2011).

By definition, nanomaterials are characterized by having one or more dimensions in the order of 100 nm or less. This property is attractive for production of high performance materials (Mariano et al., 2014). There are two distinct nanocellulosic plant-based materials that are covered in this concept: (i) cellulose nanocrystals (CNC) and (ii) cellulose nanofibrils (CNF) (Fig 1.2B). CNC and CNF are obtained by disintegrating cellulose fibers to nano-scale particles. Isolating nanocrystals or nanofibrils is a top-down process (Nechyporchuk et al., 2016). Another material with outstanding properties that can also be isolated from cellulose fibers is the microfibrillated cellulose (MFC) (Fig. 1.2A), which is similar to CNF but shows more heterogeneous fibers suspension in terms of size, with diameters ranging from nanoscale to 400 nm) (Fig. 1.2) (Chinga-Carrasco, 2011).

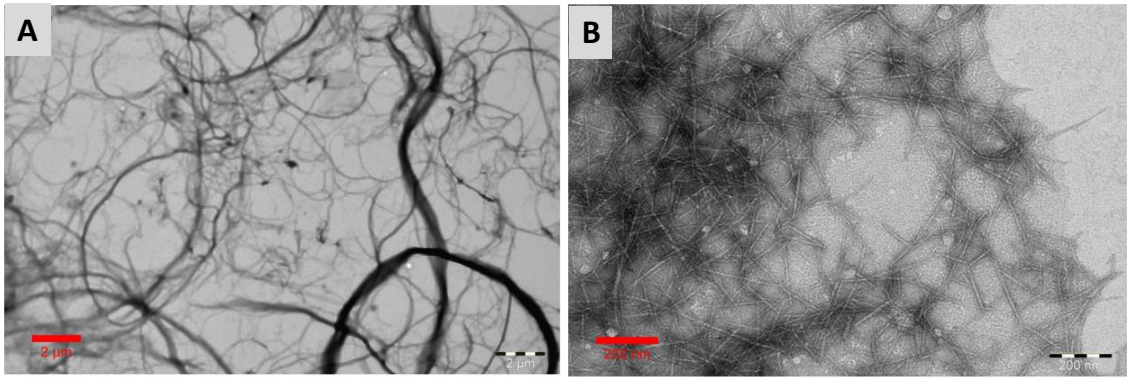

Fig. 1.2. Transmission electron microscopy of MFC and CNF obtained from BEKP by disc refiner and TEMPO-homogenization, respectively (Kumar et al., 2014).

CNC, CNF and MFC share some properties and preserve some of the cellulose fiber's characteristics. As examples, all of them are hydrophilic, present large reactive surface area and low suspension and film density (Moon et al., 2011; Nechyporchuk et al., 2016). The most remarkable different between CNC and CNF/MFC is regard to the aspect ratio, a relation of length and diameter. The morphology of CNC is typically a rod-like shape, whereas MCF and CNF are long micro and nanofibers with entangled network. But even comparing just one type of cellulose nanomaterial (CNM), a number of differences can be observed such as diameter size, degree of polymerization (DP), crystallinity index (CI) and aspect ratio (Table 1.1) (Habibi et al., 2010). This broad range in properties is because of CNC, CNF and MCF can be isolated from different biomass sources (e.g. cotton, wood, wheat straw, sugar cane bagasse) and by different mechanical, chemical and biochemical approaches.

Table 1.1. General characteristics of CNF, MFC and CNC.

	Diameter	**Length**	**CI (%)**	**DP**
CNC	3-35 nm[1]	200-500 nm[1]	53-80[2]	-
CNF	5-100 nm[1]	some µm[1]	34-60[3]	836-263[3]
MFC	20-400 nm[4]	some µm[1]	-	-

[1](Nechyporchuk et al., 2016); [2](Klemm et al., 2011) [3](Qing et al., 2013); [4](Chinga-Carrasco, 2011).

The differences among the CNMs lead to more specific application for each type of material. Nanocrystals have high crystallinity index and excellent optical properties, which are attractive to manufacture translucent and resistant films and composites with excellent

mechanical properties (Brinchi et al., 2013; Moon et al., 2011). The nanofibrils and microfibrils stand out for their high modulus of elasticity, stiffness and low oxygen permeability, thus CNF and MFC have the potential to be used in packaging and as reinforcement materials (Aulin et al., 2010). The forecasts for NCs applications indicate that some sectors will consume small amounts (e.g. drugs delivery, paint additives, emulsions), while others will require large quantities (e.g. automotive, packaging, textiles, aerogels, foams) (Shatkin et al., 2014). CNF and MFC are great material for packaging and just for this sector the forecasted demand for 2020 is 44,000 ton, jumping to 165,000 ton in 5 years (2025) (Miller, 2019).

1.2 CURRENT GLOBAL PRODUCTION OF CNF AND MFC

The potential application and future growing market of CNF and MCF have sparked substantial interest of companies in countries such as the USA, Canada, Japan, Finland, Norway and Sweden (Moon and Walker, 2012). These countries are traditional players in the forestry sector and in the pulp and paper industry, using mostly softwood as raw material. In the south hemisphere, Brazil, Chile, Australia and South Africa are the greatest players in the pulp and paper sector, exploring the isolation of cellulose fiber from hardwood, especially eucalyptus. Therefore, it is not surprising that these all these countries are the pioneers on research and production of nanocelluloses.

Table 1.2 shows a list of some current producers of MFC or CNF, their respective production capacities in 2015 and 2018, the biomass source and the type of defibrillation process. The information was presented during the International Conference on Nanotechnology for Renewable Nanomaterials in 2015 in Atlanta (USA) and in 2019 in Chiba (Japan). The start-up of operations in an industrial scale is quite recent for both CNF and CMF (e.g. American Process in 2015 and Borregaard in 2016). However, most of the companies increased their production capacity. Like all new technology, a significant effort is needed to drive the concepts of research and development of CNF/CMF to reach full commercialization and meet market demand (Walker, 2012).

Table 1.2. CNF and CMF producing companies and stated production capacity, announced at the 2015 and 2019 TAPPI Nanotechnology for Renewable Nanomaterials Conference.

Company - Country	**Product**	**Source/Method**	**2015 capacity[1]** (ton/year)	**2019 capacity[2]** (ton/year)
FiberLean Technologies - UK	MFC	Wood pulp/ Mechanical with mineral	1,000	8,800
Borregaard - Norway	MFC	Specialty cellulose/Proprietary	110	1,100
RISE - Sweden	MFC	Enzymatic pretreatment	-	25
Suzano - Brazil	MFC	Wood pulp/Mechanical	-	25
Daicel - Japan	MFC	Purified pulp/Mechanical	Lab	200
American Process - USA	CNF	Wood or agricultural residue/Mechanical	130	130
Nippon Paper - Japan	CNF	Wood pulp/TEMPO and mechanical	30	560
University of Maine - USA	CNF	Wood pulp/Mechanical	50	260

[1](Miller, 2015); [2](Miller, 2019).

Each company has a target market and produces MFC/CNF with specific characteristics for it. For example, Borregaard, located in Norway, has its internal division Exilva, which produces MFC for various applications: adhesives, agricultural chemicals, coating, construction and personal and home care (Borregaard, 2019). American Process owns BioPlus, a division responsible for the production of nanofibrils with hydrophilic and hydrophobic (lignin coated) characteristics seeking to further increase the diversity of applications (ProcessAmerican, 2019).

The large range of applications and opportunities of these biomaterials could be addressed to the different properties of CNF and MFC that can be isolated from diverse biomass sources and by different approaches. Figure 1.2 is an example of the variety of range in sizes, and, consequently, aspect ratio of CNF and MFC current available in the market. Thus, a comprehensive study of the properties and characteristic of cellulose nanofibrils and microfibrils is fundamental for the best final application and exploration of these materials.

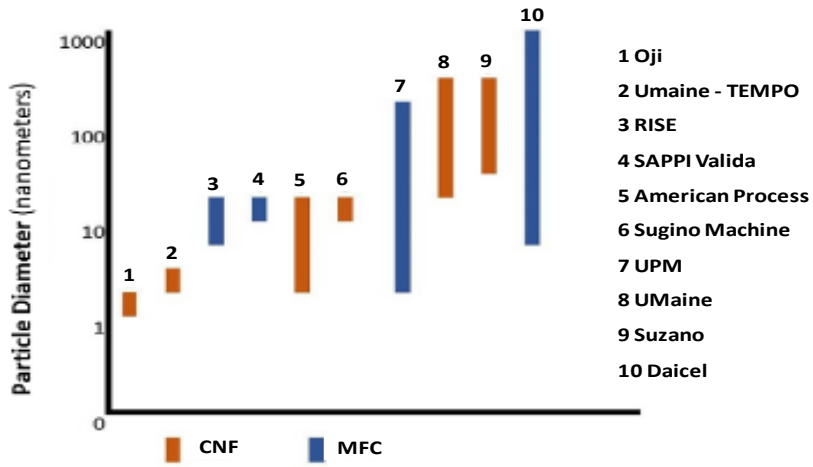

Fig. 1.3. Distribution range of particle diameters of CNF and MFC current produced by diverse companies. Adapted from Miller, 2017.

1.3 PRODUCTION ROUTES OF CNF AND MFC

The first production of micro and nanofibrils was recorded in 1983 by Turbak et al., who reported the isolation of nanofibrils by passing a suspension of hardwood pulp in a high-pressure system (homogenizer). Since then, the production of CNF is typically driven by mechanical processes, when through defibrillation and/or shear, nanofibrils are released, yielding isolated fragments of high aspect ratio (Eichhorn et al., 2010). The three most commonly used equipment to produce CNF are: (i) homogenizer, (ii) microfluidizer, and (iii) disc ultra-refiner (Spence et al., 2010a).

In addition to these conventional pathways, other methodologies are also able to efficiently isolate CNF with excellent quality. Among them, the use of twin-screw extruder has been shown to be able to refine pulp suspension in high solid content (20 wt%), to be scaled-up and produce CNF with similar properties to the CNFs isolated by homogenizer or disc ultra-refiner (Baati et al., 2017; Espinosa et al., 2019; Rol et al., 2017). Likewise, a process called nanopulping, which consists of the acceleration of cellulose fibers and fast pressure drop by an autoclave system, has also been shown to efficiently isolate NC from softwood kraft pulp (Zhu et al., 2012). Using an intense ultrasound probe, the fibrils can also be delaminated by hydrodynamic shear forces that break the hydrogen bonds (Leite et al., 2017; Li et al., 2013; Nechyporchuk et al., 2016). In the production of CNF by cryocrushing, the cellulosic pulp is immersed in liquid nitrogen to freeze the water present in the fibrils. Then, a high impact force is applied, for example, with a mortar and pistil, to release the microfibrils (Chakraborty et al., 2005).

The type of defibrillation also reflects the differences in the properties and morphology of the MFC and CNF isolated. An ultra-defibrillation increases the specific surface area (SSA), and, considering the initial SSA of bleached kraft pulp (5 m^2/g), the increase can be up to 14x (70 m^2/g) using a microfluidizer and 10x (50 m^2/g) with the disc ultra-refiner SuperMassColloider (Spence et al., 2011). This increase in SSA promotes greater networking capacity among micro/nanofibrils, resulting in films with low oxygen permeability, enhancing their application as a barrier material (Aulin et al., 2010). Increasing the SSA also increases the number of isolated nanoparticles and the number of free hydroxyl groups, which interact with a larger volume of water, forming high viscosity and stable gels at low concentration of nanofibrils. In addition, hydroxyl groups can be altered, for example through esterification, oxidation and sulfonation, modifying the properties of the biomaterial and diversifying its application (Nechyporchuk et al., 2016).

1.3.1 HIGH-PRESSURE SYSTEMS

The homogenizer and microfluidizer work at high pressure and with a pulp suspension at low solids content (0.2 to 2.0 % w/w) (Henriksson et al., 2007; Wang et al., 2015). In both devices, the abrupt drop in pressure (opening and closing of the feed valve) promote cavity formation and particles collision, and the passage of pulp suspension through the small chambers causes the shear of the fibrils (Dufresne, 2012). Several passes of the cellulosic material through the equipment (from 10 to 30 passes) are required to change of suspension's visual appearance and form a high viscosity gel at low solids content (typical characteristic of aqueous suspension of nanofibrils) (Hassan et al., 2010; Henriksson et al., 2007; Wang et al., 2015).

The most commonly used homogenizer for isolation of CNF is the Gaulin type, shown in Fig. 1.3A. The supply valve is quickly opened and closed successively, causing an abrupt drop in pressure. In addition, the impact of the pulp passage through the small slits causes the shear of the fibrils (Alain Dufresne, 2012). The nanofibrils obtained by this treatment have diameter ranging from 25-100 nm and length of up to a few millimeters (Szczesna-Antczak et al., 2012). Using the microfluidizer, (Fig. 1.3B), the pulp suspension passes through chambers of different diameters (200 and 400 µm) to increase the degree of defibrillation (Wang et al., 2015). The fibers suspension is forced through a chamber with fixed geometric shape (Y or Z), which ensures the process reproducibility (Kalia et al., 2014), resulting in CNF with similar morphology to that obtained with a homogenizer.

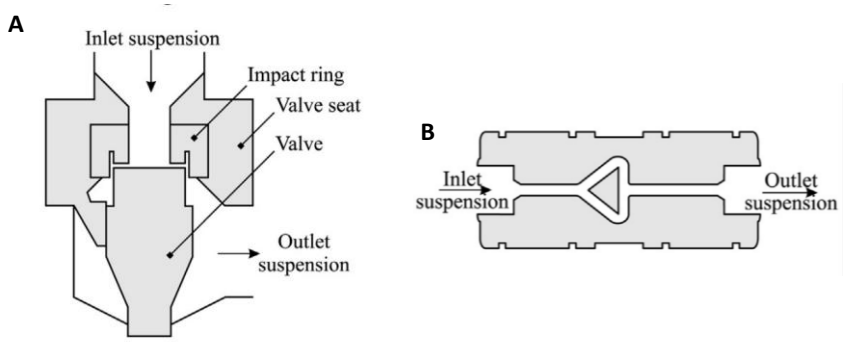

Fig. 1.4. General scheme of the mechanical operation of (A) homogenizer and (B) microfluidizer (Nechyporchuk et al., 2016).

Comparing the defibrillated pulps obtained by these devices, the nanofibrils obtained from the microfluidizer are more uniform (the distribution of particles size is more homogeneous) than those obtained by the homogenizer. Although there are minor differences between the two devices, both present some obstacles that hamper their operationalization in large scale. The major difficulty is the fluidity of the process, which is impaired by recurrent blockage/clogging of small chambers and channels due to the size of microfibrils and fibrils aggregates (Dufresne, 2013). When clogging occurs, it is necessary to stop the process for emptying the system, disassemble the equipment and cleaning the blocked points (Henriksson et al., 2007). In addition to this, the economic barrier and scaling up challenge are also related to high energy consumption (several passes through the systems) and the procedure with suspensions at low solid consistency (Kalia et al., 2014).

1.3.2 DISC ULTRA-REFINER (SUPERMASSCOLLOIDER)

Using the disc ultra-refiner, the feeding is done by gravity and the passes of the pulp suspension is forced between two discs, one rotating and one static. The centrifugal force displaces the material to the edges of the discs, where the friction between the discs and the fibrils causes the more intense fiber loosening and defibrillation, gradually exposing the inner layers of the cell wall (Dufresne, 2012). The most widely used disc refiner for CNF production is the SuperMassColloider (Masuko Sangyo Co Ltd, Japan) (Fig. 1.4). It allows processing suspensions of up to 8% (w/v) of solid content, but to date it has been reported cases where the consistency ranged only from 1.5% to 3% (w/w), underestimating the equipment operating capacity (Hassan et al., 2010; Nakagaito and Yano, 2004; Qing et al., 2013).

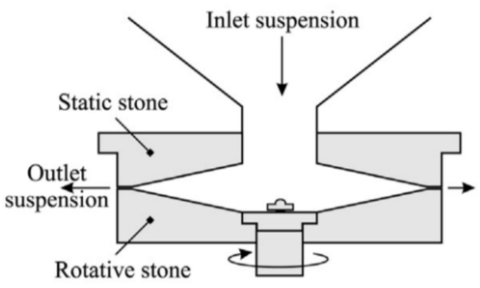

Fig. 1.5. General scheme of the mechanical production of CNF by disc ultra-refiner (Nechyporchuk et al., 2016).

As in the high-pressure systems, the disc ultra-refiner also requires repeated passes of the fibrils suspension through the equipment (around 5 to 20 times) or up to 12 hours of refining using continuous feed system, for visual changing in the appearance of the suspension, consequently, resulting in high energy consumption. (Hassan et al., 2010; Iwamoto et al., 2007; Nakagaito and Yano, 2004; Wang et al., 2012). However, the great advantage of disc ultra-refiner, comparing to the high pressure systems, is the fluidity of the system. In the microfluidizer and homogenizer, the processes are exhausting and hamper large-scale production (Kalia et al., 2014). Thus, the isolation of MCF or CNF by the high-pressure systems is infeasible without a pre-treatment step (Henriksson et al., 2007; Pääkko et al., 2007; Rol et al., 2017). The clogging/blocking do not occur in the disc ultra-refiner and the cellulosic material can be defibrillated without requiring a pre-treatment step (Nechyporchuck et al, 2016). Additionally, the scaling-up can be considered more feasible by disc ultra-refiner with regard to the higher solid content capacity of this equipment. A more detail description of mechanical isolation of CNF/MFC is described in the chapter 2.

1.4 ENERGY DEMAND AND STRATEGIES FOR REDUCTION

Spence et al., (2011) evaluated the combination of a mechanical pre-treatment (valley beater) with high pressure systems or disc ultra-refiner. The work stands out for comparing the three most used equipment for the isolation of CNF and reporting a detailed investigation of the energy consumption. For the high-pressure systems, homogenizer or microfluidizer, it was strictly necessary a mechanical pre-refining. The energy consumption using the homogenizer reached 22 kWh/kg and the microfluidizer 3 kWh/kg. The disc ultra-refiner, the only one that did not require a mechanical pre-treatment, consumed 1.5 kWh/kg of energy.

Several other groups reported energy requirements, as well as strategies of pre-treatment to reduce the energy demand (Table 1.3). The results reported should be considered

with attention as there are considerable differences among sources of lignocellulolytic biomass, devices, level of scaling, methodologies for quantification of energy consumption, sizes, quality and nomenclatures of isolated micro or nanofibrils.

The paper industry, traditionally, uses the refining process to process cellulosic pulps and produce papers with different characteristics (Blechschmidt and Heinemann, 2006). The input energy in this process varies due the final properties of the desired paper quality. For example, to produce print paper from bleached hardwood Kraft pulp, the energy demand is approximately 0.1 kWh/kg and to produce grease resistance paper from sulfite pulp the energy demand can reach 1 kWh/kg (Annergren and Hagen, 2009).

In CNF isolation process, higher energy demand result in CNFs with suitable characteristics for noble applications. Ranging the energy consumption between 1.5 and 3 kWh/kg in the defibrillation of bleached hardwood Kraft pulp, resulted in final nanomaterial with improved proprieties (e.g. physical, optical and nanofibers interactions) to be used packing applications (Spence et al., 2011). Increasing the inputted energy to 33 kWh/kg, the final obtained nanomaterial showed higher specific surface area and lower water vapor transmission rate, both important properties for food packaging application and displays.

Table 1.3. Examples of energy consumption for isolation of CNF and MFC by different devices and from different cellulosic source.

Cellulosic material	Pre-treatment	Defibrillation process	Solid content (%)	Energy consumption (kWh/kg)	Isolated material	Range or mean diameter	Reference
Bleached hardwood Kraft pulp	Mechanical	Homogenizer	0.7	33	MFC	Less than 1 µm	Spence et al., 2011
Bleached hardwood Kraft pulp	Mechanical	Microfluidizer	0.7	3	MFC	Less than 1 µm	Spence et al., 2011
Bleached hardwood Kraft pulp	None	Disc ultra-refiner	3	1.5	MFC	Less than 1 µm	Spence et al., 2011
Bleached eucalyptus Kraft pulp	Lab disintegrator	Disc ultra-refiner	2	10 – 40	CNF	10-140 nm	Wang et al., 2012
Bleached softwood Kraft pulp	None	Nanopulping	1	0.76	CNF	-	Zhu et al., 2012
Bleached softwood Kraft pulp	Lab disintegrator	Disc ultra-refiner	2	4	CNF	0.75 – 1.75 µm	Hoeger et al., 2013
Bleached softwood Kraft pulp	Lab disintegrator	Disc ultra-refiner	2	5	CNF	15 – 40 nm	Nair et al., 2014
Corn stalk delignified	Oxidation	Homogenizer	1.5	40	CNF	-	Chaker et al., 2014
Corn stalk delignified	Oxidation	Waring Blender	2	12	CNF	7 nm	Chaker et al., 2014
Sulphite softwood dissolving pulp	Carboxymethylation	Microfluidizer	1.2	3 – 6	CNF	-	Naderi et al., 2015
Bleached eucalyptus Kraft pulp	None	Twin screw extruder	20	20	MFC and CNF	-	Rol et al., 2017
Soda pulping from eucalyptus	Oxidation	Twin screw extruder	10	4.1	CNF	-	Baati et al., 2017
Bleached eucalyptus Kraft pulp	None	Disc ultra-refiner	1	12	MFC	100 nm	Berto and Arantes, 2019
Bleached eucalyptus Kraft pulp	None	Disc ultra-refiner	1	20	CNF	21 nm	Berto and Arantes, 2019

- : not available or not reported; MFC: microfibrillated cellulose; CNF: cellulose nanofibrils

The large range of energy consumption reported is observed even for the same type of equipment. For example, the energy inputted for defibrillation by disc ultra-refiner ranges from 1.5 to 40 kWh/kg (Hoeger et al., 2013; Nair et al., 2014; Spence et al., 2011; Wang et al., 2012). Considering a similar initial material (bleached hardwood Kraft pulp), Spencer et al. (2011) and Wang et al. (2012) reported distinct energy consumption, 1.5 and 40 kWh/kg, respectively. Hoeger et al. (2013) and Nair et al. (2014) reported similar energy consumption, 4 and 5 kWh/kg, respectively, using the same initial material (bleached softwood kraft pulp) and same pre-treatment (lab disintegrator). The range of energy reported applying the homogenizer is lesser discrepant, varying from 33 to 40 kWh/kg, even when using different biomass resource (bleached hardwood Kraft or delignified corn stalk) and different pre-treatment (mechanical or oxidation) (Chaker et al., 2014; Spence et al., 2011).

Despite of this range of reported energy demand by different authors, the efficiency of the pre-treatment stage is well known in order to reduce the energy consumption and improve the fluidity of the high pressure systems (Henriksson et al., 2007; Moreau et al., 2019; Nakagaito and Yano, 2004; Pääkko et al., 2007; Saito et al., 2006; Tibolla et al., 2014; Wang et al., 2015). Pre-treatments can be mechanical (Nakagaito and Yano, 2004), chemical (Saito et al., 2006), biochemical (Henriksson et al., 2007; Moreau et al., 2019; Pääkko et al., 2007; Tibolla et al., 2014; Wang et al., 2015), but the combination of them is the most applied approach. The morphological aspect of the CNF/MFC can vary among the different defibrillation processes and applied pre-treatment (Fig. 1.5) due to the differences of each pre-treatment approach.

Regardless of the differences in morphology of isolated CNFs, all pre-treatments share the same foundation: to promote specific changes in the cellulose macrofibrils, aiding and facilitating the defibrillation process. The use of reagent 2,2,6,6-tetramethylpiperidine-N-oxyl (TEMPO) as mediator for cellulose oxidation in the presence of NaClO/NaBr was proposed by Saito and Isogai (2004). The authors used cotton as substrate and verified the formation of carboxylates (COO^-) (0.7 mmol/g) and aldehydes (0.3 mmol/g) groups in the cellulose. Apparently, these functional groups had been inserted in the amorphous regions and in the surface of the crystals, since no reduction in crystallinity or changes in crystal size was observed. The presence of these groups on cellulose surface promotes the loosening of adhesion among the fibrils by electrostatic repulsive forces (Saito et al., 2006) facilitating the mechanical defibrillation. Switching to the TEMPO/NaClO2/NaClO system, at neutral pH (6.8), the formation of aldehyde groups is avoided, the DP is preserved and the oxidation is more efficient (Saito et al., 2009).

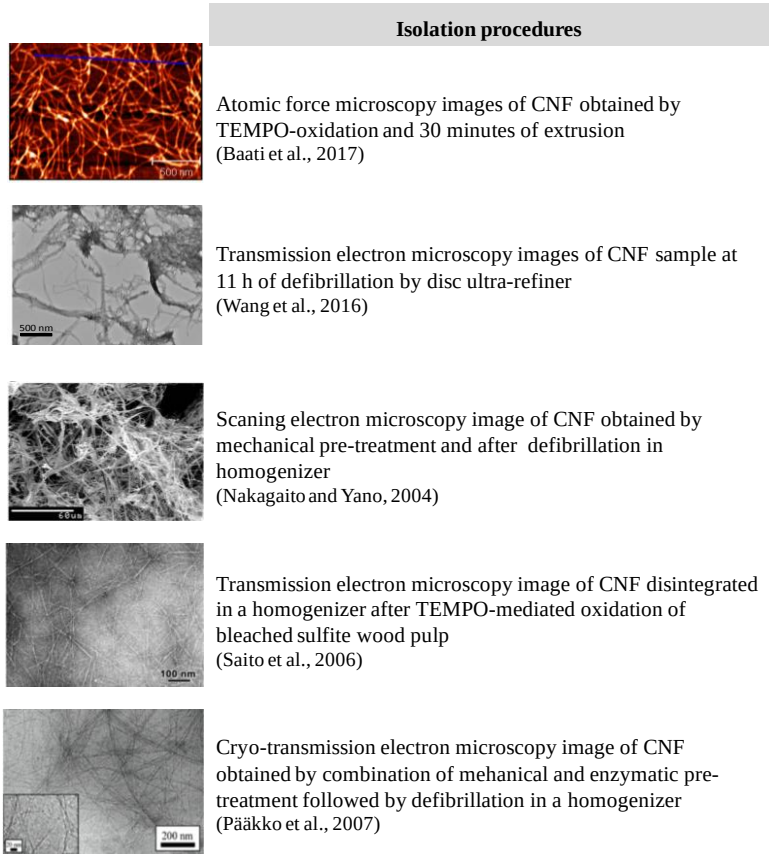

Fig. 1.6. CNFs images obtained by different microscopy techniques and isolated from different pre-treatment and defibrillation procedures.

Despite of using NaClO/NaBr or $NaClO_2$/NaClO, TEMPO-mediated oxidation reduces the number of passes required in the homogenizer to obtain the characteristic gel formation of nanofibrils suspension (Kalia et al., 2014). A significant drop in the number of passes was observed in oxidized pulps containing at least 0.3 mmol/g of carboxyl groups (Saito et al., 2006). Isogai et al. (2011) reported a reduction of energy consumption from 195 kWh/kg to 2 kWh/kg, comparing the isolation of and MFC and oxidized-CNF, respectively. Rol et al. (2017) described the isolation of CNF by twin screw extruder using TEMPO as the pre-treatment. The oxidation-driven system could reduce the energy consumption by approximately 25%. In addition to reducing the energy consumption, the application of the TEMPO-mediated system allows to isolate CNF with a diameter between 3-4 nm, resulting in extremely homogeneous suspensions and high optimal quality and low oxygen permeability films (Isogai et al., 2011; Saito et al., 2009). However, its applicability in an industrial scale is not consolidated due to the high cost of the reagent and the lack of an efficient recovery system (Zhu et al., 2011). In addition, TEMPO is a relatively toxic and environmentally

aggressive reagent (Brinchi et al., 2013) and the TEMPO-oxidized cellulose becomes resistant to biodegradation by endo and exo cellulases as COONa groups are introduced into the glucose polymer (Isogai et al., 2011). Nevertheless, Nippon Paper, located in Japan, has a production capacity of 560 ton/year of TEMPO oxidized-CNF.

An alternative pathway to the application of TEMPO-driven system is the use of a biomimetic methodology. The application of enzyme for the isolation of MFC/CNF was described for the first time by Pääkko et al. (2007) and, later in the same year, by (Henriksson et al. (2007). Both groups applied an isolated endoglucanase from the glycosyl hydrolase family 45 (GH45), combined to mechanical refining, to aid the defibrillation of dissolve grade pulp by a homogenizer. They observed that the enzymatic pre-treatment could improve the fluidity of the pulp suspension through the device. Since then, other research groups assayed several monocomponents or combination of enzymes to aid the defibrillation process, using different biomasses and devices for the defibrillation process (Table 1.4).

As can be observed in Table 1.4, there is a large range of conditions and stages to pre-treat the cellulosic material for isolation of MFC/CNF. Some examples are: (i) Pääkko et al. (2007), in which the dissolving pulp was pretreated by successive revolutions in a disc refiner, followed by an enzymatic treatment, again mechanical refining, ending with successive homogenizer passes; (ii) Qing et al. (2013) combined different processes at the pre-treatment stage, starting with enzymatic treatment, followed by successive revolutions in ultrafine disc refiners and finally several passes through the microfluidizer; (iii) Nechyporchuk et al. (2016) reported the isolation of CNF following sequential steps, initialization by pulp disintegrator and pre-refining in a PFI-mill, followed by enzymatic treatment and isolation of nanofibrils by disc ultra-refiner.

In addition to these sequential steps, the range of enzyme loading (from 0.85 to 350 EGU/g) and reaction time (1 – 72h) is very large and the optimal hydrolytic condition has not been established until this moment and neither how the enzymes aid in the defibrillation process. A more detail approach concerning the enzymatic condition for the pre-treatment and its benefits over MFC/CNF isolation is described in the following chapters. However, all authors reported excellent benefits for the application of enzymes to isolate MFC/CNF, especially regarding the improvement of fluidity and energy reduction in all equipment. The differences regarding the enzymes, especially endoglucanases from distinctive families, are described in more details in chapter 4.

Table 1.4. Examples of reported studies applying enzymes as a pretreatment for isolation of CNF by different devices and from different biomass sources.

Cellulisic material	Pre-mechanical refining	Enzyme	Solid content (%)	Time	Temp.[1] and pH	Enzyme loading	Defibrillation process	Benefits	Reference
Dissolving pulp	PFI-mill	Novozym 476	3	2 h	50 °C – 7	0.02, 0.5, 1.5 or 3% (1, 25, 75 or 150 EGU/g*)	Homogenizer	Lowest enzyme loading allowed the defibrillation	Henriksson et al., 2007
Dissolving pulp	Escher-Wiss refiner (before and after enzymatic treatment)	Novozym 476	4	2 h	50 °C – 7	0.17 or 30 µl/g (0.87 or 130 EGU/g)	Homogenizer	Lowest enzyme loading allowed the defibrillation	Pääkko et al., 2007
Bleached sisal fiber	Mechanical shearing	Celluclast or Ecopulp	5	2h	50 °C	0.1 or 10 wt% 3.5 or 35 EGU/g	Microfluidizer	It was possible to isolated CNF and CNC varying the steps sequence	Siqueira et al. (2010)
BSKP[2]	Mechanical beating	FiberZyme$^{T}_{M}$ LBR	0.5	24 h	45 °C – 7	0.05, 0.1, 1, 4 wt%	Homogenizer	Higher enzyme loading allow to increased the solid content for defibrillation	Siddiqui et al., 2011
Softwood Kraft pulp	None	Novozym 476	15	1 h	50 °C – 7	0.165 g/ 30 g fiber (27.5 EGU/g)	Nanopulping	Increased the nanopulping efficiency	Zhu et al., 2012
BEKP[3]	Blender	FiberCare or Celluclast	10	24 h	50 °C	3 FPU/g Fibercare or 2 FPU/g Fibercare + 1 FPU/g Celluclast	Disc ultra-refiner + Microfluidizer	CNF with high tensile stiffness and transparency	Qing et al., 2013
Bleached sugar cane bagasse and curauá fibers	None mechanical Chemical stages	FiberCare or Viscozyne	2	72 h	50 °C – 4.8	0.1 or 10 mg/g of Viscozyme + 0.33 or 33 mg/g of Fibercare	Sonifier	For bagasse lower enzyme loading for required to improve CNF isolation	Campos et al., 2013
Bleached banana bran	Knife mill and chemical stages	Xylanase	25	24 h	45 °C – 5	50 U/g	None	Combination of chemical and enzymatic treatment was able to isolated CNF	Tibolla et al., 2014

To be continued

BEKP[3]	Lab disintegrator and Bauer classifier	FR or GH5	5	48 h	50 or 70 °C – 5	0.1, 1 or 10 mg /g fiber	Microfluidizer	1 mg/g of GH5 preserved the DP and reduced 30% the number of passes	Wang et al., 2015
Bisulfite softwood pulp	Disintegrator and PFI-mill	FiberCare or Celluclast	2	2 h	50 °C – 5	Celluclast 2.1, 10.5, 21 EGU/g Fiber Care 21, 210, 315 EGU/g	Disc ultra-refiner	Increased the level of defibrillation even using low amount of FiberCare	Nechyporchuk et al,. 2014
BEKP[3]	Lab pulper and PFI-mill	Novozym 476	3 e 5	2 – 4 h	50 °C – 5	80, 160, 240, 320 g/ton (0.4, 0.7, 1.1, 1.4 EGU/g)	Homogenizer	Longer reaction time and higher enzyme load resulted in greater yield of defibrillation	Tarrés et al., 2016
BEKP[3]	Disc beater	FiberCare	2	2 h	50 °C – 5	300 EGU/g	Twin screw extruder	Reduced the number of passes and preserved the properties quality	Rol et al., 2017
BHKP[4]	Lab Blender	Endoglucanase, xylanase and LPMO	1	3 h	50 °C – 5	1 mg of each enzyme/g of substrate	Sonicator	The synergism among three enzymes increased the transmittance	Hu et al., 2018
Bleached Birchwood Kraft pulp	None	LPMO	3.5	24 h	50 °C – 4.8	Enzyme:substrate ratio 1:500	Ultra Turrax + Microfluidizer	LPMO treatment allowed the defibrillation	Moreau et al., 2019
BEKP[3]	Lab Disintegrator	Xylanases or Endoglucanase FR	10	48 h	50 °C – 5	0.05, 0.1, 0.2, 0.3 mL of enzyme/g of glucan in pulp	Microfluidizer	EG was more efficiency to increase the transmittance than xylanases	Zhou et al., 2019

Temp.[1]: reaction temperature; *EGU/g: EG international unit per gram of substrate; BSKP[2]: Bleached softwood Kraft pulp; BEKP[3]: Bleached eucalyptus Kraft pulp; BHKP[4]: Bleached hardwood Kraft pulp.

One of major advantage of the enzymatic pre-treatment over the oxidative pre-treatment is related to the mild condition of operation. The biomimetic pre-treatment using hydrolytic or oxidative enzymes is conducted at around neutral pH conditions, ranging from pH 5 to 7 in low molarity buffers (mostly 50 mM) (Table 1.4). In addition, the required temperature is considered industrially mild, around of 50 ° C (Table 1.4). Such operating conditions do not require corrosion resistant reactors or elevated temperatures. Besides that, enzymes themselves are another great advantage as they are non-toxic biochemical molecules that degrade in the environment and do not produce toxic secondary products.

1.5 CARBOHYDRATE ACTIVE ENZYMES

The enzymes involved in the deconstruction of cellulose and other carbohydrate chains are grouped in a database called CAZy (Carbohydrate Active Enzyme) according to the similarity of their three dimensional structure and their mechanism of action (Levasseur et al., 2013). The cellulases, the specific enzymes that act on cellulose, are clustered in the glycosyl hydrolyses group (GH) and in the auxiliary activity (AA), and subclassified in families according to their catalytic action and substrate specificity (Dashtban et al., 2010; Horn et al., 2012; Vlasenko et al., 2010).

Although all cellulases act on cellulose chain in order to deconstruct the polymer by hydrolytice reactions, there are some differences in the mechanism of action and substrate specificity for each family of cellulases (Davies and Henrissat, 1995). The classic model of cellulose deconstruction involves the synergic action of three different cellulases (cellobiohydrolases, endoglucanases and beta-gludosidases). However, more recently it was found that other enzymes with swelling (swollenin) and oxidative effect (auxiliary activity) are also involved (Horn et al., 2012), as demonstrated Fig. 1.6

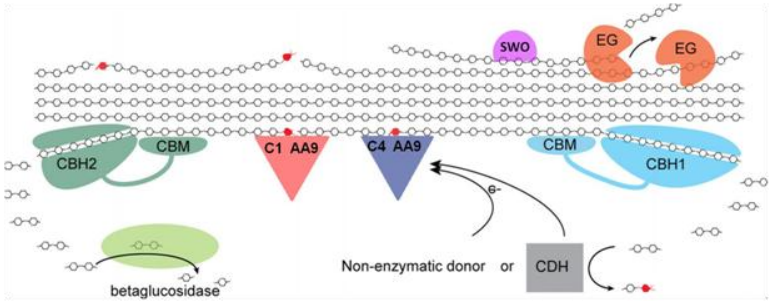

Fig. 1.7. Schematic representation of the cellulose deconstruction by hydrolytic and oxidative enzymes. (EG) endoglucanases; (CBH I and II); cellobiohydrolases; (CBM) carbohydrate binding domain; (AA9) auxiliary activity of family 9; (SWO) swollenin; (CDH) cellobiodehydrogenases (Adapted from Horn et al., 2012)

The exo-glucanases or cellobiohydrolases (CBH, EC 3.2.1.91 and EC 3.2.1.176) act on the crystalline region of cellulose, being CBHI (GH7) specific for the reducing terminal and CBHII (GH6) for the non-reducing terminal of the chain. Both, when attached to the terminal, act along the chain and release cellobiose as product (Horn et al., 2012). In general, CBHs have a bimodular structure, that is, they are connected to a carbohydrate binding module (CBM) by a polypeptide chain (polylinker). The CBM binds to cellulose, approaching the active site of the enzyme to the substrate and remains bound, promoting the catalytic action of CBH. CBHs are very effective in decomposing cellulose and are present in higher levels in commercial enzyme cocktails, therefore they are the most studied cellulases (Van Den Brink and De Vries, 2011).

Unlike CBHs, endoglucanases (EG, EC 3.2.1.4) act on the less organized fraction of cellulose and randomly cleave glycosidic bonds. EGs promote a fast decrease in the degree of polymerization of cellulose and further expose new ends in the cellulose chains. Currently, EGs are classified in the following GH families: 5, 6, 7, 8, 9, 10, 11, 12, 26, 44, 45, 48, 51, 74, 124 and 148 (CAZy, 1998). EGs may be linked to CBM and thus may also have, or no, processive action over cellulose chain (Cohen et al., 2005). Finally, β-glycosidases (EC 3.2.1.21) belongs to families GH1 and GH3 and cleave the cellooligosaccharides (mostly cellobiose), released by CBHs and EGs, to glucose monomers (Payne et al., 2015). More recently other enzymes were associated to this conventional mechanism. In addition to the cellulases, the action of the auxiliary and accessory enzymes such as polysaccharide lytic monoxoygenases (LPMOs), cellobiose dehydrogenases (CDHs) (Horn et al., 2012) and swollenin (SWO) (Saloheimo et al., 2002) were included in the deconstruction mechanism of cellulose.

CHAPTER 2 – KINETIC CHANGES IN CELLULOSE PROPERTIES DURING DEFIBRILLATION INTO MICROFIBRILLATED CELLULOSE AND CELLULOSE NANOFIBRILS BY ULTRA-REFINING

Manuscript published at *International Journal of Biological Macromolecules* on April 2019 (DOI: 10.1016/j.ijbiomac.2019.01.169)

2.1 ABSTRACT

Defibrillation of cellulose fibers can lead to the isolation of microfibrillated cellulose (MFC) or cellulose nanofibrils (CNF) with intrinsic properties suitable for various applications. However, to what extent these properties are preserved, enhanced, gained or lowered during defibrillation and how they are related remains unclear. In this study, a kinetic study of the ultra-refining of bleached eucalyptus Kraft pulp (BEKP) in a disc ultra-refiner was performed and characterized in terms of physical-structural, morphological and thermal properties and their interactions and compromises. Defibrillation of BEKP to MFC substantially decreased the fiber diameter and increased viscosity, surface area and morphological heterogeneity. It also led to a remarkable increase in transparency and essentially did not alter the thermostability but significantly degraded the crystallinity. A higher degree of defibrillation to isolate CNF led to fibers with smaller diameter and increased diameter uniformity but required a substantial amount of energy to only marginally increase viscosity and transparency. Crystallinity and thermostability were not altered, comparing with CMF. In conclusion, most changes occurred during the defibrillation of BEKP to CMF. Further defibrillation to CNFs with smaller diameters and better uniformity did not significantly reflect on other important structural cellulose physical properties, despite the much higher energy consumption and degree of defibrillation.

Keywords: nanocellulose properties, SuperMassColloider, cellulose microfibrils, cellulose nanofibrils.

2.2 INTRODUCTION

The controlled deconstruction of the natural assembly of cellulose hierarchical fiber structure to individual microfibrils and further deconstruction of the microfibrils into individual nanofibrils leads to the formation of microfibrillated cellulose (MFC, 20-400 nm wide and a few micrometers long) and cellulose nanofibrils (CNF, 5-100 nm wide and a few micrometers long), respectively (Aulin et al., 2010; Chinga-Carrasco, 2011; Pääkko et al., 2007; Saito et al., 2009). This fiber defibrillation approach has allowed micro- and nanoscale cellulose to be applied to a broad range of products in various industrial sectors. It has also been gaining growing attention in both the scientific community and the industrial sector due to the combined unique properties of these materials (Aulin et al., 2010; Czaja et al., 2007; Fang et al., 2014; Korhonen et al., 2011). The micro and nano fibrils have a high surface area, which results in a higher interaction between the fibrils, conferring their films with low oxygen permeability (Aulin et al., 2010). The high surface area is closely related to the large number of available hydroxyl groups, which interact with a larger volume of water, forming stable, high viscosity gels. In addition, the hydroxyl groups can be functionalized (e.i. esterification, oxidation and sulfonation), altering the properties of the biopolymer and diversifying its application (Nechyporchuk et al., 2016). The high aspect ratio and flexibility confer excellent mechanical properties, such as high modulus of elasticity and tensile strength (Siró and Plackett, 2010).

Typically, cellulose fiber defibrillation is done mechanically in a high-pressure system (homogenizer or microfluidizer) or using a ultra-disk refiner (Hassan et al., 2010; Henriksson et al., 2007; Nakagaito and Yano, 2004; Pääkko et al., 2007; Turbak et al., 1983; Wang et al., 2012). Although the mechanism of defibrillation varies between high-pressure systems and ultra-disk refining, based mostly on characterization studies comparing the properties of the starting cellulosic pulp and the final defibrillated cellulose, there is a growing body of evidence showing that different cellulose properties undergo distinct changes after defibrillation. For example, while the most noticeable property change after cellulose defibrillation is typically a decrease in particle diameter, consequently increasing the specific surface area, increased transparency, particle size uniformity, viscosity, and some mechanical properties also occur, all to different extents. However, the gain or improvement in these cellulose properties is, in general, accompanied by the loss of other critical structural cellulose properties such as crystallinity and degree of polymerization (DP) (Iwamoto et al., 2007; Wang et al., 2012). Therefore, cellulose fiber defibrillation seems to result from a compromise among different and in some cases opposite behavioral changes in cellulose properties. For

example, maximizing diameter reduction, uniformity, transparency, and viscosity requires a high degree of defibrillation and therefore high energy consumption, conditions in which cellulose degradation (crystallinity) appears to be inevitable.

While monitoring the physical properties of composites prepared with defibrillated softwood dissolving pulp cellulose and an acrylic resin, Iwamoto et al. (2007) observed that the decrease in crystallinity and DP that occurred during defibrillation led to losses in the properties of the composites, such as a decrease in mechanical properties and an increase in thermal expansion. This finding evidences the importance of detailed investigation of the cellulose fiber defibrillation process in terms of the physical and morphological properties.

Over the last decade, a number of studies have successfully investigated changes in the properties of cellulose fibers from various sources during defibrillation in different equipment (Iwamoto et al., 2005; Spence et al., 2011; Stelte and Sanadi, 2009; Wang et al., 2012). However, limited information is reported from investigations or attempts to relate the gain and improvement (and to what extent) in cellulose properties during defibrillation to the extent of change in crystallinity and DP, which are more prone to undergo loss during defibrillation and have recently been classified within the most important properties of defibrillated cellulose (Kangas et al., 2014). In addition, only a few studies have monitored the change in the properties of hardwood-derived cellulosic pulp occurring during defibrillation (Stelte and Sanadi, 2009; Wang et al., 2012). This is relevant since hardwood-derived cellulosic pulp is the most widely available commercial source of cellulose and has been shown to be less susceptible to defibrillation than softwood-derived pulp (Stelte and Sanadi, 2009; Syverud et al., 2011), therefore requiring more extensive defibrillation, which could lead to more extensive cellulose degradation. Nevertheless, Wang et al. (2012), studying the morphological development of cellulose fibrils of bleached eucalyptus pulp by mechanical defibrillation, observed that both the crystallinity and DP decreased with increased energy input during ultra-disk refining, but no other physical property was investigated and therefore cellulose degradation was not correlated to other changes in cellulose properties during the defibrillation process.

In this context, the present study aimed to comprehensively study the kinetic change in important physical structural properties of cellulose (morphology, surface area, uniformity, homogeneity, transparency, viscosity, crystallinity, and thermal stability) during defibrillation of bleached eucalyptus Kraft pulp (BEKP) into MFC and CNF by ultra-disk refining. In addition, the compromise between the gain, improvement or loss in cellulose properties during defibrillation is discussed. It is expected that with a detailed understanding of the

kinetic changes in important physical structural properties as related not only to the gain and improvement in specific cellulose properties during defibrillation but also to the potential loss of critical properties, it will certainly be possible to more precisely customize the defibrillation process to reach the best compromise among gain, improvement, and loss in cellulose properties while isolating the most suitable MFC and CNF for specific applications.

2.3 MATERIALS AND METHODS

2.3.1 CELLULOSIC PULP

The never dried bleached eucalyptus Kraft pulp (BEKP) was kindly supplied by Fibria Celulose S/A (Jacareí, Brazil). The major chemical composition, determined according Sluiter et al. (2012), was 78.6% cellulose and 14.6% xylan.

2.3.2 MECHANICAL DEFIBRILLATION BY ULTRA-REFINING

Three BEKP suspensions were prepared at the same concentration (1% w/w) and volume (1 L). The suspensions were defibrillated in the disc ultra-refiner SuperMassColloider (Masuko, model MKCA6-5J). The discs (model MKGA10-80) are made of a ceramic material (aluminum oxide and resin) without porosity to avoid any nanometric particle infiltration and also to allow better fit between the discs. The SuperMassColloider was connected to a digital energy meter (ForLong DRT-341D) that was used to monitor and measure the energy consumption during defibrillation, reported in kWh. As the initial solid content was the same for all the processes, the energy consumption was reported in kWh/kg.

During operation, one of the discs remained stationary and one in motion, with rotation at 1,600 rpm. The distance between the discs was determined and fixed as described by Wang et al. (2012), and these parameters were fixed for the three BEKP suspensions. Briefly, the zero motion position was determined by the noise generated by the contact position between the two discs before loading the suspension. From the zero motion position, the ultra-refiner was loaded with the cellulosic suspension and the discs were immediately adjusted to the -100 μm amplitude position between the discs. Although the position is negative, the presence of the cellulose suspension acts as a lubricant ensuring that the discs do not touch and wear out. The ultra-refiner was operated with the cooling system using water flow at room temperature; it was necessary to readjust the zero motion position for each new cycle.

2.3.3. PARTICLE SIZE DISTRIBUTION AND SPECIFIC SURFACE AREA

The particle sizes and the particle size distribution of the suspensions were determined by Low Angle Laser Light Scattering (LALLS) using the laser diffraction particle size analyzer Mastersizer 3000 (Malvern Instruments) with two sources of light, red (632.8 nm) and blue (470 nm), allowing for a measurement range of 10 nm - 3,500 µm. The equipment was coupled to a medium volume automated sample dispersion unit (Hydro MV, Malvern) with a built-in centrifugal pump to circulate the suspended sample within the analysis cell, an in-line ultrasonic probe and a stirrer to prevent sedimentation and aggregation of the particles in the sample unit tank. Analyses were conducted at low obscuration (0.5 - 4%) – a measure of the concentration of the suspension during analysis – with a stir rotation speed of 3,500 rpm and without sonication.. The input parameters were manually set to assume a non-spherical particle model that approaches the particles to the cylindrical shape (related to the fibrillar structure) with the refractive index (RI) set to 1.4683, the RI for cellulose (Sultanova et al., 2009). The Mie-scattering theory is used by the Malvern Mastersizer 3000 software to convert the data to the particle size distribution. The particle size number is related to the hydrodynamic diameter value of the equivalent particle, calculated automatically. It is important to clarify that the reported value cannot be assumed as absolute value for nanofibrils measurements, but it can be taken as a reference value to infer the degree of defibrillation.

The final particle-size distributions were reported as the particle size density number (Dx_{10}, Dx_{50} and Dx_{90}). Dx_{50} is the value that represents the average particle size, where half of the particles have a size below the displayed value. The Dx_{10} and Dx_{90} values represent the value where 10% and 90% of the particles are smaller than the displayed value, respectively. Also, the specific surface area was the determined by this same methodology. Size analyses report the average of one run, with five successive laser diffraction runs, for a total of 5 readings per sample. Before each analysis, the dispersion unit was automatically cleaned three times with ultrapure water. The Hydro Sight unit is coupled to the particle analyzer, which allows real-time viewing along with image capture of the sample in-line during particle measurement. The Hydro Sight (Malvern) resolution is equal to an optical microscope, with a viewing limit close to 1.4 - 1,4000 µm, which does not allow the visualization of nanostructures, but does monitor the decrease in particle size.

2.3.4. CRYSTALLINITY INDEX

Sample preparation for analysis by X-ray diffraction was done by drying the cellulosic material in an air circulation oven at 33 °C for 24 hours. Each dried sample was placed on a microscope slide and analyzed in an X-ray diffractometer (XRD – 6000, Shimadzu) at room temperature, with CuKα radiation and a graphite monochromator (reflection mode analysis). The measurement conditions were $10 < 2\theta < 40$; 2θ step: 0.02°, 30 s per step. All measurements in the XRD were taken in triplicate. The XRD peaks were separated by deconvolution (curve fitting) using a Gaussian function in the Origin software (version 2017, OriginLab), in corroboration to the recommended method to study crystallinity of nanocellulose by the ISO (ISO/TR 1976: 2016). The crystallinity index (CI) of the suspensions was determined according to Segal, Creely, Martin and Conrad (Segal et al., 1959), but using the deconvoluted peak height method (DPHM), which makes use of the fitted XRD data to calculate CI according to equation 1, where I_{002} is the peak approximately $2\theta = 22.5°$ and I_{am} is the minimum approximately $2\theta = 18°$.

$$CI = \frac{(I_{002} - I_{am}) \times 100}{I_{002}} \quad (1)$$

The X-ray diffractograms were also used to calculate the cellulose crystallite lateral dimension according to the Scherrer equation (equation 2) (Langford and Wilson, 1978; Scherrer, 1918), where K is the correction factor (0.91), λ is the radiation wavelength (for CuKα, λ=1.54060 Å), θ is the diffraction angle (approximately 11.25° for the (200) plane), and β is the full width (in radians) at half maximum (FWHM) intensity of the same peak (200) (Kumar et al., 2014).

$$L200 = \frac{K\lambda}{\beta \cos\theta} \quad (2)$$

2.3.5. VISCOSITY

The viscosity of the suspensions was determined in an automatic viscometer (Brookfield LVDV2T Pro digital) equipped with an apparatus for small sample volume. Analyses were carried out using Brookfield RheocalcT software (version 1.2.19). Cellulosic suspensions were prepared with a solids content of 0.25% (w/w). The spindle SCA-18 was coupled to the viscometer (with this spindle, a 6.7 ml sample volume was required) with the rotation set at 100 rpm and the temperature controlled at 25 °C using a water bath. The torque was measured simultaneously with the viscosity measurements, ensuring that it was within the 20-80% range, as recommended by the manufacturer. Each viscosity analysis was

conducted for 5 minutes, with measurements every 30 seconds. The results are reported as the mean of 10 measurements taken during a 5-min period.

2.3.6. THERMAL STABILITY

Thermal stability analyses were performed using the thermal analyzer TGA-TA Instrument DST-Q600 in an inert atmosphere (N_2, flow rate 100 ml/min), with a heating rate of 10 °C/min and a temperature range of 30 - 600 °C. The samples were prepared from films of the oven-dried cellulosic materials at 30 °C for 24 hours (the initial moisture of the material was not considered in the analysis). Samples with dimensions close to 4x4 mm were sectioned from the films and the mass was measured on a precision scale until it reached approximately 3-5 mg. An aluminum crucible was used for analysis due to its low reactivity.

2.3.7. MORPHOLOGICAL CHARACTERIZATION

Optical microscopy (OM) images were obtained using an Olympus BX53 X-cite 120 LED microscope. A drop of the aqueous suspension of cellulosic material with a solids content equal to 0.01% (w/w) was stained with Congo red as described (Ougiya et al., 1998) and placed on a microscope slide. The images were collected in monochrome mode and 100 diameters were measured using the Olympus cellsens Dimension software.

Atomic force microscopy (AFM) images were obtained using a Nanosurf FlexAFM (Switzerland) and a silicon FMR sonar probe (Nanoworld). The cantilever was operated with the intermittent contact technique at a nominal resonance frequency equal to 75 kHz and a nominal force constant (spring) of 2.8 N/m. Samples with a solids content close to 0.01% (w/v) were dispersed in an ultrasonic bath (2 minutes) immediately before being dropped onto the previously cleaved mica support. The generated topographic images were treated, and 100 diameters of at least 50 particles were measured in the Gwyddion (64 bit) software.

2.3.8. OPTICAL PROPERTY OF THE FILMS

The gain in optical property (increase of transparency) of the cellulosic materials was evaluated by analyzing their respective films. Films 2.5 cm in diameter and constant mass of 0.3 g were produced by adding 1.2 ml of the aqueous cellulosic suspensions with a solids content equal to 0.25% (w/v) in a polypropylene container with a diameter of 2.5 cm. The material was oven-dried at 50 °C for 24 hours. The transmittances of the films were measured at 600 nm using a BioTek Epoch 2 spectrophotometer. The specimens (1 cm x 2 cm) were inserted in the cuvette place at the optical path.

2.4 RESULTS AND DISCUSSION

In order to first verify the inherent variations in the mechanical ultra-refining system, three suspensions of BEKP were prepared and defibrillated in the SuperMassColloider under the same condition. During the ultra-refining of the tree suspensions, the number of cycles (beginning of the feed of the pulp suspension into the ultra-refiner up to the total exit of the suspension) and energy consumption were monitored and reported as average value. The materials were sampled after every two or three cycles and simultaneously analyzed for particle size (Dx_{10}, Dx_{50} and Dx_{90}), size distribution and specific surface area by laser diffraction.

BEKP suspensions were ultra-refined until the particle size reached nanoscale size as indicated by the Dx_{10}, Dx_{50} and Dx_{90} values (Fig. 2.1). Upon reaching an energy consumption close to 30 kWh/kg (10 cycles), the Dx_{90} of the particles was approximately 750 nm. Upon reaching the average particle size (Dx_{10}, Dx_{50} and Dx_{90}) of approximately 750-650 nm, the nanosize was used as the parameter to stop processing of the BEKP suspension.

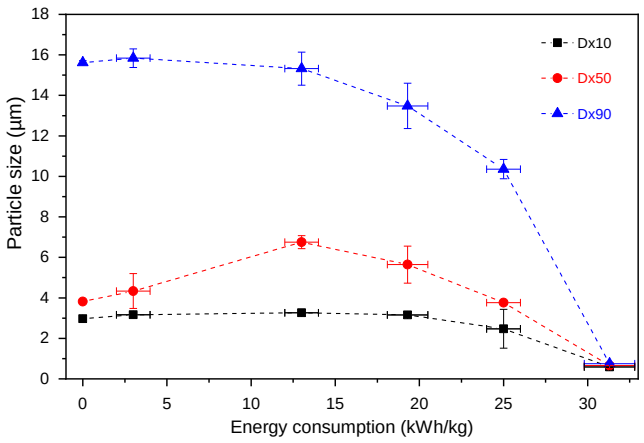

Fig. 2.1. Particle size distribution expressed as Dx10, Dx50 and Dx90 resulting from the defibrillation of three BEKP suspensions in a SuperMassColloider and reported as a function of energy consumption.

The energy consumption varied approximately 10%, reaching values between 30 and 33 kWh/kg, with a mean consumption of 31.3 kWh/kg (± 1.5 kWh/kg) to reduce the particle to mean size of 750 nm. During most of the ultra-refining, Dx_{10} essentially did not change, remaining at approximately 3,000 nm until the energy consumption reached 31.3 kWh/kg (equivalent to 10 cycles), when the reduction of Dx_{10} was detected at 500 nm. On the other hand, Dx_{90} showed a continuous and smooth decrease up to an energy consumption of 25 kWh/kg within the range of 15,000 to 10,000 nm. When the energy consumption reached 31.3

kWh/kg, a drastic reduction in the Dx_{90} from 10,300 nm to approximately 700 nm was observed. On the other hand, Dx_{50} started at a particle size equal to 3,800 nm, but increased at energy consumption close to 13 kWh/kg, reaching 7,000 nm. This increase can be attributed to the particles that were clustered in Dx_{90} and due to ultra-refining were reduced and regrouped in the Dx_{50}. After this increase, the particle size in Dx_{50} dropped smoothly to 650 nm. The relationship between particle sizes (Dx_{10}, Dx_{50} and Dx_{90}) and energy consumption showed small variations for the three different BEKP suspensions processed (Fig. 2.1). Based on this small variation, it was assumed that the ultra-refined materials resulting from the five BEKP suspensions are likely to be similar and therefore the characterization analyses were conducted with the ultra-refined materials of only one BEKP suspension. Considering that high energy consumption is a major bottleneck for the cellulose defibrillation process to MFC and CNF, the characteristics and changes in the cellulose fibers throughout ultra-refining are reported as a function of the energy consumption.

The laser diffraction particle analyzer MasterSizer 3000, which reports the mean particle sizes for Dx_{10}, Dx_{50} and Dx_{90}, also generates information about the overall particle size distribution (Fig. 2.2). Changes in the size distribution profile were expected throughout the defibrillation process since ultra-refining in the SuperMassColloider has been reported to cause reductions in particle size, especially in the longitudinal direction of the fiber (Wang et al., 2012). However, from the beginning of the ultra-refining (2 kWh/kg) to an energy consumption equal to 25 kWh/kg, the numerical particle size distribution profile was characterized by two distinct peaks (one peak at approximately 3,000 nm and a broader peak at approximately 7,000 – 8,000 nm) and did not show any significant change (Fig. 2.2) as well in the average particle size (Dx_{10}, Dx_{50} and Dx_{90}) (Fig. 2.1). A possible explanation for the fact that the size distribution pattern remained practically constant throughout the ultra-refining is that although the cellulose fiber suffered delamination in the longitudinal direction, the fiber-length was preserved, maintaining its volume equivalent with essentially no modification of the hydrodynamic diameter. A drastic change in the particle size distribution profile was only observed at a higher degree of defibrillation when ultra-refining was performed up to an energy consumption of approximately 30 kWh/kg. At this high degree of ultra-refining, the particle size distribution was characterized by a single and narrow peak at 600 nm, indicating great size uniformity of the ultra-refined material. Indeed, this is can be evidenced by the AFM images (Fig. 2.3), which shows highly uniform mean diameter of the nanofibrils with more than 90% of the nanofibrils with diameter between 0.1-10nm. Although in this study there is no evidence about the fiber longitudinal damage, it has already

demonstrated that the application of excess shear force is can lead to loss of mechanical properties and degree of polymerization (Shinoda et al., 2012). At a high degree of defibrillation, corresponding to the energy consumption of 30 kWh/kg, it was observed a drastic change in the size distribution of the volume equivalent spherical diameter.

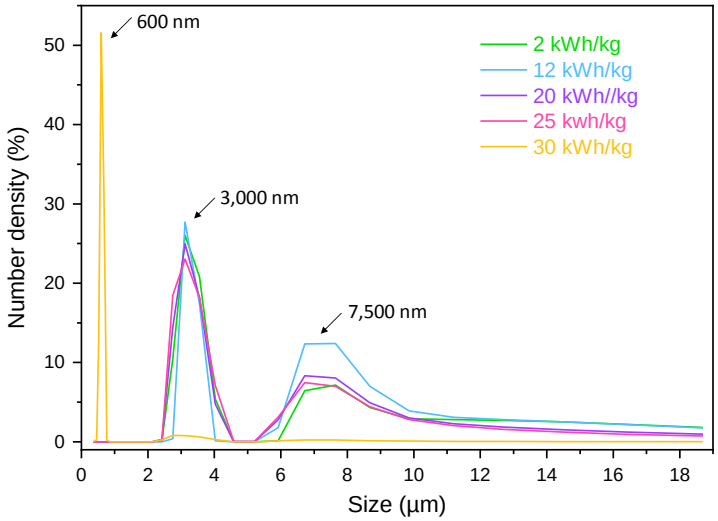

Fig. 2.2. Particle size distribution profile during BEKP defibrillation by ultra-refining in a SuperMassColloider.

2.4.1 MORPHOLOGICAL ASPECT

The first morphological analysis was performed using the Hydro Sight, an in-line imaging accessory coupled to the MasterSizer 3000 particle analyzer that functions as an optical microscope. Therefore, it was possible to observe and capture images of the particles in real time in the laser diffraction measurement (Dx90) flow (Fig. 2.3). The images allow one to follow the size reduction of the cellulose fibers during defibrillation until no particles are visible, indicating that the particles could no longer be detected by the Hydro Sight and likely were smaller than 1,400 nm, the lower limit range of the equipment according to the manufacturer. At the initial phase of the ultra-refining process, with an energy consumption of 2 kWh/kg, the BEKP suspension consisted mainly of fibers, with a Dx_{90} of approximately 15,000 nm. At an energy consumption of approximately 12 kWh/kg, a drastic reduction in the number of visible fibrillar structures could be observed, but Dx_{90} remained constant. With further defibrillation to an energy consumption of approximately 20 kWh/kg, it was no longer possible to identify the microfibrillar structures of the material in the Hydro Sight, and Dx_{90} started to smoothly decrease (Dx_{90} equal to 11,000 nm). Consequently, as the material was further ultra-refined to energy consumptions of 25 and 30 kWh/kg, no particles were

identified, and Dx_{90} showed a slight decrease to 10,300 nm and a drastic reduction to 750 nm, respectively.

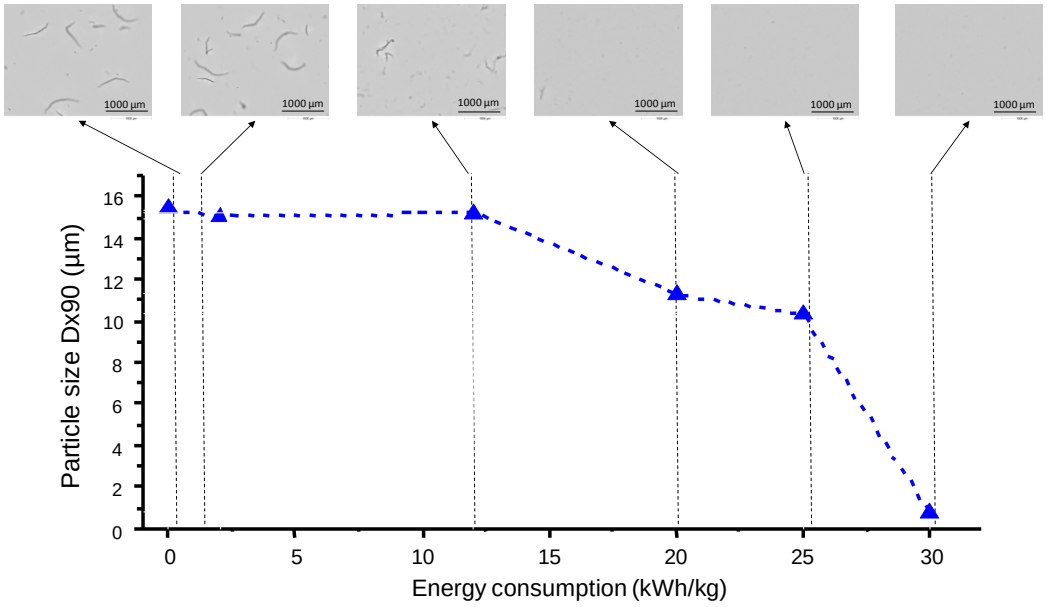

Fig. 2.3. Optical images generated by Hydro Sight, relating the morphological aspect of the material to the average particle size (Dx_{90}) measured by Mastersizer 3000 during cellulose fiber defibrillation by ultra-refining BEKP in a SuperMassColloider (the scale bar is 1000 µm).

To analyze the morphological aspect and to understand the changes during the BEKP defibrillation process, images were generated by optical microscopy (OM) and atomic force microscopy (AFM). OM images were taken from the samples where it was still possible to observe fibrillar structures in the Hydro Sight (Fig. 2.4 A, B, C), whereas the other samples were imaged by AFM (Fig. 2.4 D, E, F). The diameters of the fibers, microfibrils and nanofibrils measured by software analysis of the images generated by OM (Olympus Cellsens Dimension) and AFM (Gwyddion 64 bit) showed that drastic changes occurred in the material throughout the ultra-refining process (Table 2.1).

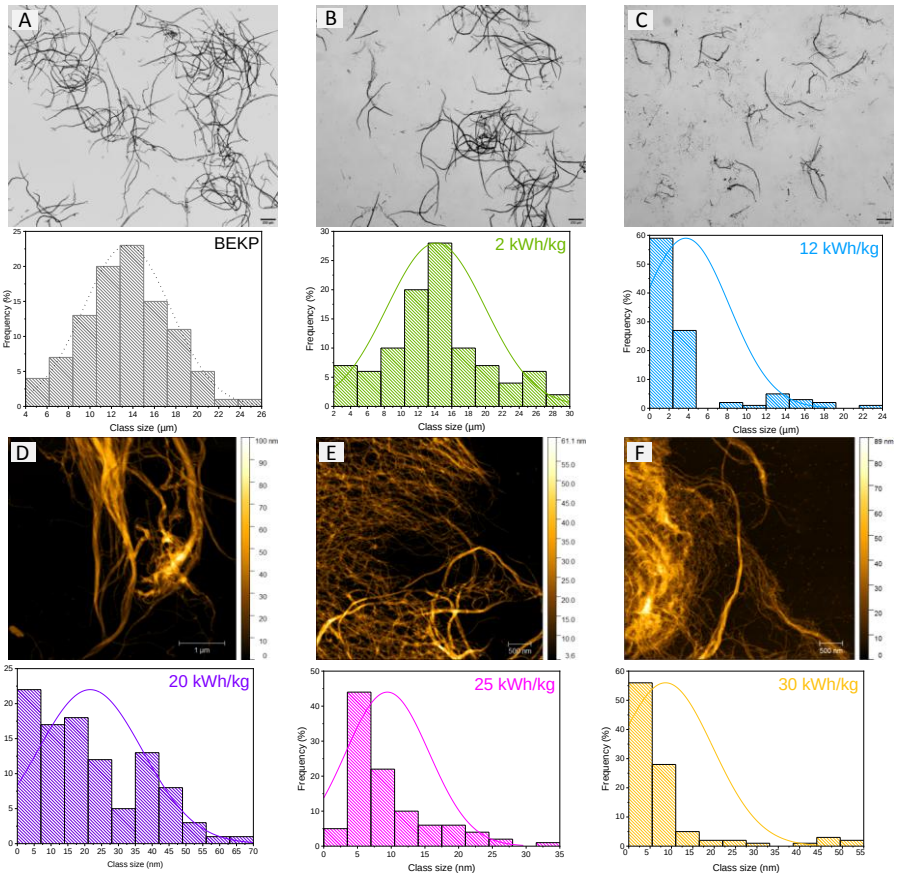

Fig. 2.4. Optical images (A, B and C) with a scale bar equal to 200 µm and atomic force microscopy (D, E and F) with a scale bar equal to 500 nm, and graphs of diameter distribution determined from the respective microscopy images of BEKP and BEKP suspensions defibrillated to different degrees of ultra-refining indicated as energy consumption.

Table 2.1. Diameters of BEKP and ultra-refined BEKP samples collected during defibrillation in a SuperMassColloider.

Energy Consumption	**Distribution range**	**Mean**
BEKP (control)	6000 – 24000 nm	13500 nm
2 kWh/kg	4000 – 24000 nm	14100 nm
12 kWh/kg	400 – 22000 nm	400 nm
20 kWh/kg	2 - 64 nm	21 nm
25 kWh/kg	2.7 - 33 nm	9.4 nm
30 kWh/kg	0.5 - 51 nm	8.6 nm

The microscopy images and image analysis allowed for the evaluation of BEKP ultra-refined to different degrees of defibrillation. Initially, BEKP (control) had a diameter

distribution range of 6,000 – 24,000 nm and a mean diameter of 13,000 nm, values in agreement with the literature (Shackford, 2003). A low degree of defibrillation corresponding to ultra-refining at an energy consumption of 2 kWh/kg did not modify the diameter distribution range (4,000 – 22,000 nm) or the mean diameter (14,000 nm). With further ultra-refining to an energy consumption of 12 kWh/kg, the fibers in the BEKP suspension still had the same diameter distribution range of 4,000 – 22,000 nm, but most fibers diameters were clustered at approximately 300 nm and the mean diameter was substantially decreased to 400 nm, indicating partial defibrillation of the BEKP fibers. This ultra-refined BEKP suspension was also characterized by residual fiber structures that were still visible in OM, which demonstrates that the suspension was not homogeneous. In addition, this partially defibrillated BEKP suspension may also contain microfibrils with diameters smaller than 400 nm, and even nanofibrils with diameter smaller than 100 nm, which are not apparent in OM.

According to the literature, MFC suspensions are generally heterogeneous with particles of uneven diameter, varying between micrometric and nanometric scales, and even with residual non-delaminated fiber fragments. For example, recently Lehmonen et al., (2017) classified as MFC a defibrillated cellulose suspension containing fibrillar fragments with diameters greater than 150 nm as well as fibrillar structures with average diameters in the 15-20 nm range. Kumar et al. (Kumar et al., 2014) produced an MFC suspension with fiber diameters ranging from 15-500 nm and low particle uniformity. Therefore, the characteristics of the defibrillated BEKP suspension obtained at an energy consumption of 12 kWh/kg is typical of an MFC suspension, which in this study is considered as a suspension containing cellulose fibers with diameters greater than 100 nm and also containing fragments of fibers with diameters within the micrometer scale and probably CNF with diameters less than 100 nm.

With a higher degree of ultra-refining at an energy consumption of 20 kWh/kg, the MFC suspension was defibrillated to a diameter distribution range of 2 - 64 nm and a mean diameter of 21 nm. These nanoscale diameter values characterize the defibrillated BEKP at an energy consumption of 20 kWh/kg as nanocellulose since it has at least one dimension smaller than 100 nm, and more specifically as CNF, which has been reported to consist of cellulose nanofibrils with diameters within the 5-100 nm range (Aulin et al., 2010; Chinga-Carrasco, 2011; Pääkko et al., 2007; Saito et al., 2009). Further ultra-refining to a higher degree of defibrillation at energy consumptions of 26 and 30 kWh/kg resulted in cellulose nanofibrils with a diameter distribution range of 2.7 - 33 nm and 0.5 - 51 nm and mean

diameters of 9.5 and 8.5, respectively. That is, further ultra-refining leads to CNF with smaller diameters and a diameter distribution skewed to smaller sizes (Fig. 2.4).

It is notable the difference between the pattern of particle size reduction determined by laser diffraction and the pattern of reduction of the fiber diameter determined by AFM morphological analysis. This divergence is a result of differences between the techniques used to complete the analysis of the materials. While the morphological analysis by AFM allows the real quantification of the diameter of the fibers, the analysis by laser diffraction allowed a real-time monitoring of the changes along the defibrillation process. However, the combination of these two techniques, allow to observe that the ultra-refining process causes delamination of cellulose fiber, gradually exposing the inner layers and releasing the microfibrils and nanofibrils, depending on the degree of defibrillation. Therefore, the reduction in particle size was expected to occur mainly in the longitudinal direction of the fibril (diameter) (Chinga-Carrasco, 2011; Henriksson et al., 2007; Wang et al., 2012). Indeed, for BEKP defibrillation to MFC (energy consumption of 12 kWh/kg) and CNF (energy consumption of 20 kWh/kg), the size reduction in the longitudinal direction can be observed by relating the mean particle size (Fig. 1), particle size distribution (Fig. 2.2) and mean diameter (Fig. 2.4). That is, the mean diameter results show a drastic reduction (Table 2.1) that was not accompanied by significant changes in particle size and size distribution (Fig. 2.1 and 2.4), indicating that the fiber length was not deep affected. At a higher degree of defibrillation (energy consumption 30 kWh/kg), the drastic change in distribution size (Fig. 2.3) suggested that ultra-refining promoted a substantial reduction in fiber length.

The dimensions of cellulose fibrils are related to a very important property, the aspect ratio between fiber length and diameter, which is one of the factors that confers excellent mechanical properties to micro- and nanofibrils (Lehmonen et al., 2017; Nakagaito and Yano, 2004). In this context, the microscopy images and particle size results shown here (Fig. 2.1, 2.3 and 2.4, and Table 2.1) suggest that during BEKP ultra-refining to MFC and CNF, most of the fibers diameters changed, indicating that the aspect ratio increased as BEKP was defibrillated do MFC and CNF, as expected. The smooth particle size reduction observed by laser diffraction could indicate that the fiber length was preserved along the mechanical defibrillation. However, as the length decreased at higher degrees of ultra-refining due to fiber damage, the aspect ratio began to be compromised. Thus, the increase in aspect ratio is not proportional to the increase in the degree of defibrillation. Apparently, there is a limit among the extensive defibrillation and the improvement in this property.

2.4.2. SUSPENSION UNIFORMITY

It is known that the homogeneity and uniformity of a polymeric matrix suspension have a close relation to film and composite quality (Iwamoto et al., 2007) and that homogeneous materials contribute to uniform formation of films and composites, avoiding stronger or weaker regions, without variations in mechanical properties among regions. Therefore, the uniformity of the ultra-refined BEKP suspensions was monitored by calculating the diameter distribution range (Table 2.1).

One of the advantages of cellulose defibrillation by ultra-refining over high-pressure systems (microfluidizer and homogenize) is that the typical clogging problems during the defibrillation does not occur (Besbes et al., 2011; Kalia et al., 2014). However, the uniformity and homogeneity of the cellulose suspensions defibrillated by ultra-refining have been contradictory. Indeed, Kalia et al, (2014) reported that the ultra-refiner SuperMassColloider resulted in a suspension of nanofibrils that was not uniform or homogenous. Some authors have suggested further processing the ultra-refined suspension in a high-pressure system to improve uniformity. For example, Qing et al. (2013) reported that after processing a suspension of nanofibrils obtained using the ultra-refiner SuperMassColloider and a microfluidizer, the diameter distribution range decreased from 9-170 nm to 3.1-4.7 nm. On the other hand, (Iwamoto et al., 2007) showed that by operating a SuperMassColloider (Masuko MKCA6-3) under certain conditions (1500 rpm, 1 wt.% and 15 cycles), it was possible to obtain a uniform CNF suspension with a diameter distribution range of 20-50 nm.

The MFC suspension produced at an energy consumption of 12 kWh/kg had a diameter distribution range of 400 – 22,000 nm and a mean diameter of 400 nm (Table 2.1, Fig. 2.4C). This heterogeneity is due to the presence of fiber fragments with larger diameters in addition to the defibrillated microfibrils, as discussed in the previous section. By prolonging the ultra-refining of the BEKP suspension to a higher degree of defibrillation and producing a suspension with nanofibrils of a mean diameter equal to 21 nm (energy consumption equal to 20 kWh/kg), the diameter size range decreased to 2 to 64 nm and the non-defibrillated fragments present in the MFC suspension no longer were visible in the CNF suspension, indicating increased particle uniformity and suspension homogeneity. Continued ultra-refining of this CNF suspension to an energy consumption of 25 and 30 kWh/kg led to CNFs with a diameter distribution between 2 - 64 and 2.7 - 33 nm, respectively, demonstrating that the improvement in fiber diameter distribution uniformity is achieved by prolonging ultra-refining in the SuperMassColloider.

2.4.3. SPECIFIC SURFACE AREA (SSA)

The improvement in mechanical properties such as tensile strength and modulus of elasticity of defibrillated cellulose has been related to the increase in the specific surface area (Dogan and McHugh, 2007). A higher specific surface area results in a better interaction of particles, forming a low density, low-porosity network that leads to a better oxygen barrier network, a property suitable for application as a packaging material (Aulin et al., 2010; Boufi et al., 2016).

The changes in the SSA during BEKP ultra-refining were monitored using the Mastersizer 3000 (Malvern) particle analyzer (Fig. 2.5). The SSA values reported by the particle analyzer cannot be considered absolute values since the nanoparticles show a high aspect ratio; therefore, they are not similar to a spherical particle. However, it is possible to follow the modification and increase in SSA during ultra-refining. As expected for this type of mechanical process (Boufi et al., 2016), ultra-refining improved the SSA (Fig. 2.5). As BEKP was ultra-refined, the SSA property was characterized by a continuous increase. Ultra-refining remarkably increased the surface area (values approximately 160 m^2/kg) of the particles in the BEKP suspensions defibrillated up to an energy consumption of 12 kWh/kg, when the ultra-refined material had characteristics of MFC according to the morphological analyses. This increase in the SSA coincided with the steep reduction in particle mean diameter (approximately 97%). Further ultra-refining to an energy consumption of 20 kWh/kg to obtain a CNF with a diameter equal to 21 nm further increased the SSA (reaching values of approximately 200 m^2/kg or a 41% increase in relation to the initial SSA). Ultra-refining to an even higher degree; that is, at an energy consumption of 25 and 30 kWh/kg, further significantly increased the SSA to 257.5 m^2/kg (55%) and 356.4 m^2/kg (68%), respectively, with a constant diameter reduction.

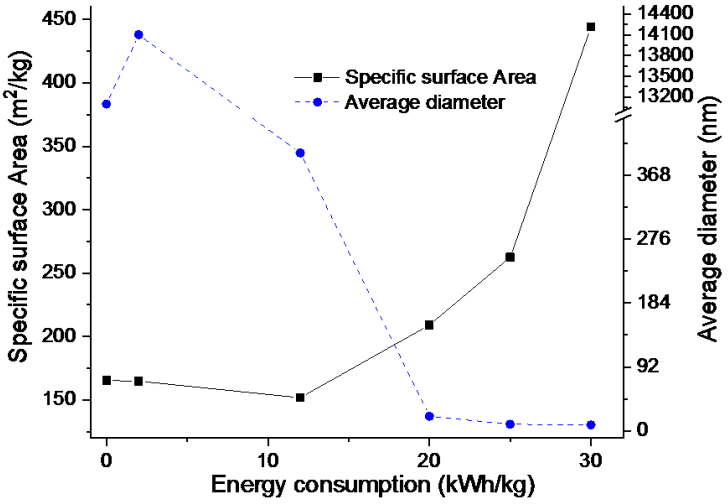

Fig. 2.5. Changes in the specific surface area (SSA) and average diameter of the particles in the ultra-refined suspension along BEKP defibrillation by ultra-refining in a SuperMassColloider.

Spence et al., (2011) determined the specific surface area by Congo red dye and Langmuir isotherms before and after defibrillation of pretreated bleached hardwood pulp in a Valley Beater into CNFs using high-pressure systems (microfluidizer and homogenizer) and ultra-refining (SuperMassColloider). The authors observed that the SuperMassColloider boosted the surface area approximately 55%, whereas with the high-pressure systems, the increase was 30% and 60% for the microfluidizer and homogenizer, respectively. These results and the results reported here indicate that ultra-refining in the SuperMassColloider is a remarkably efficient method compared to high-pressure systems to increase the surface area of cellulose particles without any clogging issues and with the potential for scaling up.

2.4.4. VISCOSITY

Cellulose fiber defibrillation is known to change the rheological properties of the aqueous suspension from low- to high-viscosity (Iwamoto et al., 2005; Qing et al., 2013). This change in viscosity is partially due to the increase in specific surface area, aspect ratio and in the availability of surface hydroxyl groups that influence the particle interactions and crosslink between the nanofibrils in suspension (Besbes et al., 2011). Therefore, the rheological properties of an aqueous suspension of defibrillated cellulose are also dependent on the defibrillation method (Moberg et al., 2017).

In order to better understand the changes in the rheological behavior of the aqueous BEKP suspension during ultra-refining, the flow property was monitored in terms of the apparent viscosity as determined by a Brookfield viscometer (at 130/1.s^{-1} of shear rate). The rheological assay using the digital viscometer is an extremely simple, accurate and sensitive method that allows rapid rheological characterization of colloidal suspensions, especially of materials produced by high shear force. However, there are various parameters that can influence the rheological response, such as, solid content, temperature, surface charge and particle size (Nechyporchuk et al., 2015). The viscosity relates the particle interactions with each other, and considering the biomass fibers, this interaction can result in a tangled and complex network (Viamajala et al., 2009). Another important aspect relative to this analysis is the interactions of hydroxyl groups on the surface of the fiber with the aqueous solution.

Taking into consideration that BEKP defibrillation by ultra-refining increased the surface area (Fig. 2.5) and aspect ratio and reduced the diameter of the fibers (Fig. 2.4 and Table 2.1), higher interactions among the particles in the ultra-refined BEKP suspension and consequently higher viscosity were expected. In fact, the apparent viscosity of the BEKP suspension increasedas the degree of ultra-refining increased (Fig. 2.6). At the beginning of the process (energy consumption of 2 kWh/kg), the apparent viscosity was 5.6 cP. Up to an energy consumption of 12 kWh/kg, the viscosity of the ultra-refined BEKP suspension (MFC) increased to 10.3 cP; that is, it increased at a rate of approximately 2.12 cP/kWh/kg. Further ultra-refining the MFC suspension to the CNF suspension increased the viscosity to 24 cP at energy consumption of 20 kWh/kg at a high rate of increase equal to 5.7 cP/kWh/kg. However, continued ultra-refining of the CNF suspension with an average diameter equal to 20 nm to CNF suspensions with smaller diameters was associated with a lower rate of viscosity increase. For example, when defibrillating the CNF obtained at 20 kWh/kg to CNF obtained at an energy consumption of 25 and then to 30 kWh/kg, the viscosity increased at a rate of approximately 0.3 and 0.5 cP/kWh/kg, respectively. However, increasing the ultra-refining from an energy consumption of 25 to 30 kWh/kg, the viscosity of the CNF suspension only slightly increased but this increase in viscosity with the additional ultra-refining was reached at a very low rate.

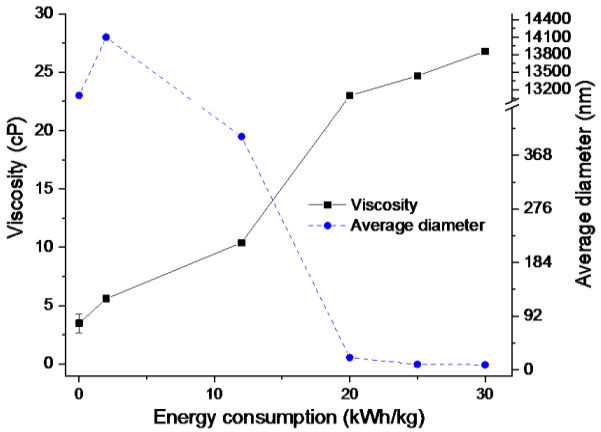

Fig. 2.6. Changes in the apparent viscosity (cP) and average particle diameter as a function of the energy consumption (kWh/kg) of the ultra-refined suspensions produced along BEKP defibrillation in a SuperMassColloider.

2.4.5. CRYSTALLINITY

The crystallinity index (CI) corresponds to the percent of cellulose which is organized in crystalline domains (Park et al., 2010). It has been reported to directly impact the mechanical, physical and chemical properties of cellulose. For example, Iwamoto et al. (2007) found that the use of nanocelluloses with higher CIs resulted in a nanocomposite with lower thermal expansion and higher modulus. On the other hand, they also reported that the use of nanocelluloses with lower CIs resulted in nanocomposites with higher thermal expansion. However, the alignment of amorphous cellulose can be improved by electrospinning, which can lead to improved cellulose mechanical properties (Magalhaes et al., 2009).

The XRD pattern of BEKP and ultra-refined BEKP suspensions were consistent with that of cellulose I (data not shown). The CI of the unprocessed BEKP was 72%, and a low degree of refining (energy consumption of 2 kWh/kg) was already enough to promote a smooth drop of the CI to approximately 65% (Fig. 2.7A). As the degree of defibrillation increased (energy consumption of 12 kWh/kg), yielding MFC, the CI further dropped to approximately 46% (CI reduction approximately 30%). With increasing defibrillation to yield CNFs (energy consumption up to 30 kWh/kg), the CI did not change significantly, despite the higher degree of refining. Therefore, the most intense drop in crystallinity occurred at the beginning of ultra-refining (12 kWh/kg), reaching a 50% reduction in CI. Several authors have proposed different methodologies for the determination of the CI and for this reason this is not yet a standard methodology to calculate the IC of the cellulose (French, 2014; Segal et al., 1959). In addition to the divergences of calculations, different materials and treatments used to isolate the cellulose result in fibers with different chemical compositions. However, it

is possible to estimate and correlate the behavior of the CI throughout the defibrillation process based on relative percentages.

Considering the relative values of IC, ssimilarly, Iwamoto et al. (2007) observed an approximately 20% drop in CI during ultra-refining of conifer dissolving pulp to CNF in a SuperMassColloider after only one cycle. Qing et al.(2013) also reported a drop (15%) in CI after BEKP was ultra-refined in a SuperMassColloider for 6 hours. Wang et al. (2012) observed a drastic drop in crystallinity at the beginning of ultra-refining (approximately 20%), followed by a smooth reduction to the end of the process, reaching a reduction in CI of 35%. Tonoli et al. (2012) suggested that the decrease in the CI observed for BEKP after ultra-refining was a result of the damage that the crystallites underwent during defibrillation. In addition, Kim et al. (2010) reported that the crystallite sizes of cellulose affect the thermal decomposition of cellulose, after observing that with increasing crystalline sizes, the thermal decomposition temperature of cellulose increased, despite not affecting the activation energy of the thermal degradation.

Therefore, in this study, the XRD diffractograms were also used to estimate the crystallite size of cellulose using the Scherrer equation for BEKP before and after ultra-refining (Fig. 2.7B). At a low degree of defibrillation (ultra-refining at an energy consumption of 2 kWh/kg), the crystallite size (5.3 nm) remained partially that of the unrefined BEKP (4.9 nm). Increasing defibrillation to an energy consumption of 12 kWh/kg to yield MFC decreased the crystallite size to approximately 4 nm (approximately 24% reduction). Further increasing the degree of defibrillation to yield CNFs (energy consumptions of 20, 25 and 30 kWh/kg) did not statistically (p-value > 0.5) alter the crystallite size.

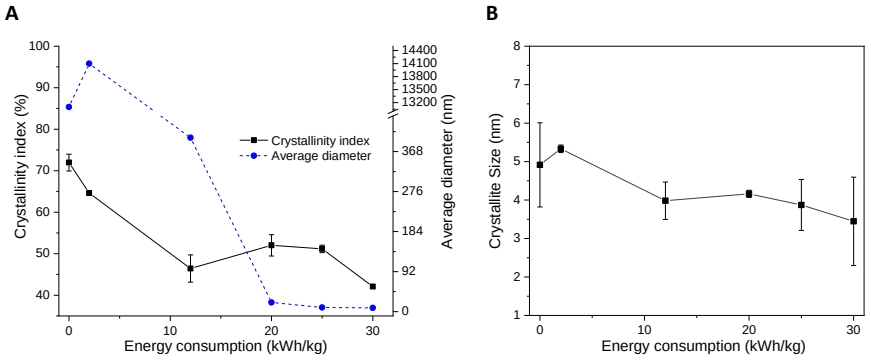

Fig. 2.7. (A) Changes in the crystallinity index (CI) and average diameter and (B) changes in the crystallite size (nm) as a function of the energy consumption (kWh/kg) of the ultra-refined suspensions obtained during BEKP defibrillation by ultra-refining in a SuperMassColloider.

2.4.6. THERMAL STABILITY

The structure and properties of cellulose are known to be influenced by temperature, and therefore the thermal properties of cellulose are another important characteristic of cellulosic materials. They are crucial, for example, for the manufacture of composites, when high temperature is required for processing (i.e., temperatures higher than 200 °C for thermoplastic polymers). It is noteworthy that one large-volume application of defibrillated cellulose is in the production of plastic composites for the automobile, packaging, aerospace and construction industries (Hubbe et al., 2017; Kalia et al., 2014; Spence et al., 2010b). Therefore, the thermal properties of BEKP during ultra-refining were investigated by monitoring the thermal stability, an essential parameter to determine the temperature range of processing and use of materials.

The typical pattern for the thermal degradation of cellulose shows three distinct degradation phases, which were also observed for BEKP (Fig. 2.8A). The first phase (between 50 °C and 105 °C) was characterized by a small initial mass loss, which has been reported to correspond to absorbed water and residual moisture (Dufresne, 2012). The second stage, between 200 and 380 °C, was characterized by an expressive mass loss, corresponding to the loss of mass of cellulosic and non-cellulosic compounds. Raising the temperature to above 400 °C resulted in only a small mass loss, characteristic of the third phase when the volatilization of the components is complete and any additional mass loss is related to the degradation of the residual coal (Dufresne, 2012).

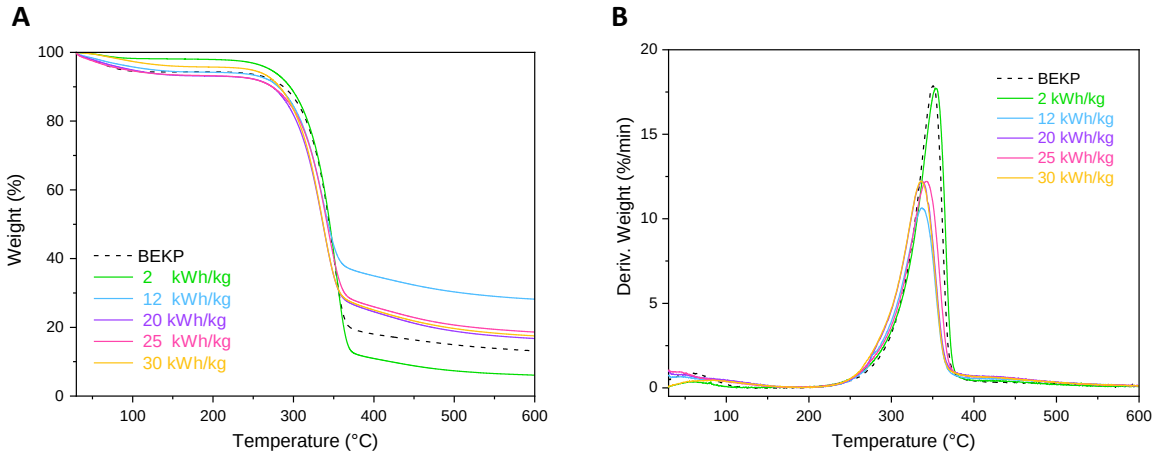

Fig. 2.8. Thermogravimetric (TG) (A) and derivative TG (DTG) (B) curves of BEKP and ultra-refined BEKP during defibrillation by ultra-refining in a SuperMassColloider at different energy consumption levels.

There have been some reports that the thermal stability of cellulose can be related to the CI. It has been shown that higher CIs shift to higher thermal stability (Kim et al., 2010; Peng and Gardner, 2013); this pattern can be seen in Figure 8. At a low degree of fibrillation (energy consumption equal to 2 kWh/kg), the initial degradation temperature (T_{onset}) was approximately 280 °C and the CI was close to 64% (Fig. 2.7A), very similar to unrefined BEKP (T_{onset} equal to 285 °C and CI 70%). The increase in defibrillation to obtain MFC (energy consumption of 12 kWh/kg), a material with lower CI (44%), was accompanied by a reduction in T_{onset} to 272 °C. The further increase in the degree of fibrillation to obtain CNFs (energy consumption equal to 20, 25 and 30 kWh/kg), did not much alter the T_{onset} values (Fig. 8A). This finding was expected since the CI values only marginally changed for this energy consumption range (Fig. 2.7). Nevertheless, although a relation was observed between CI and thermal stability, it was not proportional. For example, with BEKP defibrillation at an energy consumption equal to 30 kWh/kg, the T_{onset} was equal to 268 °C, representing only a 6% decrease in relation to the starting material (unrefined BEKP), whereas the CI showed a 41.6% decrease compared to unrefined BEKP (Fig. 2.7).

In addition to the CI, it is also expected that the thermal stability could be related to the morphological aspect of the particles (particle size and surface area), because the larger the particle size reduction, the greater the surface area exposed to heat. Indeed, simultaneous with the significant increase in the SSA and significant reduction in the mean diameter observed at an energy consumption of 12 kWh/kg to obtain MFC, a reduction in the temperature at the beginning of the inflection (Tp) was also observed (Fig. 2.8B). As can be observed in the degradation temperature derivative graph (DTG), the peak detachment corresponds to the onset of the TG curve inflection (Fig. 2.8B). The Tp of BEKP (mean diameter 13 µm) was near 353 °C, whereas for the MFC (mean diameter 400 nm) the Tp was lowered to 337 °C. With further ultra-refining, the diameter was reduced, resulting in CNFs with diameters in the range of 20 - 8.5 nm, but this slight reduction in diameter and increase in SSA (Fig. 2.6) did not cause changes in the Tp, which varied between 337 and 340 °C for the CNFs, therefore similar to Tp of the MFC. Thus, the kinetic analysis of the thermal behavior of the MFC and CNFs obtained during BEKP ultra-refining showed only small changes between BEKP defibrillated at different degrees and the initial material (unrefined BEKP), preserving the high thermal stability of the cellulosic material.

2.4.7. FILM OPTICAL PROPERTIES

The optical characteristic of cellulose is another property that is altered during defibrillation. When properly dewatered, defibrillated cellulose suspensions can result in translucent or transparent papers or films, depending on the degree of defibrillation. At a high degree of defibrillation, cellulose fibers can reach sizes (diameters) much smaller than the wavelength of visible light, remarkably reducing the light scattering effect. These highly defibrillated fibers can lead to transparent paper and films, unlike common paper made of cellulose fibers with an average diameter of approximately 2.5 μm that induces light scattering and results in an opaque material (Zhu et al., 2013). The optical properties enhanced with decreasing diameter and packaging density are advantageous for several emerging applications in optoelectronics such as displays, touch screens and interactive papers, as well as in solar cells (Hu et al., 2013; Zhu et al., 2013). Here, the change in optical properties of the defibrillated BEKP suspensions obtained during the ultra-refining process was monitored by comparative visual inspection and transmittance of the films made from unrefined BEKP and ultra-refined BEKP suspensions.

The improvement in transparency and the loss of opacity with increasing BEKP defibrillation can be clearly observed in Fig. 2.9A. As expected, the film made of the unrefined BEKP suspension was opaque, whereas a substantial decrease in opacity and consequent increase in transparency was seen for the film made with the BEKP suspension ultra-refined at low energy consumption (2 kWh/kg, low degree of defibrillation). With increased ultra-refining, the BEKP suspensions resulted in films with very high transparency, as can be seen for the films produced from the MFC suspension (energy consumption of 12 kWh/kg, average diameter equal to 400 nm) and the film from the CNF suspension obtained at 20 kWh/kg (average diameter equal to 21 nm). Extending defibrillation to energy consumptions of 25 and 30 kWh/kg, the average diameter reduced to 9.4 and 8.6 nm (Table 2.1), respectively, and the films became even more transparent. However, the biggest improvement in optical properties seems to have occurred at the beginning of the ultra-refining process (low degree of defibrillation), in agreement with Iwamoto et al. (2007), who observed an increase in transmittance of the acrylic composites with the defibrillated material of approximately 35%. In this context, the increase in transmittance of the films made with the defibrillated BEKP suspensions were enhanced up to 66%, from an energy consumption of 2 kWh/kg to 12 kWh/kg (MFC) (Fig. 2.9B), likely due to the decrease in diameter with a higher degree of defibrillation. Kangas et al. (2014) reported a similar increase in transmittance of CNF films at 800 nm with a smaller particle size.

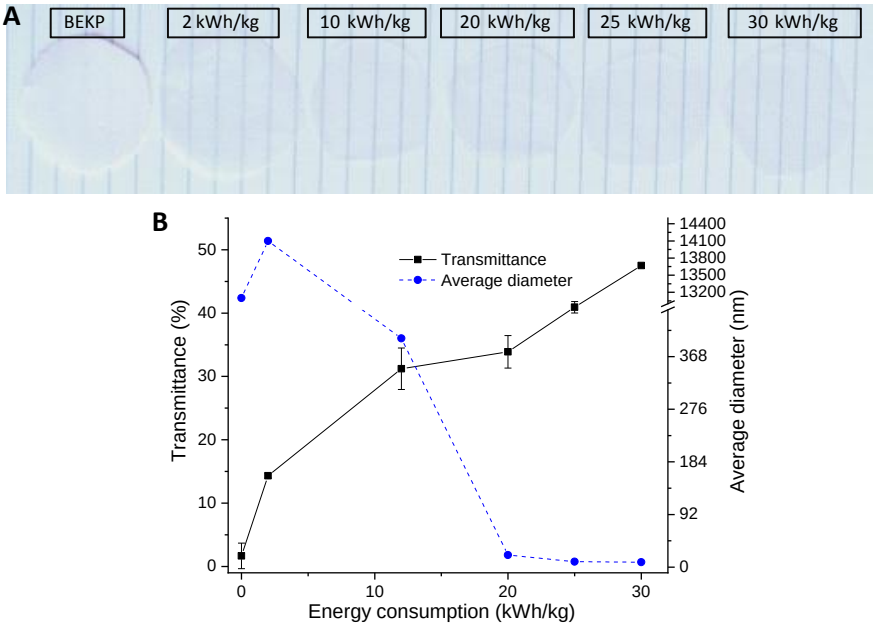

Fig. 2.9. Films made from BEKP and defibrillated BEKP suspensions at the same volume and solid concentration (B) regular transmittance at 600 nm of the films obtained during BEKP defibrillation by ultra-refining in a SuperMassColloider at different energy consumptions (kWh/kg).

2.4.8. COMPROMISE IN CELLULOSE FIBER DEFIBRILLATION

During the process of BEKP ultra-refining, defibrillated cellulose with different characteristics and properties was produced. At the beginning of the process (energy consumption at 2 kWh/kg) the degree of defibrillation was low and most properties were preserved in relation to the starting material (Fig. 2.10). At energy consumption equal to 12 kWh/kg, more intensive changes were observed, including loss, gain or enhancement of the properties. This degree of defibrillation yielded a cellulose suspension that was classified as CMF with a mean diameter equal to 400 nm. This large decrease in diameter reflected the high enhancement of the optical property and the gain in viscosity (corroborating with the higher degree of defibrillation). On the other hand, these beneficial effects were accompanied by a decrease in crystallinity and crystallite size. However, these reductions did not seem to have compromised the MCF thermal stability when compared to the initial material.

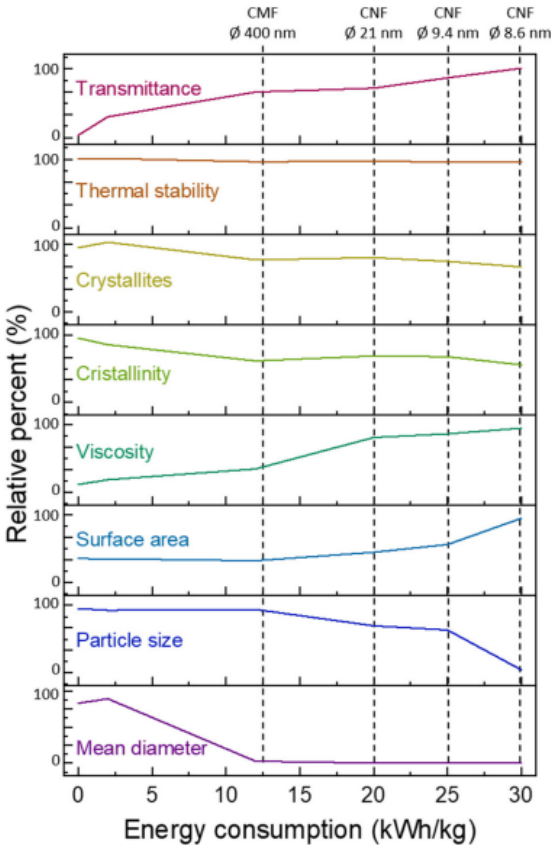

Fig. 2.10. Representative scheme of all characterized properties during ultra-refining. The Y axis is on the same scale for all properties (ranging from -20 to 120), representing the relative percent of change in property.

Setting the mechanical process to an energy consumption of 20 kWh/kg, it was obtained a defibrillated cellulose suspension that had characteristics of CNF, with an average diameter of 20 nm and a more homogeneous particle size. This higher degree of defibrillation also led to more intensive gain in viscosity and specific surface area (SSA) and enhancement of optical properties. However, this CNF did not show further decrease crystallinity, and thermal stability properties remained essentially unaltered compared with the MCF properties. Prolonging the ultra-refining of the CNF suspension by applying higher energy consumptions (25 and 30 kWh/kg) to reach higher defibrillation degrees led to a larger reduction in the average diameter (mean diameter of approximately 8.5 nm) and only marginal change in CNF properties. The values of the thermal stability, crystallite size and crystallinity remained almost the same, indicating that higher changes in these properties only occurred at the beginning of ultra-refining process. Although the viscosity and the specific surface area showed continuous enhancement along the entire process, while the optical property underwent a progressive gain. The reduction in the mean diameter of cellulose fibers mainly

compromised viscosity, specific surface area, suspension homogeneity and optical properties, but did not reflect the thermal stability and degradation of the crystallinity regions. This deeper and detailed knowledge of the changes in properties during the ultra-refining process allows for more precisely designing suitable defibrillated cellulose for specific applications with the desired characteristics.

2.5. CONCLUSION

Defibrillation of BEKP using the disc ultra-refiner SuperMassColloider was suitable for isolating MFC and CNF. The detailed kinetic study of the changes in the properties of cellulosic fibers (crystallinity, thermal stability, viscosity, surface area, optical and morphological aspects) led to understanding the effect of ultra-refining in the characteristics of the micro- and nanofibrils. The most intense enhancement in properties occurred at the beginning of the process, when 12 kWh/kg resulted in a defibrillated cellulose suspension with characteristics of MFC. Defibrillation up to MFC resulted in excellent gain in viscosity, optical property and surface area, and in loss of crystallinity and slight loss of thermal stability, while the diameter was drastically reduced (400 nm). Further ultra-refining with increased energy consumption resulted in more homogenous CNF suspensions with different diameters. Although a continuous enhancement and gain in properties was observed, the rate slightly increased during CNFs production. Detailed kinetics of the ultra-refining of cellulose fiber into microfibrils and nanofibrils in terms of properties and characteristic changes as a function of energy consumption demonstrated compromising between the degree of defibrillation and the gain, enhancement or loss of properties. A suitable degree of defibrillation is desirable for specific applications, and the kinetic study of the ultra-refining process allows one to minimize the input energy.

CHAPTER 3 – SYSTEMATIC INVESTIGATION OF NANOFIBRILS ISOLATION BY A SINGLE-STEP TREATMENT: TAILORING AND RATIONALIZATION OF THE ENZYMATIC PROCESS

3.1 ABSTRACT

The combination of a multi-step enzymatic pretreatment and mechanical defibrillation has been demonstrated as a green and low-energy consumption route to defibrillate cellulose fibers into cellulose nanofibrils (CNF). However, there is a high variability in process parameters, as well as a lack of understanding of their role in the defibrillation and in the properties of the CNF. Herein, a monocomponent endoglucanase (EG) was utilized to investigate the effect of the enzymatic processing conditions on the energy consumption and on the physical properties of CNFs and their colloidal suspensions. Compared to untreated CNF, varying the reaction time (1-3h) and enzyme loading (0.5-25 EGU/g pulp), the single-step enzymatic pretreatment reduced up to 50% the energy consumption, not affecting the crystallinity, crystal size and particle size and resulting in CNF with nearly 100% yield. While harsher conditions required the lowest energy consumption but drastically reduced the rheological properties, milder conditions did not show any energy reduction. 5.6 EUG/g for 1 h was found to preserve the rheological properties and reduce the energy input by approximately 25%. This condition did not release soluble products, slightly reduced the molecular weight and swelled the fiber. The carbohydrate binding module seems to improve the interaction of the catalytic core with the substrate, boosting the enzyme effect even at small quantity.

Keywords: single-step pretreatment; energy reduction; enzyme-substrate interaction; endoglucanases.

3.2 INTRODUCTION

Mechanical defibrillation is a widespread, sustainable method to isolate cellulose nanofibrils (CNF) from cellulosic biomasses. Either high-pressure systems (i.e., homogenizer or microfluidizer) or disc ultra-refiner are capable of reaching industrial scales, being paramount in the rising of new advanced materials from nanocelluloses (Assis et al., 2018; Nechyporchuk et al., 2016; Spence et al., 2011). Typically, pretreatments are required to allow the fluidity of the cellulose slurry through the micro channels and chambers in a microfluidizer or homogenizer device. This is key to avoid clogging of the machinery that often results in inefficiencies on the processing, especially those related to the energy consumption (Henriksson et al., 2007; Isogai et al., 2011; Moreau et al., 2019).

The most used pretreatment involves the oxidation of cellulose pulp using 2,2,6,6-TetraMethylPiperidine-1-Oxyl (TEMPO) (Saito and Isogai, 2004). Although TEMPO-oxidized CNF display smaller sizes and better colloidal stability, it presents reduced degree of polymerization and lower crystallinity, which perhaps may lead to lower rigidity of the fibers (Patiño-Masó et al., 2019; Reyes et al., 2020; Wakabayashi et al., 2020). Most importantly, TEMPO-oxidized CNF are not biodegradable by the typical cellulase routes, thus losing one of the most appealing characteristics of cellulose (Isogai et al., 2011). Chemical pretreatments, however, are not required when defibrillating wood pulp into CNF via disc ultra-refiner. Easier pulp processability in ultra-refiners has intensified the production of CNF industrially due to practical, economical and environmental benefits . However, it has been reported that pretreatments of the starting material can improve the nanofiber production efficiency, aiding to largely reduce the input energy, which is still one of the bottle necks of CNF production (Nechyporchuk et al., 2016). Enzymatic pretreatments have been proposed as more sustainable and greener alternatives to the chemical counterparts. Several enzymes, e.g. endoglucanases, xylanases, lytic polysaccharide monooxygenase or enzymatic cocktails, have been proposed to facilitate the defibrillation of pulp into CNF (Hu et al., 2018; Moreau et al., 2019; Wang et al., 2015; Yarbrough et al., 2017). Among the variety of enzymes used so far, cellulose-hydrolyzing enzymes (e.g. monocomponent endoglucanase, EG) have been explored more widely due to their effectiveness in defibrillating but also because their relative lower cost, commercial availability (e.g. FiberCare or Novozym 476) and biosafety, both when considering the enzyme nature or their released products (Campos et al., 2013; Henriksson et al., 2007; Nechyporchuk et al., 2015; Pääkko et al., 2007; Q; Tarrés et al., 2016; Zhu et al., 2012). The effectiveness of EG comes from their mechanism of action on the cellulose fibers. EG acts preferentially on the less ordered regions of the cellulose fibers, randomly breaking

accessible glycosidic bonds, introducing new reducing and non-reducing ends and thus promoting a fast decrease of the degree of polymerization (DP). Because of its features, EG has the potential to promote specific modifications, which in turn can aid in the fiber defibrillation process without compromising the crystalline regions, consequently, preserving the mechanical properties. The high mechanical performance of nanocellulose building blocks is a major factor driving their wide utilization in materials development, as the cohesion of the cellulosic constructs tends to mirror the one at molecular level (Kontturi et al., 2018).

Enzymatic pretreatments of cellulosic biomasses with monocomponent EG are undoubtedly beneficial for the production of CNFs. However, the processing conditions differ greatly among the relevant literature, having no agreement in regard to the extension of reaction time which varies from a few minutes to days (from 0.5 to 72 h), and the enzyme loading that spans across three orders of magnitude (from 0.85 to 351 EGU/g fiber) (Henriksson et al., 2007; Nechyporchuk et al., 2015; Q; Tarrés et al., 2016). Additionally to such wide ranges, there is also no consensus on the final properties of the pretreated fibers and consequently to the resulting nanofibers. For instance, a considerably mild enzymatic treatment (0.85 or 1 EGU/g – 2 h) led to 24% reduction in the degree of polymerization (DP), while in another study a much harsher treatment (150 or 185 EGU/g – 2h) was used to obtain 55% of DP reduction but the enzymatic treatment had to be combined with additional mechanical refining (Henriksson et al., 2007; Pääkko et al., 2007). In an intermediary condition (25 EGU/g – 2h), the DP was also reduced by 50%, however this condition resulted in a smoother mechanical defibrillation (Henriksson et al., 2007; Nechyporchuk et al., 2015; Wang et al., 2015). Furthermore, pretreatments have been used as a standing alone process or combined with mechanical processes prior to the final defibrillation. Such disparities, lack of consensus on the reported results and a still not defined processing strategies are still major challenges to be addressed until CNF can be widely produced and used in commercial products.

Therefore, in this work we have systematically investigated the effects of the processing parameters of a single-step enzymatic pre-treatment on the properties of CNF isolated by disc ultra-refining in a SuperMassColloider. Here it was thoroughly discussed the effects of the enzyme loading and reaction time, as well as their synergistic combinations, on the energy required for the mechanical defibrillation as well as the resulting properties of the nanofibers, such as viscosity, crystallinity, molecular weight and particle size. It was unveiled the compromise threshold between enzyme treatment, energy demand and CNF properties, which allowed the optimization of this step to obtain high-quality CNF without compromising

its key properties with about 25% reduction in the energy required at nearly maximum theoretical yield. It was possible to save the largest amount of energy (50%) under the harshest condition; however, the properties of CNF were compromise. At the mildest condition, the properties were preserved but no energy reduction was observed. Furthermore, it was investigated the mechanism of action of the EG by monitoring in real-time its adsorption on model cellulosic surfaces and the release of products from the hydrolysis. It was showed that defibrillation is assisted by decrease in the molecular weight of the fibers caused by the enzyme, which induces swelling of the fiber at larger extent thus decreases the strong interfibril interactions.

3.3 MATERIALS AND METHODS

3.3.1 CELLULOSIC PULP AND ENZYMES

The bleached eucalyptus kraft pulp (BEKP) utilized was the same as the one described in chapter 2. The monocomponent endoglucanase enzyme (FiberCare® Lot CGK20074) was kindly provided by Novozymes (Araucária, Brazil) and without further purification.

3.3.2 DETERMINATION OF ENZYMATIC ACTIVITY

The enzymatic activity of EG was determined using carboxymethyl cellulose (CMC) as substrate at 0.44% wt (medium viscosity) dissolved in buffer phosphate-citrate (50 mM pH 6.0). The activity of the enzyme was measured using dinitrosalicylic acid by a photometric procedure (Miller, 1959). The EG activity unit (EGU) was determined as one µmol of glucose released per minute per mL of the enzyme.

3.3.3 DESIGN OF EXPERIMENTS

In order to fully understand the individual and combined effect of reaction time and enzyme loading on the pretreatment of BEKP for isolation of CNF, a 2^2 full factorial design with triplicate at the central point was employed (Table 3.1). The highest enzyme loading was fixed at 25 EGU/g, the minimum at 0.5 EGU/g and central point at 12.5 EGU/g. The longest reaction time was fixed at 3 h, the shortest at 1 h and the central point was 2 h. These values were chosen based on common values reported in recent literature. Statistical analyses (ANOVA and regression analyses) were carried out using the statistical software Minitab® 18.1 (Minitab Inc. State College, PA, USA) and the index of significance was 95% (p-value < 0.05). Two different scenarios were determined with the Response Optimizer tool in

Minitab® 18.1 (Minitab Inc. State College, PA, USA). In Scenario #1, the target was to minimize the energy consumption and in Scenario #2, the target was set to minimize energy reduction and maximize the properties of CNF.

3.3.4 ENZYMATIC PRETREATMENT

All single-step enzymatic pretreatments conditions were conducted at 50 °C and 5% (w/w) solids loading (on a dry weight basis) in 50 mM phosphate-citrate buffer (pH 6.0). The reaction volume (250 mL) was conditioned in 2 L Erlenmeyer flasks and kept in an orbital shaker (Thermoscientific) at a constant shaking speed (250 rpm). At the end of the pretreatment, the reaction was boiled in water for 30 min to inactive the enzyme. Then, the fiber suspension was vacuum-filtrated, using miracloth membrane, with excess of distilled water to remove the enzymes. The liquid fraction was collected for quantification of soluble sugars, hydrolysis and solid yields (Fig. 3.1).

3.3.5 SOLID YIELD OF ENZYMATIC PRETREATMENT

The liquid fraction collected after the enzymatic pretreatment was utilized for determination of the solubilized sugars and, therefore, the hydrolysis and solid yield. First, the liquid fraction was centrifuged (13,000 *g* for 5 min), filtrated through a 0.45 µm mesh and subjected to a mild acid hydrolysis (4% H_2SO_4) to hydrolyze any released oligomer to monomeric sugars (Sluiter et al., 2012). The monomeric sugars were then quantified by high performance liquid chromatography (HPLC, Waters), equipped with a HPX87H column (Bio-Rad Laboratories) at 45 °C, eluted at a rate of 0.6 mL/min with 5 mM H_2SO_4, and using a temperature controlled refractive index detector at 35 °C.

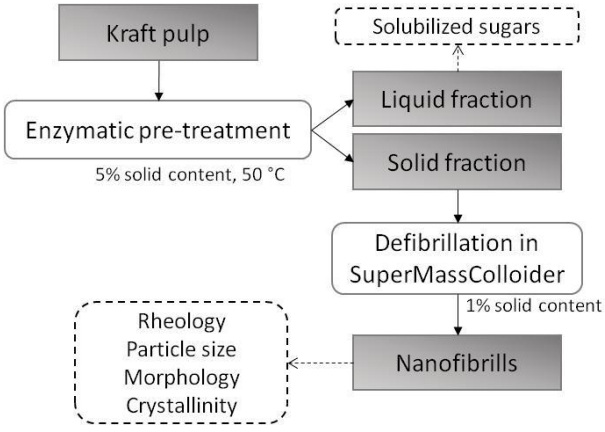

Fig. 3.1. Schematic flow chart of the pulp pre-treatment with enzymes followed by the mechanical isolation of cellulose nanofibrils.

3.3.6 MECHANICAL DEFIBRILLATION BY DISC ULTRA-REFINER

For the isolation of CNF, the enzymatically-pretreated pulps were diluted to 1% (w/w) using distillated water to be further defibrillated in a disc ultra-refiner SuperMassColloider (Masuko, model MKCA6-5J, discs model MKGA10-80) (Fig. 3.1). The distance between the grinding discs was fixed at amplitude of -100 μm and the rotation at 1,600 rpm (Berto and Arantes, 2019). The SuperMassColloider was connected to a digital energy monitor (ForLong DRT-341D), reporting the energy consumption in kWh. Simultaneously, after each grinding cycle, 1 mL aliquot was collected and rapidly analyzed in a particle size analyzer to determine the apparent wet surface area of the fibrillated fibers. A suspension of untreated BEKP was also defibrillated under the same mechanical conditions as a control.

3.3.7 CHARACTERIZATION OF THE CNF

3.3.7.1 PARTICLE SIZE AND SPECIFIC SURFACE AREA (SSA)

The apparent particle size and the wet specific surface area of the nanofibrils were determined by low angle laser light scattering (LALLS), using the laser diffraction particle size analyzer Mastersizer 3000 (Malvern Instruments) as described in Berto and Arantes, 2019. The particle size number is related to the hydrodynamic diameter value of the equivalent particle, calculated automatically, a technique used to measure spherical monodispersed particle. Although the reported value cannot be assumed as absolute value for nanofibrils measurements, it can be taken as a reference value to infer the degree of defibrillation.

3.3.7.2 VISCOSITY AND SHEAR STRESS

The viscosity and shear stress of the CNF suspensions were determined in an automatic viscometer (Brookfield LVDV2T Pro digital). The spindle SCA-18 was coupled to the viscometer, the rotation set at 100 rpm and the temperature fixed at 25 °C using a water bath. The suspensions were prepared with a solids content of 0.25% (w/w) in distilled water. Each analysis was conducted for 5 minutes, with measurements every 30 seconds and the results are reported as the average of 10 measurements.

The rheology of the CNF suspensions – isolated at the optimized condition – was evaluated using an MCR 302 rheometer (Anton Paar, Austria), equipped with a parallel flat plate geometry and smooth bottom plate at controlled temperature of 23 °C. For the shear sweep it was applied a shear rate of 0.01 – 1000 s^{-1} at angular frequencies ranging from 100 to 0.01 rad/s with a strain amplitude of 0.1% (within the linear viscoelastic region). For each

assay, triplicate measurements were conducted for each sample (validation 1 and 2), repeated separately, and the samples were changed for each collecting data.

3.3.7.3 CRYSTALLINITY INDEX

For X-ray diffraction analyses, samples were dried in an air circulation oven at 33 °C for 24 hours. The measurements were performed in an X-ray diffractometer (XRD - 6000, Shimadzu) at room temperature, with CuKα radiation and a graphite monochromator (reflection mode analysis), and the conditions were $10 < 2\theta < 40$; 2θ step: 0.02°, 30 s per step, taken in duplicate. The XRD peaks were mathematically deconvoluted using a Gaussian function in the Origin software (version 2017, OriginLab). The CI of the CNFs was determined according to Segal et al., 1959.

3.3.7.4 MORPHOLOGY EVALUATION

Negative contrast scanning electronic microscopy (Neg-SEM) images were obtained following the methodology described by Mattos et al. (2019). Briefly, for sample preparation, freshly cleaved mica discs were spin-coated with 4 nm of iridium, dipped in a polyethylenimine (PEI) solution (0.33% w/v), washed with MilliQ water, dipped in the CNF suspension (0.001% w/v) and let to dry at room temperature. The images were acquired in a field emission gun electron microscope (FEG-SEM) Zeiss Sigma VP (Germany) using the *in-lens* detector, acceleration voltage at 1.5 kV and working distance of 6 mm. The diameter of at least 20 fibers were measured using the software ImageJ.

3.3.7.5 THERMAL STABILITY

Thermogravimetric profiles of CNF obtained with and without enzymatic pretreatment were acquired in order to investigate possible structural modifications in the cellulosic matrix. Thermal stability analyses were performed in the thermal analyzer TGA-TA Instrument DST-Q500 in an inert atmosphere (N_2, flow rate 60 ml/min), with a heating rate of 10 °C/min and a temperature range of 30 - 600 °C. The samples were freeze-dried and approximately 5-8 mg was weighted in platinum pan.

3.3.8 EVALUATION OF THE EG MECHANISM OF ACTION

Optimal enzymatic processing conditions, as far as rheological properties and energy input, were used (Scenario #2): 50 °C, phosphate-citrate 50mM buffer pH 6.0, enzyme loading 5.6 EGU/g for 1 h) to investigate the effect of EG.

3.3.8.1 GEL CHROMATOGRAPHY PERMEATION

The typical behavior of depolymerization that EGs promote on cellulose chain was investigated by gel chromatography permeation (GPC), using pullulan as standard as described in Potthast et al., 2002. Briefly, a known mass of cellulosic pulp (500 mg) EG-pretreated with and the control sample were dissolved in LiCl/DMAc (lithium chloride/N,N-dimethylacetamide) at a given final of sample concentration of 1.0 mg/mL. The samples were prepared in duplicate and each was run twice using LiCl/DMAc as eluent solution.

3.3.8.2 WATER RETENTION VALUE

The water uptake caused by the extent fiber swelling by the EG was evaluated following a gravimetric methodology (Witono et al., 2014). A known mass (approximately 0.2 g) of the enzymatically pretreated pulp and control was soaked in an adequate amount of distilled water to fully immerse the sample for at least 1 h (at room temperature). Afterward, the samples were drained using nylon membrane and the masses were measured. The difference of initial and the final mass was assumed to be the remaining water, which interacted with the cellulose fibers. The measurements were conducted in duplicate.

3.3.8.3 EG– CELLULOSE INTERACTION DETERMINED BY QUARTZ CRYSTAL MICROBALANCE WITH DISSIPATION (QCM-D)

The interaction of the EG monocomponent with the cellulosic substrate was investigated using a quartz crystal microbalance (QCM) with dissipation monitoring (D-sense D-300). The frequency and dissipation data were collect using the 5^{th} overtone; however, the 3^{rd}, 5^{th}, 7^{th} and 11^{th} overtones were observed during the operation. The QCM-D gold crystals were treated with UV/ozone for 20 min and dipped in a PEI solution (0.4 mg/mL) before being covered by spin coating with a thin layer of mechanical fibrillated CNF (0.008 wt%). The crystals were placed in buffer to swell overnight and dried with nitrogen before being used. The crystals were placed in the cells and the buffer solution started being pumped at a continuous flow rate of 40 µL/min until the baseline reached the equilibrium. Afterwards, the enzyme solution was continuous pumped at the same flow rate for 60 min or until the baseline reached the equilibrium. Finally, the solution was switched back to buffer to wash the enzymes out of system.

3.4 RESULTS AND DISCUSSION

3.4.1 EFECT OF THE EG PRETREATMENT ON THE CNF PROPERTIES

The range of the processing parameters (enzyme loading and reaction time) was selected based on a collection of reported values based on the reported energy saving and on a comprehensive analysis of the reported results of the CNF properties obtained using these broad range of conditions. The conditions were limited to the enzyme loading of 25 EGU/g pulp and reaction time to 3 h, mainly because conditions over such thresholds are too detrimental to the CNF properties (Campos et al., 2013; Henriksson et al., 2007; Nechyporchuk et al., 2015; Pääkko et al., 2007; Tarrés et al., 2016; Zhu et al., 2012).

Fibers treated solely with EG at given times and loads were mechanically defibrillated in a SuperMassColloider (Fig. 3.1). The wet specific surface area (SSA) of the fiber suspensions were monitored in real time, obtained by laser diffraction using a particle analyzer. The defibrillation process was stopped when the SSA value reached ca. 200 m^2/kg (Table 3.1). Such value was used as an internal measurement of the defibrillation process for BEKP, as it corresponds to CNFs with ca. 20 nm of diameter, as previously determined by atomic force microscopy (Berto and Arantes, 2019). Although the wet method to determine SSA can be used anecdotally to monitor the defibrillation process in real-time, it cannot be assumed as an absolute surface area value as the method accounts for a hydrodynamic diameter of an equivalent spherical particle therefore underestimating significantly the real surface area of the material.

Table 3.1. Full factorial experimental design matrix with repetitions at the central point for the enzymatic pre-treatment of BEKP and the responses associated with the physicochemical properties of the obtained CNF suspensions, energy input and solubilized glucose.

Std. order	Variables		Responses						
	Enzyme loading (EGU/g)	Reaction time (h)	SSA* (m^2/kg)	Glucose released (%)	CI** (%)	Particle size (µm)	Viscosity (cP)	Shear stress (Pa)	Input energy (kWh/kg)
1	0.5	1	208.1	0.0000	60.8	10.9	23.8	3,14	16
2	25	1	209.5	0.0028	55.5	12.5	16.7	2.21	12
3	0.5	3	207.2	0.0000	56.1	10.8	18.2	2.40	21
4	25	3	204.1	0.0288	62.5	13.6	15.1	1.99	10
5	12.5	2	224.6	0.0084	52.3	11.9	19.7	2.61	13
6	12.5	2	214.0	0.0072	62.3	12.2	17.8	2.35	13
7	12.5	2	226.7	0.0095	55.4	12.0	19.3	2.55	11
Control	-	-	209.6	n.d.	54.7	11.3	23.1	3.05	20.5

SSA*- specific surface area; CI** - crystallinity index. n.d. – not determined.

All enzymatic pre-treatments led to negligible release of glucose (**Table 1**) and xylan (data not shown) from the pulp, allowing to near perfect recovering of pulp for further processing into nanofibers. Therefore, it was assumed that the total solid yield after the enzymatic pretreatment was nearly 100% for all conditions tested and the hydrolysis yield was not considered as a response for the statistical analyses. However, variations in the enzymatic treatment severity led to notable changes in the properties of the obtained CNFs and their suspensions (Table 3.1). The effects of the enzymatic pretreatment variables on the CNF properties and on the input energy were evaluated according to their statistical differences and variances (ANOVA, Table 3.2). The full ANOVA analysis (analysis of variance) and the graphic representation (Pareto chart) for each response can be found in supplementary material I and II, respectively. The significance of each main variable (factor) and their interaction are reported as *p*-value and values smaller than 0.05 indicate that the factor is statistically significant. The curvature *p*-value is higher than the statistic significant of the factors (enzymatic loading and reaction time) to all responses (CI, particle size, viscosity, shear stress and input energy). In this matter, no factor has a curve relation with any response indicating the indicated nominal model of each response can be applied.

Table 3.2. Response matrix of p-value of the ANOVA test.

	Curvature	EL*	RT**	Interaction	R^2	R^2 adjusted	Adjusted model
CI***	0.656	0.908	0.811	0.282	37.39	-	-
Particle size	0.058	0.990	0.929	0.970	0.37	-	-
Viscosity	0.577	0.012	0.029	0.124	94.42	88.84	Viscosity = 24.91 – 0.2076 EL – 1.805 RT
Shear stress	0.576	0.012	0.029	0.125	94.35	88.71	Shear stress s=3.289 – 0.02733 EL – 0.2388 RT
Input Energy	0.111	0.036	0.518	0.187	84.80	69.61	Energy = 17.62 – 0.3061 EL

EL*- enzyme loading; RT**- reaction time; CI***- crystalline index.

CNFs with the same degree of defibrillation, which is denoted by a constant SSA of ca. 200 m^2/kg, displayed statistically equal CI% regardless the pretreament parameters and their range values (Table 3.2). Therefore, CI% was not considered for further construction of predictive statistical models. The CI% of the CNFs obtained from enzymatically pretreated pulps ranged from 52 to 62%, independently of enzyme dosages or reaction time (Table 3.1). EGs act preferentially on the disordered regions of cellulose, which in theory should increase the crystallinity of the cellulose. However, while some authors have reported that enzymatic treatment of cellulose with EG in fact increase the CI% of cellulose (Hu et al., 2018; Nechyporchuk et al., 2015; Qing et al., 2013), others have observed a reduction (Campos et al., 2013; Siqueira et al., 2019). For example, Nechyporchuk et al., (2016) observed that the CI% increased from 82% for the starting cellulosic pulp to approximately 86% after the enzymatic treatment at higher dosage (21, 210 or 315 EGU/g 2h), while Siqueira et al., 2019 reported a decrease of in the CI from 90% for the starting material to 88% for the pulp treated with EG at 400 EGU/g - 72h.

The average particle size of the CNFs, which are determined by laser diffraction considering the hydrodynamic diameter value of the equivalent spherical particle, ranged from 11 to 13 µm (Table 3.1). There was no behavioral trend as far as the enzymatic loading and reaction time. With harsh enzymatic pretreatments producing bigger CNFs while controls produced smaller ones. This infers that the intrinsic variability of the mechanical fibrillation, which leads to highly polydisperse nanofibers, overlapped any effect on the nanofiber size coming from the enzymatic pretreatment of the pulp. In addition, particles of similar size were expected as the mechanical processing was stopped at the same SSA values, both properties being highly connected. The enzyme pretreatment likely promoted enhanced defibrillation,

increasing the overall branching character of the CNF network, reducing the length of its unities. This assumption was confirmed by ANOVA analysis (Table 3.2). That is, for both main factors and their interaction, the *p*-value was higher than 0.05 (Table 3.1), indicating that neither the reaction time, enzyme loading and their interaction promoted statistically significant change in the average particle size of the CNF suspension in comparison to the control CNF.

The effect of the EG pretreatment was more evident on the rheological properties of the CNF suspensions, which describe a collective colloidal behavior of the cellulose nanofibrils. Both enzymatic loading and reaction time, as well as their synergistic action, led to significant changes in the viscosity and shear stress of the CNF suspensions (Table 3.2). There was a significant decrease in viscosity and shear stress for the pretreatment at the harshest condition (25 EGU/g for 1 or 3 h) and a less pronounced change for the central, milder condition (12.5 EGU/g - 2h) as compared to the control CNF (Table 3.1). With the mildest condition (0.5 EGU/g), it is likely the extension of reaction time weighed more in the rheology changes. From the coefficients of the adjusted models in Table 3.2, one can see that the reaction time has a more significant effect (one order of magnitude higher) on both viscosity and shear stress when compared with enzyme loading. In fact, both the enzyme loading and the reaction time were significant as far as the rheology measurement (*p*-value < 0.05) of the CNF suspension, but their interaction was not significant. Such observation arises from the most impactful effect of the reaction time that is independent of the enzyme loading. This effect can be associated with the expected decrease of the DP and accessibility of cellulose surfaces. EGs can reach and break accessible glycosidic bonds, thus reducing the DP as will be discussed later. This has been shown to have a strong influence on the viscosity and shear stress of CNF suspensions (Henriksson et al., 2007; Ibarra et al., 2010). Considering that only a very limited fraction of the cellulose is accessible to the enzyme, longer reaction times allowed higher EG-cellulose interactions thus leading to an efficient activity of the enzyme over the cellulose chain.

3.4.2 EFFECT OF THE EG PRETREATMENT ON THE ENERGY CONSUMPTION FOR DEFIBRILLATION

The energy consumption for defibrillation was only significantly affected by the enzymatic loading (Table 3.2). With the higher enzymatic loading (25 EGU/g for 1 or 3h), the energy consumption was reduced from 20.5 (control sample) to approximately 10 kWh/kg, reaching 52% reduction. Lowering the enzyme loading to 12.5 EGU/g and reaction time to 2

h, the energy consumption was reduced by 38%, from 20.5 to 13 kWh/kg. However, the energy consumption and the enzyme loading were not proportionally related. For instance, a twice harsher pre-treatment (enzyme loading from 12.5 to 25 EGU/g) did not lead to a twice higher energy reduction. This clearly marks a threshold for energy saving led by enzymatic pre-treatment, with no advantage of using very high enzyme loading as has been often seen in the corresponding literature (Campos et al., 2013; Nechyporchuk et al., 2015; Zhu et al., 2012). Considering that the extension of reaction time and its interaction with enzyme loading were not statically significant, both factors were removed from the model that was used to predict the optimal conditions to reduce the energy consumption while preserving the CNF properties.

The enzyme load, within the range tested, had a positive effect on energy reduction as evidenced by its negative term in the adjusted equation for energy consumption (Table 3.2). As previously discussed, the reaction time had no effect on energy reduction (*p*-value greater than 0.05, Table 3.2). This indicates that maybe short reaction times (at least 60 min) is enough for the enzyme to promote fiber modifications that facilitate the defibrillation, therefore decreasing the required energy input. Similarly, Tarrés et al., 2016 also observed that reaction time (2-4 h) did not influence on increasing the surface area of the nanofibers provided that high enzyme loadings were used. On the other hand, when the enzyme loading is increased, from 0.5 to 25 EGU/g, it intensifies the action of the EG on the cellulose chain, consequently promoting highly efficient defibrillation saving energy to a great extent, with 52% decrease from control values.

3.4.3 OPTIMIZATION OF ENZYMATIC PRE-TREATMENT FOR THE CNF ISOLATION: COMPROMISE BETWEEN ENERGY INPUT AND CNF PROPER

From the observed experimental responses arising from changes in the EG pretreatment parameters we could draw a more precise prediction of different scenarios/conditions to further find optimal conditions for the enzymatic pretreatment with EG as far as energy saving for defibrillation and rheology of CNF suspensions. For the predictions, the same weight and importance was considered for all the responses (viscosity, shear stress and energy consumption), which were statistically significant according to the ANOVA analysis (Table 3.2). The optimization process is based on the creation of possible scenarios where the most energy reduction (Scenario #1) or the compromise between the most energy reduction and the properties of CNF (Scenario #2).

The first scenario (Scenario #1) targeted the maximum energy reduction (reducing from 20 to 10 kWh/kg), and the predicted condition for it was the same achieved by applying the highest enzyme loading (25 EGU/g) for the longest reaction time (3 h). In this scenario, the energy saving was 50% in comparison to the control, but with a cost to the rheological properties. It was observed that, when compared to the control sample, the viscosity of the EG pretreated (25 EGU/g for 3h) CNF reduced from 23.1 to 15.1 cP and the shear stress reduced from 3.05 to 1.99 Pa. Controlling the viscosity of CNF suspensions warrants better suitability on applications were control over flow by shear are necessary, as is the case of direct ink writing printing, filament extrusion or spray applications. Although viscosity can be readily adjusted by the mass fraction of CNF suspensions, the need for higher solid fraction to achieve a given viscosity is detrimental to the profitability of the practical application. Therefore, although such enzymatic pretreatment condition lead to high energy saving, by 50%, they may not be suitable for large scale operations as they are too detrimental for the CNF properties.

In another scenario (Scenario #2), it was targeted to find a compromise between minimization of the energy consumption and maximization of the rheological properties. The processing conditions was optimized to account for the minimum energy input (10 kWh/kg) and highest rheological properties (shear stress and viscosity, 3.13 Pa and 23.76 cP, respectively). To fulfill the criteria imposed by such scenario, it was predicted that the enzymatic pretreatment should be carried out using an enzyme loading of 5.6 EGU/g for 1 h of reaction. In such conditions, combining the individual the nominal models of each response, the model predicted (by the adjusted model of the interaction of each response and factor) indicated that it would require an energy input of 15.9 kWh/kg (22 % reduction) to isolate CNF while preserving the rheological properties (viscosity 21.9 cP and shear stress 2.89 Pa) (Table 3.3), achieving a desirability composite (calculated by utility transfer function – weight geometric mean desirability individual) equal to 66 %, indicating the combination of different variables are able to achieve a positive result for global combination of all responses. The individual desirability for shear stress and viscosity was equal to 79% and 46% for energy consumption, showed the shear stress and the viscosity predicted values can be easiler achieved and the energy consumption. Considering that under this scenario the properties of the CNF were preserved, this condition was taken for the purpose of further investigating the mechanism behind the energy reduction promoted by the enzymatic treatment. In order to validate Scenario #2, BEKP was enzymatically pretreated under the predicted optimum conditions (5.6 U/g for 1h), defibrillated and characterized following the same methods

previously described. The experimental responses for the CNF suspensions fell within the predicted values (**Table 3.3**). The experimental average energy consumption was 15 kWh/kg, the viscosity 21.59±1.07 cP and the shear stress 2.58±0.14 Pa. Thus validating the predicted Scenario #2 and giving optimized conditions to pretreat pulp aiming at an efficient and more sustainable CNF defibrillation.

Table 3.3. Prediction and experimental responses for CNF generated under the optimal condition (5.6 U/g - 1 h) for scenario #2.

			Predicted		Experimental values		
	Scenario 2	Target	Solution	IC 95%	#1	#2	Average
Input energy (kWh/kg)	Minimum	10	15.89	13.03-18.74	15	15	15
Viscosity (cP)	Maximum	23.76	21.93	19.52-24.34	23.72	19.45	21.59±1.07
Shear Stress (Pa)	Maximum	3.13	2.89	2.57-3.21	3.16	2.58	2.58±0.14
Desirability	-	-	0.662	-	-	-	-

The properties of the CNF produced from the optimized (5.6 EGU/g for 1h) enzymatic pre-treated pulp fibers were deeper investigated as far as morphology, thermal stability and rheology. The CNF suspension isolated by the enzymatic pretreatment (EG-CNF) was compared to a control sample isolated without the pretreatment (CNF).

The morphology of the nanofibrils was analyzed by negative contrast scanning electron microscope (Neg-SEM). The overall morphology as well as their width distribution are shown in Fig. 3.2. The general aspect of EG-CNF and CNF is similar, displaying an entangled network of high aspect ratio nanofibrils with widths below 50 nm. In both suspensions, one can notice nanofibrils with high level of defibrillation, with small widths homogeneously distributed across the fibrillar network. However, it is also possible to see fibril bundles with larger diameters (ca. 100 nm). This is a typical characteristic of CNFs obtained by mechanical defibrillation (Chinga-Carrasco, 2011; Kumar et al., 2014).

CNFs are industrially competitive and their intrinsic morphological features have shown to achieve upper boundaries as far as mechanical performance in materials (Kontturi et al., 2018). The median widths of the EG-CNF are slightly smaller (26 nm) when compared to the control CNF (31 nm), with size ranges spanning from 3 to 116 nm compared to 8 to 150 nm, respectively (Fig. 3.2). Considering a preserved length for the fibrils (Table 1), a smaller width infers a slight higher aspect ratio for the EG-CNF. The absence of bigger fiber bundles

may warrant more homogenous materials assembled from such EG-CNF, as well as potentially stronger considering that with narrower particle distribution the interparticle interactions can be better controlled. That is, a homogenous suspension displays also a better networking formation capability, while heterogeneous suspensions form big aggregates and inefficient networking (Zimmermann et al., 2010). The width distribution results (Fig. 3.2) also show that EG-CNF has a considerable narrower diameter size range, clustering around 85% within 3 – 40 nm, and entangled fibrillar structures that leads to good networking formation. Compared to the reference CNF, the enzymatic treatment resulted in a slightly more uniform suspension, as CNF has clustered 78% of widths distributed within the 8 to 40 nm range.

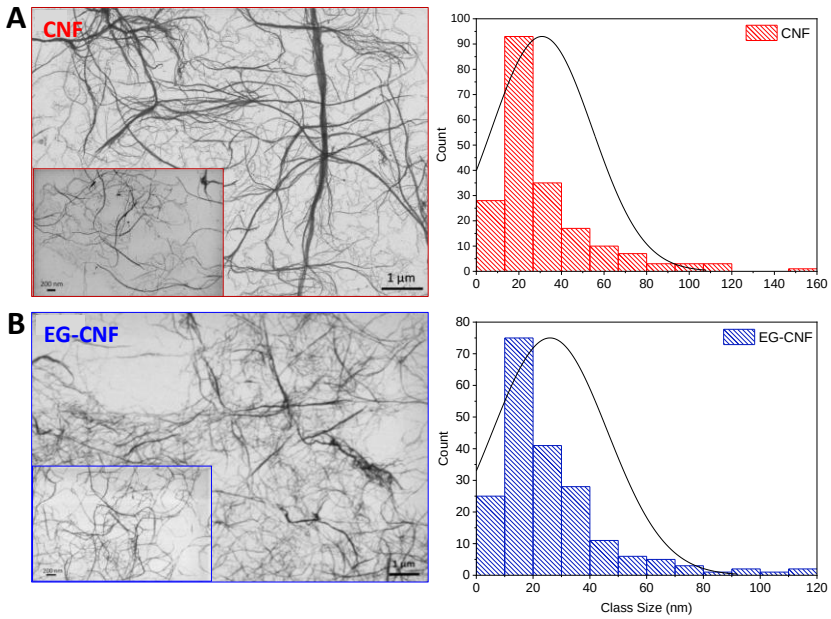

Fig. 3.2. Morphological aspect by high contrast SEM images and the respective distribution of diameter size of nanofibrils isolated from BEKP by defibrillation in a SuperMassColloider (A) without and (B) with an enzymatic pretreatment with EG under scenario #2 (5.6 U/g - 1 h).

The high aspect ratio of the nanofibrils and their entangled network influence strongly on the rheology behavior of the suspension. The storage and loss moduli profile of EG-CNF and CNF in aqueous suspension (1 % wt) has the typical gel-like behavior (Fig. 3.3A). The storage modulus was 10-fold greater than loss modulus, indicating the viscoelasticity of the suspensions coming from the strong interfibril interaction within the entangled network, the same profile of CNF obtained by mechanical and enzymatic pretreatment described by Paakko et al 2007. The EG-CNF suspension has a slightly higher storage (G`) and loss (G``)

moduli than the CNF suspension, which can be attributed to the entangled network but also to a greater interaction of the surface of the fibril with water molecules. A similar profile was observed for the representative curves of shear stress as a function of strain (Fig 3.3B), showing that, again, EG-CNF suspension displays a modestly higher increase in the elastic modulus compared to CNF.

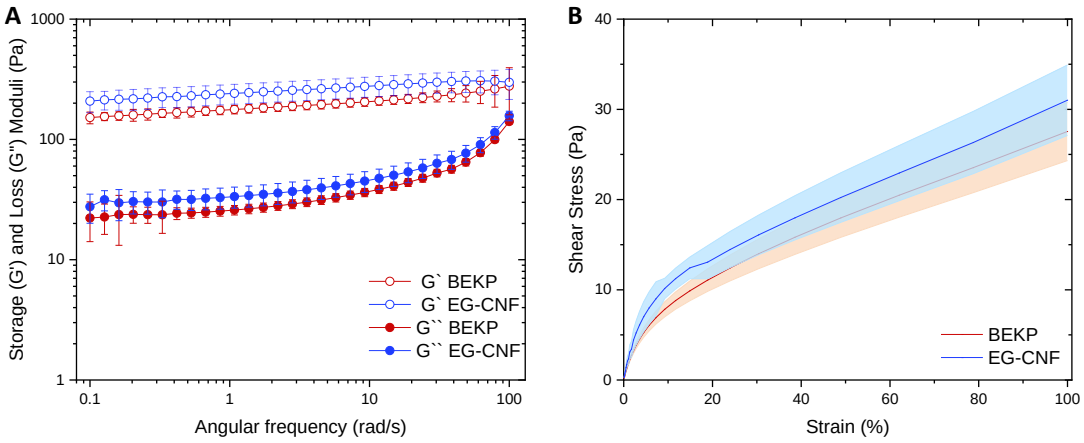

Fig. 3.3. Rheological characterization of CNFs obtained applying the optimal EG pre-treatment condition (blue, EG-CNF) and without enzymatic treatment (red, CNF). (A) Storage (empty symbols) and loss (filled symbols) moduli as function of angular frequency at 1% of solid content using parallel flat plate geometry; (B) the shear stress under different shear rate.

There is slight variations in the EG-CNF properties compared to those from CNF derived from the EG action on cellulose fibers. Additionally, the pretreatment with EG led to significantly high reduction in the energy consumption for defibrillation. The enzyme action on cellulose with no release of soluble products, observed under the mild enzymatic pretreatment (5.6 EGU/g – 1 h), improved the cellulose surface reactivity allowing higher interactions with water, thus modifying the rheological behavior of the suspension. In a related study, Ibarra et al. (2009) demonstrated that this specific monocomponent EG is very efficient to increase the reactive of cellulose surface. The authors attributed the increase to i) the inverting catalytic mechanism, which it is more efficient on the disordered regions along the cellulose fibrillar structure and ii) to the presence of a secondary protein domain, the carbohydrate binding module (CBM), which gives the EG a high binding efficiency (Ibarra et at. 2009).

Another key property of CNF is the thermal stability, especially considering the final application of nanofibrils as a reinforcement component of polymeric composites that are

usually processed by thermal routes. The thermogravimetric curves (derivatives) of both EG-CNF and CNF displayed similar profiles. The initial degradation temperature (T_{onset}) of EG-CNF and CNF was found to be ca. 230 °C, which agrees with the thermal degradation of pure cellulose (Poletto et al., 2014). CNF, however, is slightly more thermal stable at T_{onset} than EG-CNF (Fig 3.4 inset). It is likely that such result came from the action of the EG on the disorder segments of cellulose that deconstructed the chains into smaller molecular weight (Mw) fragments. These smaller fragments are likely more susceptible to thermal degradation than higher Mw fragments. This can be attributed to action of the EG that decreases the DP, resulting in an early-initial thermal degradation.

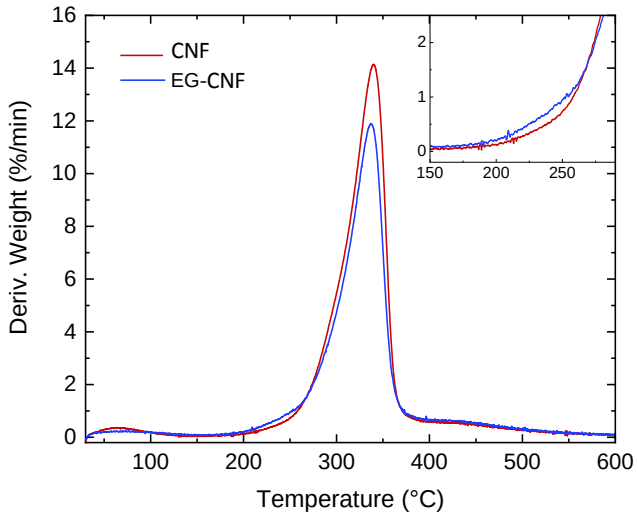

Fig. 3.4. Derivative thermogravimetric (DTG) of) of EG-CNF and CNF films with a zoom in detail from 150 to 300 ℃.

Herein, the condition of scenario two for the enzymatic pretreatment of BEKP for isolation of CNF in a SuperMassColloider, smoothly shifted the rheology, morphology and the thermal stability, in addition to save energy on defibrillation process. Apparently, EG applied in low enzyme dosage and short reaction time is enough to promote smooth modifications in cellulose chain. Moreover, these slight modifications seemed to be sufficient to facilitate the defibrillation process, saving energy and preserving key properties. Our work agrees with previous efforts on such matters (Pääkko et al., 2007; Quing et al., 2012; Tarrés et al., 2016; Zhu et al., 2012), thus contributing to a consolidation of the knowledge on a single step enzymatic pretreatment for facilitated defibrillation. However, the mechanism of the enzyme mode action that is responsible to facilitate the defibrillation is still not fully understood, which limits more advances in the field.

3.3.7. RATIONALIZING OF THE EG MECHANISM OF ACTION FOR ASSISTING DEFIBRILLATION

The monocomponent used herein (EG) did not release soluble products from the cellulose fiber in the assayed conditions, even at the harshest conditions (Table 3.1). Despite that, it was possible to save up to 50 % of energy required for defibrillation in the SuperMassColloider, and 25% when the pretreatment condition was optimized to preserve rheological properties. To have a better understanding on how the EG promotes changes in the substrate that leads to efficient defibrillation at significantly lower energy input, we investigated structural modifications of cellulose fibers promoted by the enzyme. Further, the substrate-enzyme interactions were explored deeper by using QCM-D.

The structural changes in the cellulose chain were investigated in the treated pulp. The BEKP enzymatically treated by the monocomponent EG at the condition optimum in Scenario #2 (EG-BEKP) was compared with a non-pretreated BEKP. For a logical investigation, it is important to consider the catalytic mechanism of EGs and the typical modifications expected from this specific group of enzymes (endoglucanases). EGs are well-known cellulases that reduce the DP by randomly cleaving the glycosidic bonds and inserting new non-reducing and reducing ends in less organized regions of cellulose. This tends to reduce the molecular size of cellulose chains, leading to smaller cellulose fragments at the molecular level (Fig. 3.5A). The analyses of molecular weight distribution of the EG-BEKP and BEKP allowed to show structural differences between the two pulps. The EG-BEKP treated at the Scenario #2 displayed an average molecular weight of approximately 284,117 Da, which represents a reduction of 17 % compared to the BEKP (341,484 Da) (Fig. 3.5B). Ibarra et al., 2010 reported a reduction of molecular weight of approximately 8% using the same enzyme and dissolved pulp from hardwood as substrate. This different proportion in reduction can be related to the differences of the substrate and their recalcitrance to the enzyme. By analysing the molecular weight distribution, one can observe that the starting material (BEKP) is heterogeneous in nature and clusters fragments in two distinguished peaks. The same profile was observed the treated pulp (EG-BEKP). However, EG-BEKP had the molecular weight distribution shifted towards the lower molecular mass region. This also confirms the typical action of EG on reducing the DP, even at the very mild reaction condition applied, making the cellulose surface more reactive (Ibarra et al., 2010), therefore facilitating the defibrillation.

The surface modification promoted by EG can improve the interaction of the cellulose's surface with water. Specifically, this EG has been described to efficiently improve fiber swelling, having an evolutionary similarity with enzymes specialized in swelling of

cellulose fibers (i.e., swollenin) (Berto et al., 2019; Igarashi et al., 2008; Nakamura et al., 2015). The water retention value (WRV) was determined by the tea-bag methodology (Fig 3.5C). EG-BEKP had higher water retention capability when compared to control pulp (BEKP), indicating a possible increase in the swelling capacity of the fibers accentuated by the EG treatment. WRV can be also intensified by the surface activation caused by the CBMs. The interaction/penetration of CBM in the cellulose hierarchical structure promotes a re-arrangement of the cellulose chains, without hydrolytic effect, and more molecules of water can interact with the cellulose surface, a phenomenon called amorphogenesis (Arantes and Saddler, 2010; Bernardes et al., 2019).

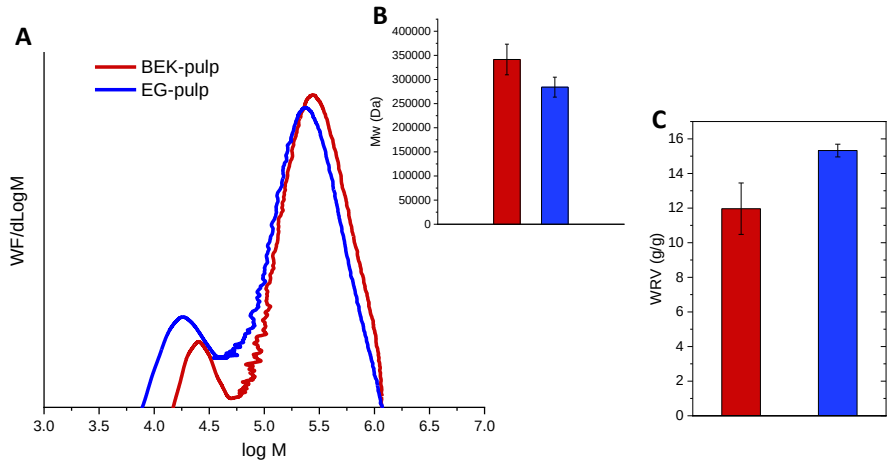

Fig. 3.5. Molecular weight analysis using gel-permeation chromatograph of non-treated pulp (red, BEK-pulp) and treated with EG (blue,EG-pulp). (A) Distribution of retention volume versus RI of molecular weight; (B) average molecular weight and; (C) water retention value (WRV) by tea-bag methodology.

Furthermore, the cellulose-enzyme interfacial interactions were evaluated by QCM-D (Fig. 3.6). For the analyses, CNF was used as cellulose model substrate and spin coated in a gold quartz crystal. The crystal coated with the thin CNF film was placed on the QCM-D system and the temperature was raised to 50 °C in the presence of buffer (phosphate-citrate 50 Mm pH 6.0) until the frequency reached the equilibrium baseline. Afterward, a solution of EG at 5.6 EGU/g was pumped into the system at a flow rate of 40 µL/min for at least 60 min. EG showed a rapid adsorption on the cellulosic surface taking place right after its injection in the system (first 15 minutes) followed by a gradual adsorption that did not reach a plateau over 1h (Fig .3.6 – black line). Such profile shows a high time-dependency for the enzyme to efficiently adsorb on the cellulose surfaces, explaining why the reaction time is a significant

variable to modify the viscosity and shear stress of the CNF suspension produced from EG-BEKP. The enzyme was more efficient to adsorb on the cellulose surface at the begging of injection, which is close correlated to the available free-surface of the substrate. The dynamics of adsorption slow down rapidly, possibly driven by the more intense traffic of enzyme on the cellulose surface. Even at a lower rate, the frequency continued to decrease, which can be justified by the EGs that were still adsorbing and by the water molecules that interacted more strongly with the surface. Additionally, adsorption in multilayer, meaning EGs interacting with EGs, cannot be neglected. The increase in WRV (Fig. 3.5C) and the decrease in the molecular weight (Fig 3.5A and 3.5B) can be correlated with this observation. The change in frequency, which correlates with the mass adsorbed on the substrate, was remarkably lower when compared to the adsorption of other proteins on cellulosic surfaces (Josefsson et al., 2008). The difference in intensity of the frequency is closely related to the total of protein mass applied in each study. While Josefsson et al., (2008) applied 10 µg of the EG Novozym 476, herein it was used enzyme solution to account for 5.6 EGU/g. Although much higher enzyme dosages achieve faster adsorption, they were shown to be unnecessary to favor defibrillation.

Contrary to the frequency, the dissipation achieved a plateau after 50 min of injection (Fig. 3.6). Thus, the modification of the viscoelasticity property of the cellulose thin film occurs within the first 50 min of enzyme action. Such modification is a result of two distinct phenomenal i) the adsorption of enzyme on the cellulose surface that adds a new layer of protein onto the film and ii) structural modification on the cellulose surface that allows better water interaction with the cellulose. As the energy consumption response was not affected by the reaction time), it is likely that closely associated with the modification of viscoelasticity rather than solely to the enzyme adsorption. The presence of CBM could be the key feature for the efficient energy reduction, as such domains can promote structural modification (Arantes and Saddler, 2010; Bernardes et al., 2019) and bind to the cellulose surface in a short period of time. In our study, the CBM, apparently, is fundamental to aid the binding of EG on the surface of cellulose fibers, considering that a low enzyme dosage and short reaction time were employed. The catalytic domain could efficiently act and promote superficial modification without having a more drastic catalytic activity, for example, realizing products and preserving the morphology and rheology, in addition to saving 25% of energy during the defibrillation process.

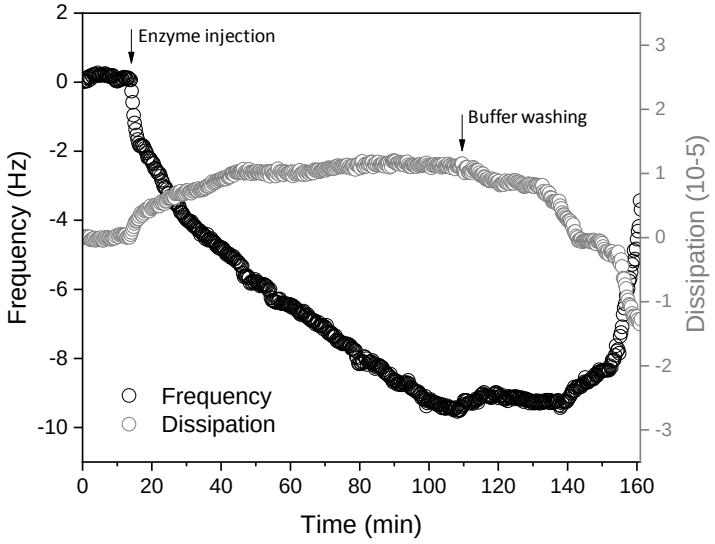

Fig. 3.6. Interaction of nanocelluloses surface (frequency and dissipation) with monocomponent EG as function of time by QMC-D technique, where the black line is the frequency curve and grey line is the dissipation curve.

The analyses of molecular weight distribution, water retention value (WRV) and enzyme-cellulose interaction suggest that the monocomponent EG, when used at the optimized conditions (5.6 EGU/g for 1h), slightly reduced the DP, swelled the fiber at greater extent and adsorbed to the cellulose surface. All together changing the molecular structure of the cellulose and changing its viscoelasticity behavior. The combination of such considerably mild modifications allowed the defibrillation process of BEKP to consume less energy while preserving the morphology of the nanofibrils and improving the rheology of the obtained EG-CNF suspension.

The enzyme was not capable to release sugar, specially, at the optimized pretreatment condition (5.6 EGU/g – 1 h). Therefore, there was no contribution of the EG hydrolytic action on the reduction of the energy demand in the defibrillation process. Typically, EGs are investigated and explored to reduce the viscosity (Ibarra et al., 2010), increase the cellulose surface (Rahikainen et al., 2019) and as a biocatalytic component to act in synergism with others cellulases to fully deconstruction of cellulosic biomass (Berto et al., 2019; Chylenski et al., 2017; Haq et al., 2015). However, for isolation of CNF by disc ultra-refining the hydrolytic effect for product releasing was not beneficial for the improvement of the process (reduce the energy consumption and preserve the great quality of the final nanomaterial). Instead, it appears that the structural modifications in cellulose promoted by the EG and its CBM were more helpful for this application. This insight allows to a new avenue for

exploring hydrolytic enzymes, screening new enzymes and engineering proteins to promote structural modifications with very low or without hydrolytic effect and, potentially, to improve even more the enzymatic pretreatment for CNF isolation.

3.5 CONCLUSION

Herein, it was presented a comprehensive investigation of a single-step enzymatic pretreatment using a monocomponent EG for CNF isolation by disc ultra-refiner. By varying the enzyme loading and reaction time, it is possible to significantly reduce (25-50%) the energy input for defibrillation. Whereas at harsher EG pre-treatment conditions a great extent of energy intake is reduce (50%) with a cost to the quality of the resulting CNF, at a milder condition 25% of energy input is reduced but the rheology of CNFs is preserved. Thus, with pretreatment it is possible to select the conditions to achieve the desired final property and rate of energy saving. The process conditions were optimized to find a compromise between energy input and quality of the defibrillation. It was demonstrated that the EG applied at 5.6 EGU/g and 1 h condition was the optimal compromise between energy input and properties. The EG pretreatment, with negligible hydrolytic effect, i) improved the cellulose-water interactions that led to greater swelling of the fibers, ii) introduced new reducing and non-reducing ends that slightly reduced the molecular weight, iii) and modified the cellulose due to the strong binding of EG's CBM. The coordination of all these effects and the tailored condition for enzymatic pretreatment step could reduced the energy consumption using a SuperMassColloider for defibrillation and isolate CNF with high quality properties, being a potential approach to tackle the high energy consumption. Moreover, the enzymatic pretreatment reported can be easily conducted in only a single-step, in addition to being a green and sustainable route to facilitate the CNF isolation from bleached pulp.

CHAPTER 4 – EFFECT OF ENDOGLUCANASE FROM DIFFERENT FAMILIES ON THE ISOLATION PROCESS OF CELLULOSE NANOFIBRIL

4.3. ABSTRACT

Endoglucanases (EG) are cellulases that act preferentially on the less organized regions of cellulose fibers, but some possess significantly distinct properties that can be exploited for specific applications. They are clustered in different glycosyl hydrolase (GH) families in regard to differences in non-cellulosic substrate specificity, tri-dimensional structure and catalytic mechanism. Additionally, EGs may also differ in relation to the presence a carbohydrate binding domain (CBM), thought to improve the approximation of the catalytic domain to the substrate, consequently improving the enzyme action. The beneficial effect of the application of EG for isolation of cellulose nanofibrils (CNF) has been already reported, however it is still unknown which enzyme property contributes the most. Herein, the effects of EGs from different GH families (5, 6, 7 and 12, with or without CBM) at low enzyme dosage and short reaction time were investigated in the enzymatic pretreatment of a commercial Kraft pulp, followed by disc ultra-refiner for isolation of CNF. The GH5 and GH12, lacking the CBM domain, reduced the energy consumption to approximately 15%, compared with the control without pretreatment. The most efficient energy reduction, 25 and 32%, was achieved with GH5 and GH6, respectively, both linked to a CBM. All EGs reduced the molecular weight distribution of the pulp, did not release soluble products and improved the rheological property of CNF suspensions. Exceptionally, EG from GH7 linked to CBM did not reduce the energy demand and neither modified the molecular weight, but its hydrolytic activity was significant as demonstrated by the release of soluble products. Together, these findings evidence that the beneficial effect of EGs for isolation of CNF is attributed to the efficient adsorption onto the substrate and the combined effects of molecular weight reduction without cellulose solubilization.

Keywords: endoglucanase families; enzymatic pre-treatment; amorphorgenesis, enzyme-substrate interaction, Carbohydrate modulus domain.

4.4. INTRODUCTION

Several authors have reported the efficiency of enzymatic pre-treatments to allow the flow of cellulosic suspension in high pressure systems (Henriksson et al., 2007; Pääkko et al., 2007) or to reduce the energy consumption at disc ultra-refiner (Nechyporchuk et al., 2016) for isolation of CNF. A very specific cellulase, called endoglucanase (EG, EC 3.2.1.4), for less ordered regions of cellulose fibers has been applied in these studies and the most used is a commercial monocomponent EG (Novozym 476 or FiberCare). For the pre-treatment, there are several combinations of enzymatic and mechanical steps and a large range of enzymatic pre-treatment conditions, which can result in CNFs with different properties and characteristics. In addition, different enzymatic pre-treatment conditions effect on CNFs production and their final properties. Modifying the enzymatic pre-treatment from harsher (25 EGU/g – 3 h) to mild (0.5 EGU/g – 1 h) condition, it was possible to tailor the desirable final property (*e.g.* higher viscosity or lower shear stress), as well as save a considerable amount of energy. In addition, the optimal condition for the maximum energy reduction and maximum preservation of the properties was predicted and validated. FiberCare was assayed to assist the pre-treatment of BEKP in one-single step followed by defibrillation in disc ultra-refiner. Low enzyme dosage and short reaction time (5.6 EGU/g and 1h) were applied in the pre-treatment resulting in 25% of energy demand preserving the rheological and morphological properties.

The commercial EG (FiberCare) and other EG classified in a different family (glycosyl hydrolase family 5, GH5 with great thermal stability) were used to pretreat BEKP (previously disintegrated and size classified) and isolated CNF from using a microfluidizer (at 0.3% of solid content) (Wang et al. 2015). These enzymes resulted in CNFs with different characteristic, even applying the same enzyme dosage (0.1, 1 or 10 mg of protein per g of pulp). The pulp pre-treated with the commercial EG resulted in CNFs with better optical property (higher transmittance) after the same number of passes of the suspension through the microfluidizer than CNFs obtained with GH5 pre-treatment. On the other hand, GH5 was more efficient to preserve the length of the nanofibrils and the DP, isolating CNF with great potential to be applied as a reinforcement component. The contrast of the obtained CNFs is related to the peculiarity of each EG and their inherent catalytic action on cellulose (*e.g.* the different preferences for CMC or residual activity in *p*-NPC) (Wang et al., 2015).

This single study (Wang et al., 2015) is a tip of an iceberg to look for the effect of distinct cellulases for isolation of CNFs with different properties. Considering just the EGs, a cellulase with high affinity for the less organized regions of cellulose fibers, they are clustered

in 15 different families (5, 6, 7, 8, 9, 10, 12, 26, 44, 45, 48, 51, 74, 124 and 148) (www.cazy.org). This classification is based on differences in the catalytic mechanism, substrate specificity and three-dimensional structure (Henrissat et al., 1991).

An outstanding study reported the hydrolytic efficiency of EGs from GH families 5, 6, 7, 9, 12 and 45 from different microorganisms on different model substrates (Vlasenko et al. 2010). EG from family 6 (GH6), besides the typical activity in PASC (phosphoric acid swollen cellulose, a model amorphous cellulosic substrate), also showed activity in xylan and arabinoxylan. GH5 (EG from family 5), in addition to the affinity on amorphous cellulosic substrate, also exhibited activity towards mannan and galactomannan. Otherwise, EG from family 45 (GH45) had greater selectivity for the less organized regions and showed hydrolytic activity only in amorphous cellulosic substrate. The EGs from family 12 and 7 (GH12 and GH7, respectively) were more versatile than EGs from other families, showing activity in xyloglucan, xylan and arabinoxylan. In the same study, the thermal stability and optimal temperature values of the EGs were presented, all of which had higher activity at 60 °C. Regarding the thermal stability, except for GH7, all EGs maintained activity at 60 °C. However, GH5 and GH45 maintained activity at 70 °C.

In addition to differences in substrate specificity that occur among EG families, the presence of associated domains like CBMs (carbohydrate binding module) and the catalytic mechanism also influence the catalysis action of the enzyme. Ibarra et al. (2010) evaluated the action of a CBM-linked GH45, a CBM-free GH45 and a CBM-free GH7 on two different cellulosic materials (coniferous and hardwood dissolving pulps) for viscose production. The EGs from family 45 were more efficient in increasing the accessibility of the cellulose than GH7. The CBM-associated GH45 also was more efficient in reducing viscosity and the degree of polymerization. In this sense, the presence of CBM and the reversing hydrolytic mechanics were fundamental for better performance of an EG for this specific application. The differences among EGs also were reported by Siqueira et al. (2019), where EGs from family 7 and 5 were not able to produce cellulose nanocrystals, however, EG from GH45 could release some cellulose nanocrystals. The same performance profile of GH45, 5 and 6 to increase cellulose accessibility was reported by Rahikainen et al. (2019). Again, GH45 was more efficient to reduce the molecular weight and the viscosity of the treated pulp than GH5 and GH6. The authors also demonstrated the great role of CBM when hydrolysis is conducted in low dry matter condition (1%), but at high consistency (10%), CBM was not beneficial for the enzyme performance.

The diversity in EGs mode of action makes these enzymes promising targets for the production of CNF. In this context, this work explores the effect of well characterized EGs from GH families 5, 7, 12 and 45, with and without CBM, in a single-step pre-treatment applied for isolation of CNF. A comprehensive study was performed to investigate the effect of EG properties in the reduction of the energy demand for the mechanical defibrillation phase while preserving the properties of the CNF. It was investigated the characteristic of the enzymes and their benefits for isolation of CNF, considering the typical behavior of EGs in reducing the DP, the presence of CBM to adsorb on cellulose surface and promote structural surface modification.

4.5. MATERIALS AND METHODS

4.5.1. CELLULOSIC PULP

Bleached eucalyptus kraft pulp (BEKP, never dried) was kindly supplied by Suzano Celulose S/A (Jacareí, SP, Brazil). The chemical composition of BEKP, determined as described by Sluiter et al. (2012), was 78.6% cellulose and 14.6% xylan.

4.5.2. EG FROM DIFFERENT FAMILIES

The EGs GH5 from Aspergillus fumigatus var niveus (AFUMN) and GH12 from Aspergillus terreus were produced in house. EGs GH5 from Rasamsonia emersonii (previously Taloromyces emersonii, GH6 from Thermobifida halotolerans and GH7 from Trichoderma longibrachiatum were purchased from Megazymes (Bray, Co, Ireland).

Amino acid sequences (accession numbers: AAL33630, KEY77237, ACZ34302 and XP_001218516), were obtained at National Center for Biotechnology Information (NCBI - https://www.ncbi.nlm.nih.gov/). The catalytic amino acid and mechanism are in accordingly information at Carbohydrate Active Enzymes Database (CAZy - http://www.cazy.org), molecular weight and isoelectric point were obtained at ProtParam platform (http://web.expasy.org/protparam/) using the predict amino acids sequence (Table 4.1). The optimal pH and temperature for the commercial enzymes were used as described by the supplier (Table 4.1). For GH12, these parameters were previously determined (Segato et al., 2017).

Table 4.1. Biochemical properties of EGs applied in this study.

Cazy family	Organism	Catalytic Aminoacid	Catalytic machanism	Molecular weight (kDa)	CBM[3]	Activity (EGU/mL)*	Optimal pH	Optimal temperature (°C)
GH6	*T. halotolerans*	Asp[1]	Inverting	42.9	Yes	250	8.5	50
GH12	*A. terreus*	Glu[2]	Retaining	23.9	No	12	5.0	55
GH5	*T. emersoni*	Glu	Retaining	34.7	No	570	6.0	40
GH5	*A. fumigatus*	Glu	Retaining	49.1	Yes	13	4.5	50
GH7	*T. longibrachiatum*	Glu	Retaining	45.9	Yes	933	4.5	40

Asp[1]- aspartate; Glu[2] - glutamate; CBM[3] – carbohydrate binding module; Activity* - determined using CMC

4.5.3. *IN HOUSE* PRODUCTION OF ENZYMES

EG GH12 and GH5 produced and purified *in house* were heterologously expressed using *Aspergillus nidulans* strain A773 as a host (Segato et al., 2012). Briefly, the protein expressions were induced by 3 % maltose (present in the broth medium culture) for 48 hours. The downstream steps for purification were: filtration through a qualitative membrane (Miracloth, MilliporeSigma, Burlington, MA, USA), to separate the mycelial mat from culture medium, concentration by ultra-filtration (10 kDa cut off Biomax® membrane in an Amicon® Stirred-cell, MilliporeSigma), followed by anionic exchange resin (DEAE sepharose CL6B, GE Healthcare Life Sciences, Marlborough, MA, USA) by salt gradient elution and size exclusion chromatograph (HiLoad 16/600 Superdex 75 pg) coupled to an Äkta Pure M25 (GE Healthcare Life Sciences) by buffer elution. The specific biochemical properties of each enzyme were considered in the purification steps (Table 4.1)

4.5.4. ENZYMATIC ACTIVITY AND ENZYMATIC PRETREATMENT

The EGs activities were measured following the photometric procedure (Miller, 1959), using carboxymethyl cellulose (CMC) at 0.44% wt (medium viscosity) as substrate dissolved in specific buffer condition for optimal pH and optimal temperature. The EG activity unit (EGU) was determined as μmol of glucose released per minute per ml of the EG.

For the enzymatic pretreatment, the enzyme loading was fixed at 5.6 EGU/g and the reaction time was 1 h, and 5% (w/w) BEKP solid loading (on a dry weight basis), as reported in chapter 3. The reaction volume (250 ml) was conditioned in 2 L Erlenmeyer flasks and kept in an orbital shaker (Thermo Fisher Scientific, Waltham, MA, USA) at 250 rpm. The enzymatic pretreatment was performed under the specific and optimal condition of pH and temperature for each enzyme (Table 1). To inactivate the enzyme after 1 h, the reaction was boiled in water for 30 min, vacuum-filtrated and washed, using Miracloth membrane, with excess of distilled water to remove the enzymes.

4.5.5. MECHANICAL DEFIBRILLATION

Mechanical defibrillation was conducted on the cellulosic material previously treated with the EGs, as described in chapter 2.

4.5.6. RHEOLOGICAL PROPERTIES

The rheological behavior of CNF suspensions – isolated using different EGs – was evaluated using an MCR 302 rheometer (Anton Paar, Graz, St, Austria), equipped with a parallel flat plate geometry and smooth bottom plate at controlled temperature of 23 °C as described in detail in chapter 3, item 3.3.11.

4.5.7. GEL PERMEATION CHROMATOGRAPHY

The change in the molecular weight of cellulose fiber was evaluated by gel permeation chromatograph following the protocol reported by Potthast et al. (2015) and briefly described in chapter 3, item3.3.13.

4.5.8. MORPHOLOGY

To investigate the morphological aspect of the CNFs obtained applying different EGs, the micrographs were generated by negative contrasted scanning electron microscopy (Neg-SEM) images (Mattos et al., 2019) as described in chapter 3 item 3.3.10.

4.5.9. ENZYME – CELLULOSE INTERACTION EXPERIMENTS

The interaction of the EGs from different families with the cellulosic surface was investigated using a quartz crystal microbalance (QCM) with dissipation monitoring (D-sense D-300) as described in chapter 3.

4.6. RESULTS AND DISCUSSION

The application of an enzymatic pre-treatment to cellulose fibers prior to the isolation of nanocelluloses is well known. However, most studies explored, in detail, the use a commercial monocomponent EG (FiberCare or Novozym 476) or complex commercial cocktails. Concerning the historic literature, the earlier studies reported the application of Novozym 476 (Henriksson et al., 2007; Pääkko et al., 2007), known to be a monocomponent EGs from family GH45 linked to a CBM1 from *Humicola insolens* (Ibarra et al., 2010). Over the time, a new enzymatic commercial monocomponent EG (designated as FiberCare) started to be reported and applied for CNF isolation (Campos et al., 2013; Nechyporchuk et al., 2014; Rol et al., 2017). As both enzymes solution have been shown benefits for CNF production, there is an initial speculation regarding to FiberCare and Novozym 476 be the same or similar enzymatic extract.

There are a few studies that have investigated the effect of enzymes classified in different families at CAZy database on the production of CNFs and their properties. EGs are a group of cellulases, which preferably act on less organized regions of the cellulose fiber, differ among themselves being classified into 15 GH families. In addition, there are an extensive number of studies prospecting and featuring EGs from different families and from different organizations, however the studies on the applications of this wide range of enzymes are still limited.

In this study, we report the application of EGs from different GH families that are associated or not to a CBM, in the pre-treatment of cellulose fibers for subsequent isolation of CNF using a disc ultra-refiner. The representatives EGs from GH families 5, 6, 7 and 12 were selected due their specific particularities and current application in different industrial sectors. Family GH5 EGs are well known for being the key EG component of enzymatic cocktails for lignocellulosic deconstruction (Payne et al., 2015). Here, EGs from family GH5 with and without a CBM (GH5_CBM and GH5, respectively) were used. EGs belonging to family GH7 present the typical behavior of EG by hydrolyzing the model amorphous cellulosic substrates CMC and PASC but they also can act on a broad range of substrates such as xylan, xyloglucan and arabinoxylan (Vlasenko et al., 2010). GH5_CBM and the GH7 are from a fungi source, and both have linked a CBM type 1, the typical CBM structure related to genes from fungi genomes. GH6 (EG from family 6) has the inverting mechanism of catalyses and is the representative EG produced by bacteria, having the associated domain (CBM2). EGs from family GH12 are generally described as low molecular weight protein and does not exhibit the CBM domain in its structures (Payne et al., 2015).

EGs from these different families have variation regarding the biochemical properties, such as optimal pH and temperature (Table 4.1). The pH and temperature range varied from 4.5 to 8.5 and 40 to 55 °C, respectively. For this reason, these properties were considered and specific conditions were employed for each enzyme during the enzymatic pre-treatment step. The enzyme loading was fixed in 5.6 EGU/g, at 5% dry matter and 1 h of reaction. Considering that the enzymes showed variation in their specific activity determined by CMC (Table 4.1), the total mass of protein added probably varied among the enzymes.

4.6.1. EXPLORING THE DIFFERENCES OF EGs

The genome search showed that *R. emersonii*, *T. halotolerans* and *T. longibrachiatum* has only one gene encoding EGs from family GH5, GH6 and GH7, respectively, which are the component of commercial preparation used in this study. The amino acid sequence analyzes allowed the identification of regions at the enzymes and based in its position a linear structure was proposed for each enzyme (Fig. 4.1). EGs, representative from each family, exhibit variations in number of amino acids in the structure of catalytic domain (the catalytic site, where the catalysis take place) and the position of catalytic site (acidophilic and nucleophile). Differences in primary structure may influence the folding and conformation of the three-dimensional structure of enzymes. In addition, differences are observed, when present, in the size of CBMs and their position along the linear distribution of amino acid residues. It was also noted that the linker length, which is the structure that connects the CBM to the catalytic domain, varies among the different structures.

The EG representing family GH6 is a bacterial enzyme and, therefore, has a CBM2, which is a common associated module in prokaryotic than in eukaryotic enzymes with 5663 and 156 entries in CAZy database, respectively. This module is structured by the interaction of 89 amino acid residues ordered in a β-sandwich fold composed of antiparallel β-sheets. The CBM2 linked to EG GH6 shows higher molar mass (9 kDa) compared to CBM1, connected to GH5 and GH7 (3 kDa) (Fig. 4.1). GH6 also differs from other EGs because of its inversion catalysis mechanism, wherein the catalytic reaction occurs in a single step with the assistance of acid/base amino acids catalytic, typically being aspartate. In addition, the optimum pH of GH6 is 8.5, distinguishing from the other EGs that work in lower pH reaction medium (Table 4.1).

The lowest molecular weight enzyme is GH12, with a predicted size of 24 kDa (Table 4.1). This characteristic is typical of EGs from family GH12, as well as the absence of the associated module (CBM) and linker (Fig. 4.1). Enzymes from family GH12 are nonspecific besides acting on the hydrolysis of β-1,4 bonds in the less organized regions of cellulose, they also show activity on non-cellulosic substrates such as xylans and mannan (Henriksson et al., 2007; Segato et al., 2017).

Alike GH12, EGs from family GH5 also show activity in non-cellulosic substrate, such as mannan and glucomann (Vlasenko et al., 2010). In this study, two GH5 from filamentous fungi, one CBM-linked GH5 and one without CBM were used. As expected, GH5 without CBM had the smallest predicted size, around 35 kDa, while GH5 with CBM

had the highest predicted molecular weight, around 49 kDa (Table 4.1). The difference in protein size is a combined effect of the presence of CBM and the linker that connects the binding module to the catalytic core (Fig. 4.1). Indeed, the size of catalytic domain is quite similar between the GH5 proteins, consisting of approximately 260 amino acid residues. Since they are classified in the same family, both enzymes demonstrate the same mechanism and catalytic amino acid (retaining and glutamine, respectively). However, there are still biochemical differences between the enzymes from family GH5 regarding the optimal pH and temperature (Table 4.1).

EGs from family GH7 are known to show less specificity to cellulosic substrates, having hydrolytic activity in xyloglucans, xylan, arabinoxylan and cellobiose (pNPC, model synthetic substrate) (Vlasenko et al., 2010). The GH7 used in this study, as well as the GH5s and GH12 also is source from filamentous fungus. Analyzing the primary structure and molecular weight, it can be seen that GH7 is quite similar to GH5_CBM with a molecular weight equal to 46 kDa (Table 1). Although the similarity in size, the GH7 catalytic core has the largest number of amino acids needed for structural conformation (358 amino acids), whereas GH5_CBM has 266 amino acids involved in its structure (Fig. 4.1). Despite the CBM of both enzymes having 29 amino acids residues involved in their structure, the size of the linker and catalytic core are different between them. GH7 has a shorter linker, which allows inferring that CBM is closer to the catalytic core. It may potentiate the catalyzes since the enzyme approach to the substrate is more efficient.

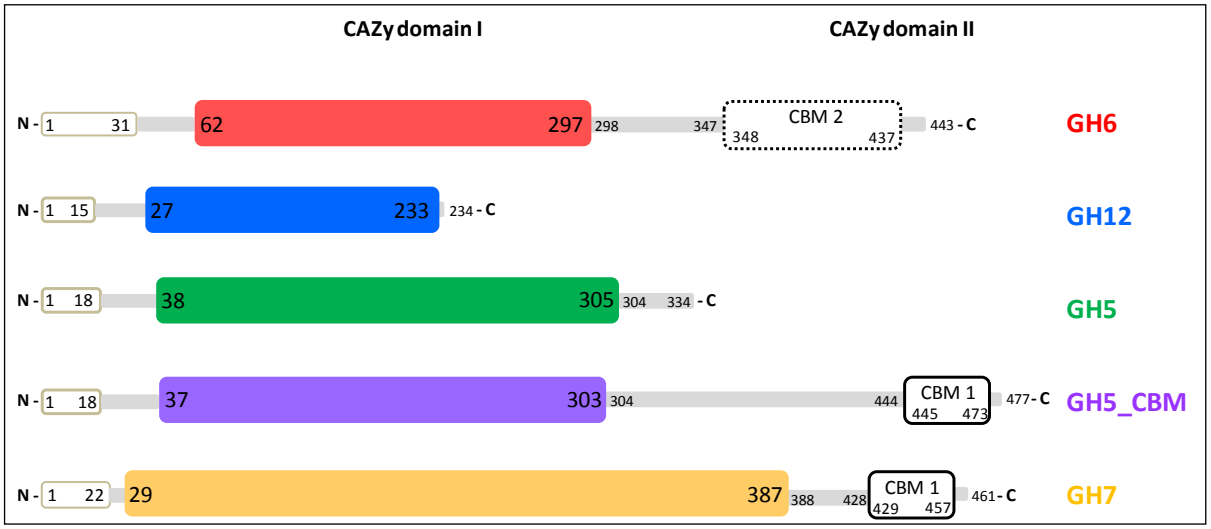

Fig. 4.1. Predicated positions of amino acids at the linear structure from N terminal to C terminal of EGs. The catalytic domains are shown in distinct colors (domain I) and CBMs are referred as domain II.

4.6.2. INTERACTION OF EGS WITH CELLULOSE SURFACE

To study how EGs interact and act on the cellulosic substrate, their interaction with cellulose was demonstrated using QCM-D by monitoring changes in frequency and dissipation during the incubation period with different purified EGs (Fig. 4.2). The frequency curve allows to evaluate gain or loss of weight (Fig. 4.2A) and the dissipation graph is related to the viscolastic modifications of the cellulose surface (Fig. 4.2B), both as function of time.

Some studies have already demonstrated the deconstruction kinetics of thin cellulose films (containing amorphous and crystalline regions) by enzyme complexes (Ahola et al., 2008; Fritz et al., 2015; Turon et al., 2008) . Studies with a single-isolated EG using the QCM-D technique have been reported on amorphous model substrate (Martin-Sampedro et al., 2012; Suchy et al., 2011) . Suchy et al. (2011) reported the systematic study on the degradation of amorphous cellulose (TMSC, trimethylsilyl cellulose) by one-component EG (EG I from *T. reesei*, EG from family 7 GH7), at different enzyme concentrations (1 - 0.01 µM). Martín-Sampedro et al. (2013) used the same enzyme to investigated the degradation kinetics of CTA (cellulose triacetate), also an amorphous cellulose substrate. The authors observed the same behavior of GH7 on amorphous substrates: an abrupt reduction of the frequency right after the enzyme being injected and immediately afterward the frequency curve started to increase. The authors attributed the immediate increase in frequency to the prompt hydrolytic effect of GH7 on the substrate, intensely solubilizing the cellulose.

In this work, using a substrate (CNF) containing crystalline as well as amorphous regions, the frequency curve profile was not similar to the profiles reported by Suchy et al. (2011) and Martín-Sampedro et al. (2013). The action of GH7 on the complex cellulosic substrate, continuously and dramatically reduced the frequency over the first 20 minutes of the reaction, in other words, the cellulose film was gaining mass (Fig. 4.2A, orange line). At the same time, the intense increase of the dissipation curve was observed (Fig. 4.2B, orange line), which allows to infer that this enzyme is causing viscoelastic modification on the surface of the material. After the frequency reduction, a short moment of equilibrium is noticed, in which the frequency reaches the maximum peak and the rate of increasing of dissipation curve is lowered. Then, the frequency curve increases, that is, the enzyme-substrate complex starts to lose mass and the dissipation curve continuously reduced the rate of increase until it practically achieves stability. After one hour of continuous injection

of enzyme, the system was washed out with fresh buffer. Like reported by Martin-Sampedro et al. (2012) and Suchy et al. (2011), rinsing buffer in the system did not show any effect on dissipation and promoted a small increase in frequency.

With the exception of GH7, the other EGs (GH5, GH5_CBM, GH6 and GH12) showed similar interaction behavior with the cellulosic substrate (Fig. 4.2), having similar curves profile as FiberCare (chapter 3, Fig. 3.6). Although there are subtle differences among them, compared to GH7, all bounded to the cellulose surface to a lesser degree and there was no increase in frequency over the period enzyme injection (Fig. 4.2A). The dissipation curve profile was also very similar among GH5, GH5_CBM, GH6 and GH12, showing intensity modification of the viscoelastic properties of the cellulose film.

The two enzymes without CBM (GH12 and GH5) had a similar substrate interaction profile. The reduction in frequency rate of the two enzymes was lower compared to GH5_CBM and GH6. However, even at a slower rate, GH12 reached the same intensity as GH5_CBM and GH6 at the end of the enzyme injection period. This differentiated adsorption profile may be related to the presence/absence of CBM, which efficiently binds and approximates the catalytic core to the substrate.

Regarding the dissipation profile over time, GH5 showed less change in intensity. Again, GH12 showed an initial behavior similar to GH5 but, during injection, at a slower rate, it reached dissipation intensity equal to GH6. GH6 and GH5_CBM had very similar behavior, reaching the same dissipation intensity after a few minutes of the contact of the enzymes with the substrate. The GH6 differed because after the beginning of the wash with buffer, it presented a small decrease in the dissipation intensity.

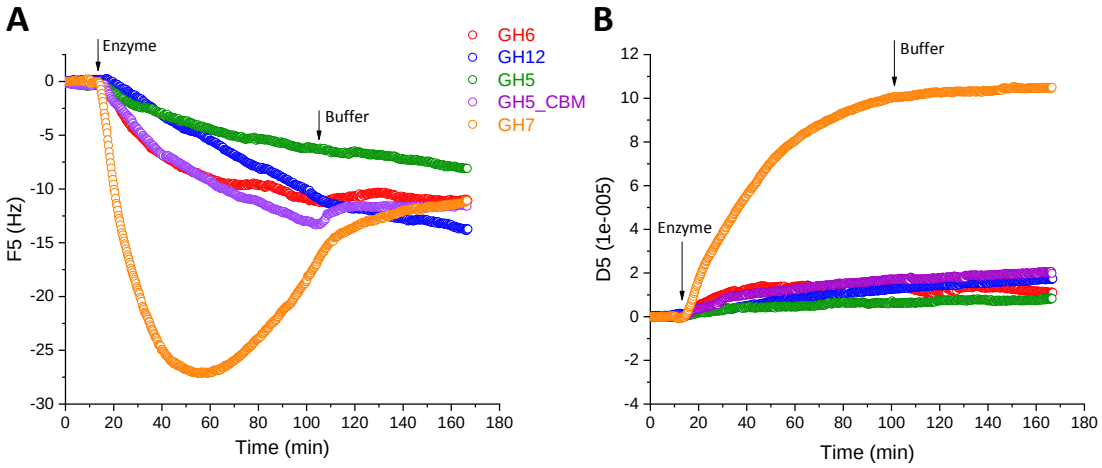

Fig. 4.2. Representative change in (A) frequency and (B) dissipation for CNF surface treated with different EGs at the same dosage and time. The frequency and dissipation are the normalized fifth overtone. The arrows indicated the time at which the CNF surfaces were exposed to enzymes or buffer.

Due to the observed differences in the interaction profiles of the different EGs with the substrate, it is possible that distinct phenomena occurred over the period of enzyme incubation. The models hypothesizing the probable stages of the enzyme-substrate interaction are shown in Fig. 4.3, using GH7 and GH6 as models. As the behavior of GH5, GH5_CBM, GH6 and GH12 were very similar, differing only in relation to small variations of frequency intensity and dissipation, GH6 was chosen as representative of this group of enzymes.

GH7 was the only EG that apparently showed hydrolytic activity according to QCM-D frequency and dissipation analysis. Looking at the frequency graph (Fig. 4.2A), GH7 was extremely efficient at binding to the substrate, which is indicated by the drastic and sharp drop in frequency, the so-called first stage, extending for 55 minutes (Fig. 4.3). The dissipation graph also shows a significant increase in the curve, which can be related to the presence of the enzyme attached to the substrate, resulting in change of the surface viscoelastic property due to the presence of proteins (Fig. 4.3 – orange line). After this period, it begins the so-called second stage, where there is an increase in frequency, associated with loss/reduction of mass. However, no decrease in dissipation is observed, instead there is a reduction in the rate of increase until practically an equilibrium.

A hypothesis for the observed reduction of mass (increasing frequency) is that it may be associated with the hydrolytic effect of the enzyme solubilizing the cellulose, but may also be associated with the fact that the enzyme bound to the substrate is being carried

from the system. By co-relating the frequency and dissipation profile, it can be inferred maybe there is a small hydrolytic effect (due to the continuous increasing of frequency), new enzymes are not binding to the substrate and probably more water molecules may be interacting with cellulose (due to the constant dissipation curve). This phenomenon is in agreement with the results reported by Siqueira et al. (2019), where an EG from GH7 (used in higher dosage and longer reaction time) was very efficient in cellulose fiber fragmentation, increasing the surface area and allowing more water molecules to interact with the fiber. Finally, at the final stage (third stage) of washing the surface with fresh buffer, the dissipation reaches the equilibrium and a slight increase in frequency is noted. It is possible to infer that a small fraction of the residual enzyme or product are still being carried from the system, but given the dissipation equilibrium the cellulosic surface has reached its saturation equilibrium with water.

When interacting with complex cellulose substrate, GH6 (and the other EGs) showed different behavior compared to GH7 (Fig. 4.3 – red line). The first stage of enzyme-substrate interaction had lower intensity of frequency drop, extending for 30 min. After this period, the rate in frequency drop decreased until reach a equilibrium level in the second stage. The same profile was observed in the dissipation curve, which had a more intense increase in the first 30 min (first stage) and after that period reached the equilibrium (second stage). Apparently, GH6 adsorbed more intensely to the thin cellulose film in the first 30 min of interaction (fall of the frequency curve). The increase in viscoelasticity (dissipation curve) may be associated with the enzyme's own adsorption to the substrate and may be interpreted as a softer new layer bound to the cellulose surface. Another hypothesis is related to the increased interaction of water with the substrate, *e.g.*, the swelling/loosening effect that the enzyme can cause on cellulose.

The increase in dissipation may be attributed to the partial degradation of the substrate and also to the increase of water uptake, forming a gel-like material (more soft and mobile) (Suchy et al. 2011). Turon et al. (2008) reported a possible sequence of substrate modifications by the cellulase complex: first the dissipation also showed a increase curve due to modification of viscoelasticity of the cellulose film; after the maximum energy dissipation is achieved, the dissipation commences to reduce due to the deconstruction and loss of the integrity of cellulosic film. However, the profiles of dissipation curve using a complex cellulase system diverge from the profile modification by a single EG. In the case of this study, a single EG, with exception of GH7, was not enough to deconstruct and release product from the cellulose film and drop the dissipation

curve. Instead, GH5, GH5_CBM, GH6 and GH12 were able to adsorve on cellulose surface and promote some superficial modifications.

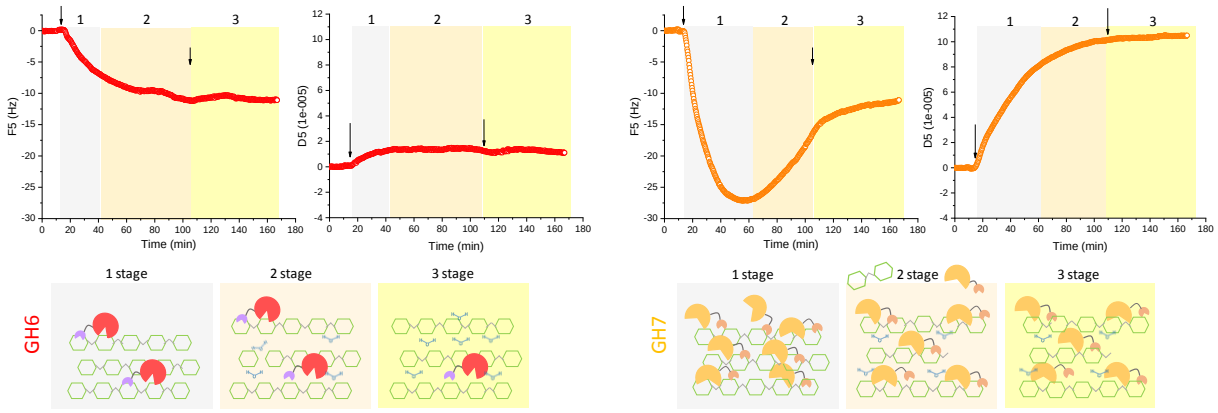

Fig. 4.3. Change in frequency and dissipation as a function of time for incubation of cellulose with GH6 (red line) or with GH7 (orange line) and schematic illustration of the stages during the interaction kinetic of EGs with CNF thin layer.

Top: arrows indicate the moment when the enzyme solution or fresh buffer injection take place; numbers are correlated with the stage of kinetic interaction of EGs with cellulose substrate; Bottom: the green symbol are representative of glucose residue bond by β-1,4 glycosidic linkage. The red and yellow circles represent GH6 and GH7, respectively. The purple and pink circles represent the CBM I and CBM II, respectively, bonded to the matching EG by linker. The molecules of water are represented by the blue H-O-H structure; the illustration is not in scale.

4.6.3. MOLECULAR WEIGHT (MW)

Gel permeation chromatography allowed to observe the effect of the different EGs on the distribution of MW and the average molecular size (MS) of BEKP (Fig. 4.4). The curves of MW distribution for the reference sample (BEKP without enzymatic treatment) and the BEKP pre-treated by the EGs had the typical shape for Kraft pulp from hardwood. That is, two distinct peaks, one for low and other for high MW distribution (Sjöholm et al., 2000).

Knowing the that typical behavior of EG is to act on less organized region of cellulose and quickly reduce the degree of polymerization but keeping in mind the differences among EGs previously discussed, some differences were observed in regard to the modification of cellulose MW distribution (Fig. 4.4A) and the average MS (Fig. 4.4A). EGs GH6, GH5, GH5_CBM and GH12 promoted a reduction of the MS distribution, shifting the peak to the left (to small size). Also, the average MW of pulp treated by these EGs was reduced from 341,484 (BEKP) to approximately 320,000 Da (mean average of

MW weight of all pulp treated by EGs). Likewise, under the same reaction condition FiberCare shifted the MW distribution to lower size and reduced the MW average (284,117 Da) more intensively than the other EGs, described in eelier chapter.. Although there are a slight differences in relation to the modifications by EGs, all of them promoted the typical changes of an EG-treatment: shifted the peak towards lower values (Gehmayr et al., 2011).

Unlike the other EGs, GH7 had no effect on reducing the molecular weight distribution (Fig. 4.4B), in accordance with the average molecular weight (Fig. 4.4B). Ibarra et al. (2010) also did not observe alteration in DP when using a EG from GH7, even at higher enzyme dosage (30 EGU/g – 1h). Correlating the lack effect on MW and the results on frequency and dissipation (Fig. 4.2), it is possible that GH7 acted on the already existing reducing or non-reducing ends. In this sense, this specify EG did not insert new ends, although some partial solubilization of cellulose was observed.

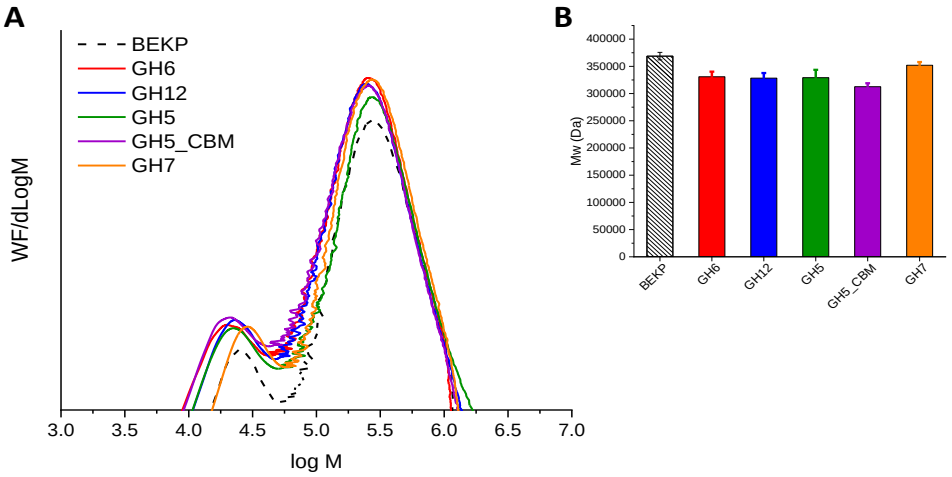

Fig. 4.4. Gel permeation chromatography by size exclusion of BEKP after pre-treatment with EGs from families GH5, 6, 7 and 12: (A) Molecular weight distribution and (B) average size of molecular weight (Mw).

4.6.4. DEFIBRILLATION PROCESS

The pulps treated with the different EGs were defibrillated in the disc ultra-refiner until a SSA of approximately 200 m^2/kg was reached, as described and justified in the previous chapter, item 3.4. Thus, it assured that all CNFs obtained from the enzymatically pre-treatment pulps using EGs from different families reached the same degree of refining. Under the same conditions, a pulp suspension without undergoing any enzymatic treatment was also refined, thereafter referred to as the control reference (BEKP). The energy consumption was monitored during defibrillation, as shown in Fig. 4.5. The control pulp (BEKP) reached the same energy consumption previously described in chapters 2 and 3

(20.5 kWh / kg), which is considered the maximum consumption for CNF production, applying the refining parameters described (1% of dry matter content, 1,600 rpm and -100 µm of disc distance).

Enzymatic pre-treatments with EGs from different families were effective in reducing energy demand in different extension, with the exception of GH7. The pulp treated with GH7 resulted in the same energy consumption as the control pulp, reaching the range of 20 kWh/kg. As shown in the enzyme-substrate interaction assay, GH7 again behaved differently from other enzymes in the consumption of energy. GH7 was the only EG that had a hydrolytic effect on the cellulose film (Fig. 4.2) and possibly the partial solubilization of cellulose had a negative effect on the reduction of the energy consumption.

There was a reduction in energy consumption for the pulps treated with GH5, GH5_CBM, GH6 and GH12, but there were differences among the extent of energy reduction. The difference of energy reduction among the samples was confirmed by statistical analyses (Tukey test) and corroborates with the similarities and differences between the EGs (Fig. 4.5). Interestingly, EGs, GH5 and GH12, , which do not have a CBM, had the least effect on reducing energy consumption, reaching 17.5 kWh/kg that represents 14.6% reduction in relation to the control pulp. The greatest reductions in energy consumption were achieved for the pre-treated pulps with GH5_CBM and GH6, both connected to CBM. GH5_CBM pulp refining achieved energy consumption equal to 15.5 kWh/kg, representing 24.4% reduction. GH6 pre-treatment resulted in the largest reduction in energy consumption (31.7%), consuming only 14 kWh/kg. A similar energy reduction (30 %) was achieved applying a GH5 from *P. horikoshii* at an enzyme dosage equal to 1 mg/g and longer reaction time (48 h) to pre-treated BEKP and prior to delamination in a microfluidizer (Wang et al., 2015).

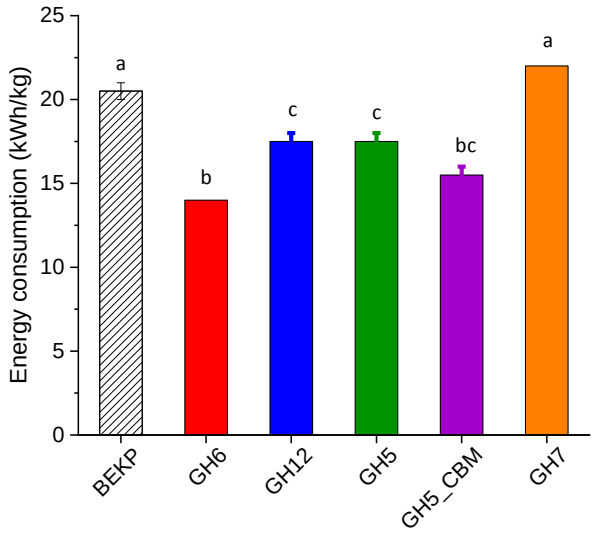

Fig. 4.5. Energy consumption monitored during the defibrillation process in disc ultra-refiner of pulp pre-treated by EGs from different families. The control reference (without pre-treatment) is called BEKP.

Differences among the EGs, indeed, had different effects on the energy consumption in the defibrillation of each pre-treated pulps by each enzyme. A very pertinent observation is concerning the presence/absence of the CBM. With the exception of GH 7, all EGs that have the binding structure had the greatest effect on reducing energy consumption, including the commercial EG, FiberCare (potential having the CBM). The presence of CBM, probably in addition to more efficiently approximating the catalytic core to the substrate, possibly also had an effect on the structural modification of the cellulose surface, the so-called amorphogenesis effect (Arantes and Saddler, 2010; Bernardes et al., 2019). This possible structural modification caused by CBM may have a greater beneficial effect on reducing energy demand than EG's own catalytic activity. This hypothesis is evidenced by the energy consumption result of the pulp treated with the GH7.

GH7 was the only EG that had a hydrolytic effect (partial solubilization of cellulose, as the frequency increased, Fig. 4.2A), and the only one that did not reduce the energy consumption. Even though this enzyme has CBM associated to the catalytic core, the hydrolytic action impaired the possible gain in reducing energy consumption. Probably the CBM bind to the of less organized fraction of cellulose and cause structural changes in this region. As there was some hydrolysis of this fraction, CBM did not promote the amorphogenesis effect. In addtion, when observing the effect of GH7 on pulp molecular weight after enzyme treatment, this enzyme showed no reduction in molecular weight,

differently of what was recently reported by Rahikainen et al. (2019) when using 1 g of protein/g of softwood Kraft pulp during 2h. One explanation for this effect is that GH7 used in the mild condition (5.6 EGU/g – 1h) did not insert new terminals into the cellulose chain, but acted and released sugars from the existing terminals, not modifying the molecular weight. In addition, Rahikainen et al. (2019) reported that GH7 was the less efficient EG (than GH5 and GH45) to reduce the viscosity of the cellulosic pulp, did not promote morphological modification of the fiber and also was less selective for cellulose as reported by Vlasenko et al. (2010). The combination of the hydrolyses on the less ordered region and the non reduction the molecular weight could be addressed to the lack to energy reduction on defibrillation process. On the other hand, GH6 was the more efficient enzyme to reduce the energy consumption. This profile can be a combination of several effects: the presence of CBM to promote structural modification (Arantes and Saddler, 2010; Bernardes et al., 2019), the lack the hydrolytic effect (Fig. 4.2) and the catalytic core with the inverting mechanism, as the same as EG from family 45, being efficient to increase the reactive of the pulp (Ibarra et al., 2010).

4.6.5. MORPHOLOGICAL ASPECT OF CNFs

The CNFs obtained by enzymatic pre-treatment with the different EGs have been morphologically characterized. The micrographs obtained by high contrast SEM were used to analyze the morphological structure of the CNFs and to determine the sizes of the diameters (distribution and average diameter) (Fig. 4.6). It was not determined the length due to the entangled network conformation and the long dimension in the fiber direction, not allowing the visualization to identify the beginning and the end of a single nanofibril structure.

Although EGs showed different interaction profiles with the cellulosic substrate, energy consumption in the defibrillation process and in the distribution of molecular weight, the morphological aspects of the CNFs obtained by enzymatic pre-treatment did not show any difference among them. The entangled structure and the high aspect ratio were preserved and the distribution of the diameters and the mean diameters were very similar among them (Fig 4.6). The same entangled network conformation was observed for the FiberCare pre-treated CNF (Chapter 3).

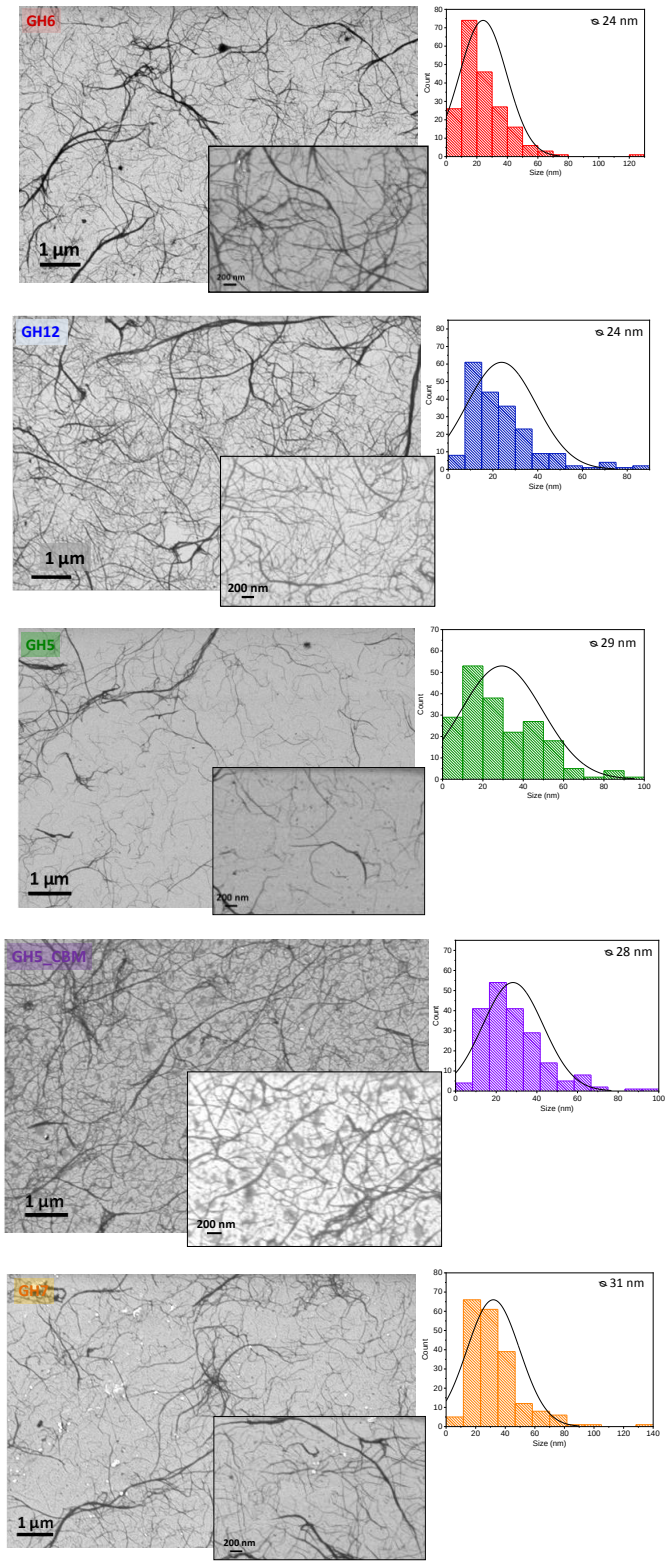

Fig. 4.6. Micrographs obtained by scanning electron microcopy with high contrast of nanofibrils isolated with enzymatic pre-treatment with (A) endoglucanase GH6; (B) endoglucanase GH12; (C) endoglucanase GH5; (D) endoglucanase GH5_CBM and endoglucanase GH7 (B). Scale bar equal to 1 µm and the zoom-in micrographs with a

scale bar equal to 200 nm. Graphs of diameter distribution were determined from the respective images.

The EGs that most reduced the energy consumption the (GH6) and EG that was not able to reduce the consumption and had a distinctive behavior of interaction with cellulose (GH7), when applied in the enzymatic pre-treatment, led to the isolation of CNFs with very similar structural dimensions. Nanofibrils isolated by GH6-pre-treatment had a mean average diameter of 24 nm. GH7 pre-treatment resulted in nanofibrils with average diameter equal to 31 nm, being quite similar to the control reference (BEKP without enzymatic pre-treatment (chapter 3, Fig. 3.2). GH12 pretreatment resulted in nanofibrils with mean diameter similar to those isolated from the pre-treatment with GH6, approximately 24 nm. GH5 and GH5_CBM produced nanofibrils with no difference in mean diameter, which was approximately 28 nm.

The small variation of the mean diameter among the nanofibrils are to negligible and, because of that, apparently, the differences among EGs and the presence/lack of CBM had no influence in the final morphological structure of isolated nanofibrils. In chapter 2, an EG from family GH45 also resulted in CNF with morphology very similar to the reference. All CNFs obtained by enzymatic pre-treatment showed the entangled network formation, consequently, preserving rheological properties (Pääkko et al., 2007; Wang et al., 2015). Furthermore, the GH6 pre-treatment was able to reduce the energy consumption in 30% without compromising the morphological structure. As the morphology of the isolated nanofibrils was not compromised, the morphology of pre-treated pulps possible was also preserved. Apparently, the reduction in energy demand is associated to molecular modification (*e.g.*, change in molecular weight and interaction of enzyme-substrate) than to macro-structural modification.

Some authors have reported that EGs from different families promoted distinctive visual modifications to cellulosic pulp fibers such as surface fibrillation or fiber fragmentation (Rahikainen et al., 2019; Siqueira et al., 2019). However, there are some divergences concerning how intense and which type of modification EGs from different families promote on pulp fibers. Siqueira et al. (2019) demonstrated that GH7 from *T. longibrachiatum* linked to CBM was very efficient to fragment BEKP fibers. On the other hand, Rahikainen et al. (2019) reported that GH7 from *T. ressei*, also associated to a CBM, did not alter the fiber structure. This divergent behavior can be related to the enzymatic hydrolysis condition. The more harsh condition (400 EGU/g – 72 h) promoted the

fragmentation (Siqueira et al., 2019) and the milder condition (0.2 mg/g – 2 h) did not promote visual modification of cellulose surface (Rahikainen et al., 2019). This observation can be correlated with the lack of morphological differences observed in this study and with the used condition in enzymatic pre-treatment. It is possible that the very mild condition (5.6 EGU/g -1 h) did not promoted surface modification or fragmentation. This observation is supported by Wang et al. (2015) who reported that the increase in the enzyme dosage (GH5 from *P. horikoshii*) from 1 to 10 mg/g resulted in reduction of the length nanofibrils isolated by 30 passes in a microfluidizer.

4.6.6. RHEOLOGICAL PROPERTIES

The rheological properties (shear stress storage and loss moduli) of the suspensions of CNFs obtained with the enzymatic pre-treatment using the different EGs were also investigated (Fig. 4.7). The control pulp (BEKP), used as a reference without enzymatic treatment, was also characterized. All results were obtained using 1% dry matter content and at fixed temperature (23 °C) to ensure the quality of the differentiation among the samples, attributed to the possible action of the enzymes.

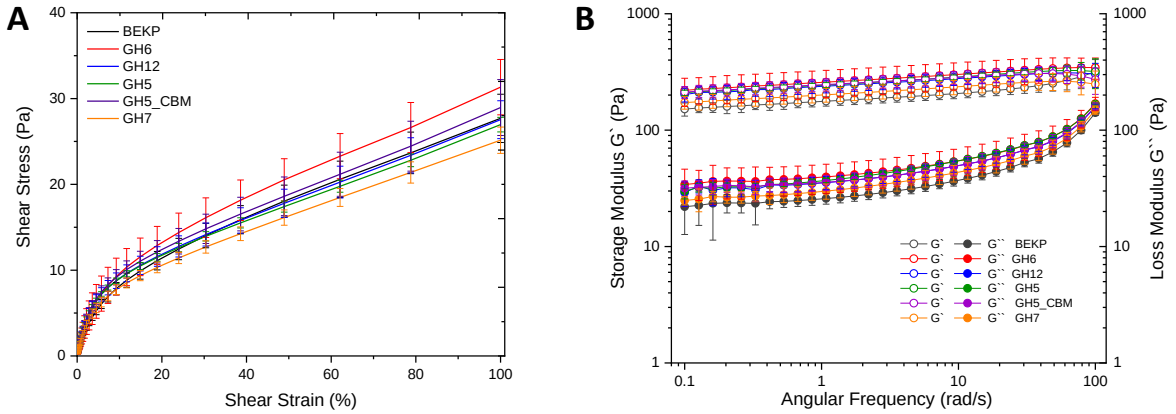

Fig. 4.7. Rheological characterization of CNFs obtained by enzymatic pre-treatment using EGs from different families. (A) The shear stress under different shear rate and (B) storage (empty symbols) and loss (filled symbols) moduli as a function of the angular frequency at 1% solid content using parallel flat plate geometry.

As a typical behavior of gel-like suspension, all CNFs suspensions showed a higher storage modulus than loss modulus (Fig 4.7B). Even at low solid concentration (1% w/w) the storage modulus was around 10-fold higher than loss modulus. However, some slight variations can the observed among the samples. The CNFs suspension pre-treatment with

EGs linked to the CBM (GH5, GH5 CBM, GH6 and GH12) had greater moduli when compared to the reference suspension (BEKP) and the same of the CNF resulted from FiberCare pre-treatment obtained in the previous chapter. Also, the shear stress of CNF isolated using these same enzyme was greater (GH6) or at least equal to the control reference (GH5, GH5 CBM and GH12) (Fig 4.7A).

The enzymatic pre-treatment promoted a beneficial effect to isolated CNF. Apparently, the slight surface modification (Fig. 4.2B) was enough to increase the water interaction with cellulose surface and also adequate to preserve the entangled formation, resulting in outstanding rheological behavior. In the case of CNF obtained from GH7 pre-treatment, the storage and loss modulie and the shear stress were quite lower than the reference value. It might be related to the hydrolytic action of the enzyme, partially solubilizing the less organized region (Fig. 4.2A) and at the same time not inserting new chain ends.

4.7. CONCLUSION

EGs from four different GH families (5, 6, 7 and 12), were assessed under the mild reaction condition in a single-step pre-treatment of BEKP for further CNF isolation in a disc-ultra-refiner. The presence or lack of a CBM was another enzymatic property investigated. The enzymatic pre-treatment reduced the energy consumption at the defibrillation process in an extent that ranged from 14 to 30%, with the expectation of GH7, which did not reduce the energy demand under the tested condition. The EGs associated to CBM (GH6 and GH5_CBM) were the most efficient enzymes in reducing energy (up to 30%). These enzymes did not have a noticeable hydrolytic action on cellulose polymer but promoted structural modification (*e.g.*, reduced the molecular weight and increased the viscoelasticity of the cellulose surface) and adsorption on the cellulose surface. Apparently, the surface modification had a more beneficial effect for saving energy than the hydrolytic action. Further investigation of the isolated CNFs demonstrated that the morphological and rheological properties were preserved and, in same case, even improved (e.g. GH6 improved the rheological property).

5. MAIN CONCLUSIONS AND FUTURE WORK PROPOSE

The kinetic study of the defibrillation of bleached eucalyptus Kraft pulp using the disc ultra-refiner SuperMassColloider was suitable for isolating MFC and CNF. The most intense modification in properties occurred at the beginning of the process, resulting MFC. Further defibrillation resulted in CNF with smaller diameter. The detailed study of key properties and energy consumption allows to achieve a suitable degree of defibrillation for the desirable applications. Further systematic investigation of ultra-refining parameters should be conduct aiming to increase the high content and, consequently, improving the efficient of the system.

The understanding of the effect of different enzymatic pre-treatment conditions in a single-step using an EG monocomponent for CNF isolation by disc ultra-refiner allow to tailor the properties of the final nanomaterial and the energy demand. The optimal condition to save the maximum amount of energy while still preserving the rheological property was predicted and validated. At this condition, the EG-driven pre-treatment improved the cellulose-water interaction, introduced new ends and reduced molecular weight, but do not solubilized. The single-step enzymatic pre-treatment, which it is a green and sustainable route, was demonstrated to be a potential approach for the high energy consumption and by varying the pre-treatment conditions it is also possible to tailor the final properties of the CNF to achieve the most desirable property, which will depend on the target application.

Further investigation of EGs from four different families (5, 6, 7 and 12) of glycoside hydrolase (GH), with different properties, in a single-step pre-treatment for CNF isolation revealed that under the same reaction condition, the different EGs reduced the energy consumption to different extents, with the expectation of the GH7, which did not reduce the energy demand and the only that released soluble products. The EGs linked to a CBM were the most efficient enzymes in reducing energy and improving the rheology and preserving the morphology. These enzymes did not have a noticeable hydrolytic action on cellulose but promoted structural modification and adsorption on the cellulose surface. Apparently, these effects were more beneficial than their hydrolytic action for saving energy during the defibrillation process. The disclosure about the features of EGs and CBM that could influence the energy demand in the defibrillation process can be further explored. There is a large range of different EGs linked to one or more CBMs that could boost the process. In addition, there are CBMs from different families and the investigation of CBMs by themselves could be another approach for CNF production.

6. REFERENCES

Ahola, S., Salmi, J., Johansson, L.S., Laine, J., Österberg, M., 2008. Model films from native cellulose nanofibrils. Preparation, swelling, and surface interactions. Biomacromolecules 9, 1273–1282. https://doi.org/10.1021/bm701317k

Arantes, V., Saddler, J.N., 2010. Access to cellulose limits the efficiency of enzymatic hydrolysis: the role of amorphogenesis. Biotechnol. Biofuels 3, 1–11. https://doi.org/10.1186/1754-6834-3-4

Assis, C.A. de, Iglesias, M.C., Bilodeau, M., Johnson, D., Phillips, R., Peresin, M.S., Bilek, E.M. (Ted), Rojas, O.J., Venditti, R., Gonzalez, R., 2018. Cellulose micro- and nanofi brils (CMNF) manufacturing - financial and risk assessment. Biofuels, Bioprod. Biorefining 12, 251–264. https://doi.org/10.1002/bbb.1835

Aulin, C., Gallstedt, M., Lindström, T., 2010. Oxygen and oil barrier properties of microfibrillated cellulose films and coatings. Cellulose 17, 559–574. https://doi.org/10.1007/s10570-009-9393-y

Baati, R., Magnin, A., Boufi, S., 2017. High solid content production of nanofibrillar cellulose via continuous extrusion. ACS Sustain. Chem. Eng. 5, 2350–2359. https://doi.org/10.1021/acssuschemeng.6b02673

Bernardes, A., Pellegrini, V.O.A., Curtolo, F., Camilo, C.M., Mello, B.L., Johns, M.A., Scott, J.L., Guimaraes, F.E.C., Polikarpov, I., 2019. Carbohydrate binding modules enhance cellulose enzymatic hydrolysis by increasing access of cellulases to the substrate. Carbohydr. Polym. 211, 57–68. https://doi.org/10.1016/j.carbpol.2019.01.108

Berto, G.L., Arantes, V., 2019. Kinetic changes in cellulose properties during defibrillation into microfibrillated cellulose and cellulose nanofibrils by ultra-refining. Int. J. Biol. Macromol. 127, 637–648. https://doi.org/10.1016/j.ijbiomac.2019.01.169

Berto, G.L., Velasco, J., Tasso Cabos Ribeiro, C., Zanphorlin, L.M., Noronha Domingues, M., Tyago Murakami, M., Polikarpov, I., de Oliveira, L.C., Ferraz, A., Segato, F., 2019. Functional characterization and comparative analysis of two heterologous endoglucanases from diverging subfamilies of glycosyl hydrolase family 45. Enzyme Microb. Technol. 120, 23–35. https://doi.org/10.1016/j.enzmictec.2018.09.005

Besbes, I., Alila, S., Boufi, S., 2011. Nanofibrillated cellulose from TEMPO-oxidized eucalyptus fibres: Effect of the carboxyl content. Carbohydr. Polym. 84, 975–983. https://doi.org/10.1016/j.carbpol.2010.12.052

Borregaard, 2019. Borregaard Exilva - Application [WWW Document]. Web Page. URL https://www.exilva.com/ (accessed 12.7.19).

Boufi, S., González, I., Delgado-Aguilar, M., Tarrès, Q., Pèlach, M.À., Mutjé, P., 2016. Nanofibrillated cellulose as an additive in papermaking process: a review. Carbohydr. Polym. 154, 151–166. https://doi.org/10.1016/j.carbpol.2016.07.117

Brinchi, L., Cotana, F., Fortunati, E., Kenny, J.M., 2013. Production of nanocrystalline cellulose from lignocellulosic biomass: Technology and applications. Carbohydr. Polym. 94, 154–169. https://doi.org/10.1016/j.carbpol.2013.01.033

Campos, A. De, Carolina, A., David, C., Eliangela, C., 2013. Obtaining nanofibers from curaua fibers using enzymatic hydrolysis followed by sonication. Cellulose 20, 1491–1500. https://doi.org/10.1007/s10570-013-9909-3

CAZy, 1998. CAZy: Carbohydrate-Active enZYmes Database [WWW Document]. Web Page. URL http://www.cazy.org/ (accessed 1.10.20).

Chaker, A., Mutjé, P., Vilar, M.R., Boufi, S., 2014. Agriculture crop residues as a source for the production of nanofibrillated cellulose with low energy demand. Cellulose 21, 4247–4259. https://doi.org/10.1007/s10570-014-0454-5

Chakraborty, A., Sain, M., Kortschot, M., 2005. Cellulose microfibrils: A novel method of preparation using high shear refining and cryocrushing. Holzforschung 59, 102–107. https://doi.org/10.1515/HF.2005.016

Chen, Y., Jiang, Y., Wan, J., Wu, Q., Wei, Z., Ma, Y., 2018. Effects of wet-pressing induced fiber hornification on hydrogen bonds of cellulose and on properties of eucalyptus paper sheets. Holzforschung 72, 829–837. https://doi.org/10.1515/hf-2017-0214

Chinga-Carrasco, G., 2011. Cellulose fibres, nanofibrils and microfibrils : the morphological sequence of MFC components from a plant physiology and fibre technology point of view. Nanoscale Res. Lett. 6, 417. https://doi.org/10.1186/1556-276X-6-417

Chylenski, P., Forsberg, Z., Ståhlberg, J., Várnai, A., Lersch, M., Bengtsson, O., Sæbø, S., Horn, S.J., Eijsink, V.G.H., 2017. Development of minimal enzyme cocktails for hydrolysis of sulfite-pulped lignocellulosic biomass. J. Biotechnol. 246, 16–23. https://doi.org/10.1016/j.jbiotec.2017.02.009

Cohen, R., Suzuki, M.R., Hammel, K.E., Cohen, R., Suzuki, M.R., Hammel, K.E., 2005. Processive endoglucanase active in crystalline cellulose hydrolysis by the brown rot basidiomycete Gloeophyllum trabeum. Appl. Environ. Microbiol. 5, 2112–2417. https://doi.org/10.1128/AEM.71.5.2412

Czaja, W.K., Young, D.J., Kawecki, M., Brown, R.M., 2007. The future prospects of microbial cellulose in biomedical applications. Biomacromolecules 8, 1–12. https://doi.org/10.1021/bm060620d

Dashtban, M., Maki, M., Leung, K.T., Mao, C., Qin, W., 2010. Cellulase activities in biomass conversion: measurement methods and comparison. Crit. Rev. Biotechnol. 30, 302–309. https://doi.org/10.3109/07388551.2010.490938

Davies, G., Henrissat, B., 1995. Structures and mechanisms of glycosyl hydrolases. Structure 3, 853–859.

Dogan, N., McHugh, T.H., 2007. Effects of microcrystalline cellulose on functional properties of hydroxy propyl methyl cellulose microcomposite films. J. Food Sci. 72. https://doi.org/10.1111/j.1750-3841.2006.00237.x

Dufresne, A., 2013. Nanocellulose: A new ageless bionanomaterial. Mater. Today 16, 220–227. https://doi.org/10.1016/j.mattod.2013.06.004

Dufresne, Alain, 2012. Nanocellulose : From Nnature to high performance tailored materials. Munchen, DEU.

Dufresne, Alain., 2012. Thermal properties, 1st ed, Nanocellulose : from nature to high performance tailored materials. Walter de Gruyter, Munchen, DEU.

Eichhorn, S.J., Dufresne, A., Aranguren, M., Marcovich, N.E., Capadona, J.R., Rowan, S.J., Weder, C., Thielemans, W., Roman, M., Renneckar, S., Gindl, W., Veigel, S., Keckes, J., Yano, H., Abe, K., Nogi, M., Nakagaito, A.N., Mangalam, A., Simonsen,

J., Benight, A.S., Bismarck, A., Berglund, L.A., Peijs, T., 2010. Review: Current international research into cellulose nanofibres and nanocomposites. J. Mater. Sci. 45, 1–33. https://doi.org/10.1007/s10853-009-3874-0

Espinosa, E., Rol, F., Bras, J., Rodríguez, A., 2019. Production of lignocellulose nanofibers from wheat straw by different fibrillation methods. Comparison of its viability in cardboard recycling process. J. Clean. Prod. 239, 118083. https://doi.org/10.1016/j.jclepro.2019.118083

Fang, Z., Zhu, H., Li, Y., Liu, Z., Dai, J., Preston, C., Garner, S., Cimo, P., Chai, X., Chen, G., Hu, L., 2014. Light management in flexible glass by wood cellulose coating. Sci. Rep. 4, 1–7. https://doi.org/https://10.1038/srep05842

Fengel, D., Wegener, G., 1989. Wood : Chemistry, ultrastructure, reactions, Walter de Gruyter. Berlin. https://doi.org/10.1163/157006610X530330

French, A.D., 2014. Idealized powder diffraction patterns for cellulose polymorphs. Cellulose 21, 885–896. https://doi.org/10.1007/s10570-013-0030-4

Fritz, C., Ferrer, A., Salas, C., Jameel, H., Rojas, O.J., 2015. Interactions between cellulolytic enzymes with native, autohydrolysis, and technical lignins and the effect of a polysorbate amphiphile in reducing nonproductive binding. Biomacromolecules 16, 3878–3888. https://doi.org/10.1021/acs.biomac.5b01203

Gehmayr, V., Schild, G., Sixta, H., 2011. A precise study on the feasibility of enzyme treatments of a kraft pulp for viscose application. Cellulose 18, 479–491. https://doi.org/10.1007/s10570-010-9483-x

Habibi, Y., Lucia, L.A., Rojas, O.J., 2010. Cellulose nanocrystals: Chemistry, self-assembly, and applications. Chem. Rev. 110, 3479–3500. https://doi.org/10.1021/cr900339w

Haq, I. ul, Akram, F., Khan, M.A., Hussain, Z., Nawaz, A., Iqbal, K., Shah, A.J., 2015. CenC, a multidomain thermostable GH9 processive endoglucanase from Clostridium thermocellum: cloning, characterization and saccharification studies. World J. Microbiol. Biotechnol. 31, 1699–1710. https://doi.org/10.1007/s11274-015-1920-4

Hassan, M.L.., Mathew, A.P., Hassan, E. a, Oksman, K., 2010. Effect of pretreatment of bagasse pulp on properties of isolated nanofibers and nanopaper sheets. Wood fiber Sci. 42, 362–376.

Henriksson, G., Lennholm, H., 2009. Pulp and paper chemistry and technology wood chemistry and wood biotechnology, Volume 1. ed, Pulp and paper chemistry and technology: Wood chemistry and wood biotechnology. Berlin.

Henriksson, M., Henriksson, G., Berglund, L. a., Lindström, T., 2007. An environmentally friendly method for enzyme-assisted preparation of microfibrillated cellulose (MFC) nanofibers. Eur. Polym. J. 43, 3434–3441. https://doi.org/10.1016/j.eurpolymj.2007.05.038

Henrissat, B., Vegetales, M., Grenoble, F., 1991. A classification of glycosyl hydrolases based sequence similarities amino acid. Biochem. J. 280, 309–316. https://doi.org/10.1007/s007920050009

Hoeger, I.C., Nair, S.S., Ragauskas, A.J., Deng, Y., Rojas, O.J., Zhu, J.Y., 2013. Mechanical deconstruction of lignocellulose cell walls and their enzymatic saccharification. Cellulose 20, 807–818. https://doi.org/10.1007/s10570-013-9867-9

Horn, S.J., Vaaje-Kolstad, G., Westereng, B., Eijsink, V.G., 2012. Novel enzymes for the degradation of cellulose. Biotechnol. Biofuels 5, 45. https://doi.org/10.1186/1754-6834-5-45

Hu, J., Tian, D., Renneckar, S., Saddler, J.N., 2018. Enzyme mediated nanofibrillation of cellulose by the synergistic actions of an endoglucanase, lytic polysaccharide monooxygenase (LPMO) and xylanase. Sci. Rep. 8, 4–11. https://doi.org/10.1038/s41598-018-21016-6

Hu, L., Zheng, G., Yao, J., Liu, N., Weil, B., Eskilsson, M., Karabulut, E., Ruan, Z., Fan, S., Bloking, J.T., McGehee, M.D., Wågberg, L., Cui, Y., 2013. Transparent and conductive paper from nanocellulose fibers. Energy Environ. Sci. 6, 513–518. https://doi.org/https://10.1039/C2EE23635D

Hubbe, M. a., Ferrer, A., Tyagi, P., Yin, Y., Salas, C., Pal, L., Rojas, O.J., 2017. Nanocellulose in thin films, coatings, and plies for packaging applications: A review. BioResources 12, 2143–2233. https://doi.org/10.15376/biores.12.1.2143-2233

Ibarra, D., Köpcke, V., Ek, M., 2010. Behavior of different monocomponent endoglucanases on the accessibility and reactivity of dissolving-grade pulps for viscose process. Enzyme Microb. Technol. 47, 355–362. https://doi.org/10.1016/j.enzmictec.2010.07.016

Igarashi, K., Ishida, T., Hori, C., Samejima, M., 2008. Characterization of an Endoglucanase Belonging to a New Subfamily of Glycoside Hydrolase Family 45 of the Basidiomycete 74, 5628–5634. https://doi.org/10.1128/AEM.00812-08

Isogai, A., Saito, T., Fukuzumi, H., 2011. TEMPO-oxidized cellulose nanofibers. Nanoscale 3, 71–85. https://doi.org/10.1039/c0nr00583e

Iwamoto, S., Nakagaito, A.N., Yano, H., 2007. Nano-fibrillation of pulp fibers for the processing of transparent nanocomposites. Appl. Phys. A Mater. Sci. Process. 89, 461–466. https://doi.org/10.1007/s00339-007-4175-6

Iwamoto, S., Nakagaito, A.N., Yano, H., Nogi, M., 2005. Optically transparent composites reinforced with plant fiber-based nanofibers. Appl. Phys. A Mater. Sci. Process. 81, 1109–1112. https://doi.org/10.1007/s00339-005-3316-z

Josefsson, P., Henriksson, G., Wågberg, L., 2008. The physical action of cellulases revealed by a quartz crystal microbalance study using ultrathin cellulose films and pure cellulases. Biomacromolecules 9, 249–254. https://doi.org/10.1021/bm700980b

Kalia, S., Boufi, S., Celli, A., Kango, S., 2014. Nanofibrillated cellulose: Surface modification and potential applications. Colloid Polym. Sci. 292, 5–31. https://doi.org/10.1007/s00396-013-3112-9

Kangas, H., Lahtinen, P., Sneck, A., Saariaho, A.-M., Laitinen, O., Hellén, E., 2014. Characterization of fibrillated celluloses: a short review and evaluation of characteristics with a combination of methods. Nord. Pulp Pap. Res. J. 29, 129–43. https://doi.org/10.3183/NPPRJ-2014-29-01-p129-143

Kim, U., Hyun, S., Wada, M., 2010. Thermal decomposition of native cellulose : In fl uence on crystallite size. Polym. Degrad. Stab. 95, 778–781. https://doi.org/https://10.1016/j.polymdegradstab.2010.02.009

Klemm, D., Kramer, F., Moritz, S., Lindström, T., Ankerfors, M., Gray, D., Dorris, A., 2011. Nanocelluloses: A new family of nature-based materials. Angew. Chemie - Int. Ed. 50, 5438–5466. https://doi.org/10.1002/anie.201001273

Kontturi, E., Laaksonen, P., Linder, M.B., Nonappa, Gröschel, A.H., Rojas, O.J., Ikkala, O., 2018. Advanced materials through assembly of nanocelluloses. Adv. Mater. 30. https://doi.org/10.1002/adma.201703779

Korhonen, J.T., Kettunen, M., Ras, R.H.A., Ikkala, O., 2011. Hydrophobic nanocellulose aerogels as floating, sustainable, reusable, and recyclable oil absorbents. ACS Appl. Mater. Interfaces 3, 1813–1816. https://doi.org/https://10.1021/am200475b

Kumar, V., Bollstrom, R., Yang, A., Chen, Q., Chen, G., Pekka, S., Bousfield, D., Toivakka, M., 2014. Comparison of nano- and microfibrillated cellulose films. Cellulose 21, 3443–3456. https://doi.org/https://10.1007/s10570-014-0357-5

Langford, J.I., Wilson, A.J.C., 1978. Seherrer after sixty years: A survey and some new results in the determination of crystallite size. J. Appl. Crysrallography 11, 102–113.

Lavoine, N., Desloges, I., Dufresne, A., Bras, J., 2012. Microfibrillated cellulose - Its barrier properties and applications in cellulosic materials: A review. Carbohydr. Polym. 90, 735–764. https://doi.org/10.1016/j.carbpol.2012.05.026

Lehmonen, J., Pere, J., Hytönen, E., Kangas, H., 2017. Effect of cellulose microfibril (CMF) addition on strength properties of middle ply of board. Cellulose 24, 1041–1055. https://doi.org/10.1007/s10570-016-1146-0

Leite, A.L.M.P., Zanon, C.D., Menegalli, F.C., 2017. Isolation and characterization of cellulose nanofibers from cassava root bagasse and peelings. Carbohydr. Polym. 157, 962–970. https://doi.org/10.1016/j.carbpol.2016.10.048

Levasseur, A., Drula, E., Lombard, V., Coutinho, P.M., Henrissat, B., 2013. Expansion of the enzymatic repertoire of the CAZy database to integrate auxiliary redox enzymes. Biotechnol. Biofuels 41, 1–14.

Li, W., Zhao, X., Huang, Z., Liu, S., 2013. Nanocellulose fibrils isolated from BHKP using ultrasonication and their reinforcing properties in transparent poly (vinyl alcohol) films. J. Polym. Res. 20. https://doi.org/10.1007/s10965-013-0210-9

Magalhaes, W.E., Cao, X., Lucia, L.A., 2009. Cellulose nanocrystals/cellulose core-in-shell nanocomposite assemblies. Langmuir 25, 13250–13257. https://doi.org/10.1021/la901928j

Mariano, M., El Kissi, N., Dufresne, A., 2014. Cellulose nanocrystals and related nanocomposites: Review of some properties and challenges. J. Polym. Sci. Part B Polym. Phys. 52, 791–806. https://doi.org/10.1002/polb.23490

Martin-Sampedro, R., Filpponen, I., Hoeger, I.C., Zhu, J.Y., Laine, J., Rojas, O.J., 2012. Rapid and complete enzyme hydrolysis of lignocellulosic nanofibrils. ACS Macro Lett. 1, 1321–1325. https://doi.org/10.1021/mz300484b

Mattos, B.D., Tardy, B.L., Rojas, O.J., 2019. Accounting for substrate interactions in the measurement of the dimensions of cellulose nanofibrils. Biomacromolecules 20, 2657–2665. https://doi.org/10.1021/acs.biomac.9b00432

Miller, G.L., 1959. Use of Dinitrosalicylic Acid Reagent for Determination of Reducing Sugar. Anal. Chem. 31, 426–428. https://doi.org/10.1021/ac60147a030

Miller, J., 2019. Nanocellulose: Packaging applications and commercial development. TAPPI Int. Conf. Nanotechnol. For. Prod. Ind.

Miller, J., 2017. Nanocellulose : producers, products and applications: a guide for end users. TAPPI Nano 175.

Miller, J., 2015. Nanocellulose: State of the Industry. TAPPI Int. Conf. Nanotechnol. For. Prod. Ind.

Moberg, T., Sahlin, K., Yao, K., Geng, S., Westman, G., Zhou, Q., Oksman, K., Rigdahl, M., 2017. Rheological properties of nanocellulose suspensions : effects of fibril / particle dimensions and surface characteristics. Cellulose 24, 2499–2510. https://doi.org/https://10.1007/s10570-017-1283-0

Moon, R., Walker, C., 2012. Research into cellulose nanomaterials spans the globe. Paper360° May/June, 32–34.

Moon, R.J., Martini, A., Nairn, J., Simonsen, J., Youngblood, J., 2011. Cellulose nanomaterials review: structure, properties and nanocomposites, Chemical Society Reviews. https://doi.org/10.1039/c0cs00108b

Moreau, C., Tapin-Lingua, S., Grisel, S., Gimbert, I., Le Gall, S., Meyer, V., Petit-Conil, M., Berrin, J.G., Cathala, B., Villares, A., 2019. Lytic polysaccharide monooxygenases (LPMOs) facilitate cellulose nanofibrils production. Biotechnol. Biofuels 12, 13–17. https://doi.org/10.1186/s13068-019-1501-0

Naderi, A., Lindström, T., Sundström, J., 2015. Repeated homogenization, a route for decreasing the energy consumption in the manufacturing process of carboxymethylated nanofibrillated cellulose? Cellulose 22, 1147–1157. https://doi.org/10.1007/s10570-015-0576-4

Nair, S.S., Zhu, J.Y., Deng, Y., Ragauskas, A.J., 2014. Characterization of cellulose nanofibrillation by micro grinding. J. Nanoparticle Res. 16. https://doi.org/10.1007/s11051-014-2349-7

Nakagaito, a. N., Yano, H., 2004. The effect of morphological changes from pulp fiber towards nano-scale fibrillated cellulose on the mechanical properties of high-strength plant fiber based composites. Appl. Phys. A Mater. Sci. Process. 78, 547–552. https://doi.org/10.1007/s00339-003-2453-5

Nakamura, A., Ishida, T., Kusaka, K., Yamada, T., Fushinobu, S., Tanaka, I., Kaneko, S., Ohta, K., Tanaka, H., Inaka, K., Higuchi, Y., Niimura, N., Samejima, M., Igarashi, K., 2015. "Newton's cradle" proton relay with amide-imidic acid tautomerization in inverting cellulase visualized by neutron crystallography. Sci. Adv. 1, 1–8. https://doi.org/10.1126/sciadv.1500263

Nechyporchuk, O., Belgacem, M.N., Bras, J., 2016. Production of cellulose nanofibrils: A review of recent advances. Ind. Crops Prod. 9, 25. https://doi.org/10.1016/j.indcrop.2016.02.016

Nechyporchuk, O., Pignon, F., Belgacem, M.N., 2015. Morphological properties of nanofibrillated cellulose produced using wet grinding as an ultimate fibrillation process. J. Mater. Sci. 50, 531–541. https://doi.org/10.1007/s10853-014-8609-1

Ougiya, H., Hioki, N., Watanabe, K., Morinaga, Y., Yoshinaga, F., Samejima, M., 1998. Relationship between the physical properties and surface area of cellulose derived from adsorbates of various molecular sizes. Biosci. Biotechnol. Biochem. 62, 1880–1884. https://doi.org/10.1271/bbb.62.1880

Pääkko, M., Ankerfors, M., Kosonen, H., Nykänen, A., Ahola, S., Österberg, M., Ruokolainen, J., Laine, J., Larsson, P.T., Ikkala, O., Lindström, T., 2007. Enzymatic hydrolysis combined with mechanical shearing and high-pressure homogenization for nanoscale cellulose fibrils and strong gels. Biomacromolecules 8, 1934–1941.

https://doi.org/10.1021/bm061215p

Park, S., Baker, J.O., Himmel, M.E., Parilla, P.A., Johnson, D.K., 2010. Cellulose crystallinity index: measurement techniques and their impact on interpreting cellulase performance. Biotechnol. Biofuels 3, 1–10. https://doi.org/10.1186/1754-6834-3-10

Patiño-Masó, J., Serra-Parareda, F., Tarrés, Q., Mutjé, P., Espinach, F.X., Delgado-Aguilar, M., 2019. TEMPO-oxidized cellulose nanofibers: A potential bio-based superabsorbent for diaper production. Nanomaterials 9. https://doi.org/10.3390/nano9091271

Payne, C.M., Knott, B.C., Mayes, H.B., Hansson, H., Himmel, M.E., Sandgren, M., Stahlberg, J., Beckham, G.T., 2015. Fungal cellulases. Chem. Rev. 115, 1308–1448. https://doi.org/10.1021/cr500351c

Peng, Y., Gardner, D.J., 2013. Influence of drying method on the material properties of nanocellulose I: thermostability and crystallinity. Cellulose 20, 2379–2392. https://doi.org/https://10.1007/s10570-013-0019-z

Poletto, M., Ornaghi Júnior, H.L., Zattera, A.J., 2014. Native cellulose: Structure, characterization and thermal properties. Materials (Basel). 7, 6105–6119. https://doi.org/10.3390/ma7096105

Potthast, A., Radosta, S., Saake, B., Lebioda, S., Heinze, T., Henniges, U., Isogai, A., Koschella, A., Kosma, P., Rosenau, T., Schiehser, S., Sixta, H., Strlič, M., Strobin, G., Vorwerg, W., Wetzel, H., 2015. Comparison testing of methods for gel permeation chromatography of cellulose: coming closer to a standard protocol. Cellulose 22, 1591–1613. https://doi.org/10.1007/s10570-015-0586-2

Potthast, A., Rosenau, T., Buchner, R., Röder, T., Ebner, G., Bruglachner, H., Sixta, H., Kosma, P., 2002. The cellulose solvent system N,N-dimethylacetamide/lithium chloride revisited: The effect of water on physicochemical properties and chemical stability. Cellulose 9, 41–53. https://doi.org/10.1023/A:1015811712657

ProcessAmerican, 2019. American Process - Bio Plus division [WWW Document]. Web Page. URL https://www.americanprocess.com/bioplus/ (accessed 12.10.19).

Qing, Y., Sabo, R., Zhu, J.Y., Agarwal, U., Cai, Z., Wu, Y., 2013. A comparative study of cellulose nanofibrils disintegrated via multiple processing approaches. Carbohydr. Polym. 97, 226–234. https://doi.org/10.1016/j.carbpol.2013.04.086

Rahikainen, J., Ceccherini, S., Molinier, M., Holopainen-Mantila, U., Reza, M., Väisänen, S., Puranen, T., Kruus, K., Vuorinen, T., Maloney, T., Suurnäkki, A., Grönqvist, S., 2019. Effect of cellulase family and structure on modification of wood fibres at high consistency. Cellulose 26, 5085–5103. https://doi.org/10.1007/s10570-019-02424-x

Reyes, G., Lundahl, M.J., Alejandro-Martín, S., Arteaga-Pérez, L.E., Oviedo, C., King, A.W.T., Rojas, O.J., 2020. Coaxial Spinning of All-Cellulose Systems for Enhanced Toughness: Filaments of Oxidized Nanofibrils Sheathed in Cellulose II Regenerated from a Protic Ionic Liquid. Biomacromolecules 21, 878–891. https://doi.org/10.1021/acs.biomac.9b01559

Rol, F., Karakashov, B., Nechyporchuk, O., Terrien, M., Meyer, V., Dufresne, A., Belgacem, M.N., Bras, J., 2017. Pilot-Scale twin screw extrusion and chemical pretreatment as an energy-efficient method for the production of nanofibrillated cellulose at high solid content. ACS Sustain. Chem. Eng. 5, 6524–6531. https://doi.org/10.1021/acssuschemeng.7b00630

Saito, T., Hirota, M., Tamura, N., Kimura, S., Fukuzumi, H., Heux, L., Isogai, A., 2009. Individualization of nano-sized plant cellulose fibrils: Achieved by direct surface carboxylation using TEMPO catalyst. Int. Conf. Nanotechnol. For. Prod. Ind. 2009 1, 49–72.

Saito, T., Isogai, A., 2004. TEMPO-mediated oxidation of native cellulose . The effect of oxidation conditions on chemical and crystal structures of the water-insoluble fractions. Biomacromolecules 5, 1983–1989.

Saito, T., Nishiyama, Y., Putaux, J.L., Vignon, M., Isogai, A., 2006. Homogeneous suspensions of individualized microfibrils from TEMPO-catalyzed oxidation of native cellulose. Biomacromolecules 7, 1687–1691. https://doi.org/10.1021/bm060154s

Saloheimo, M., Paloheimo, M., Hakola, S., Pere, J., Swanson, B., Nyyssönen, E., Bhatia, A., Ward, M., Penttilä, M., 2002. Swollenin, a Trichoderma reesei protein with sequence similarity to the plant expansins, exhibits disruption activity on cellulosic materials. Eur. J. Biochem. 269, 4202–4211. https://doi.org/10.1046/j.1432-1033.2002.03095.x

Scherrer, V.P., 1918. Bestimmung der inneren struktur und der größe von kolloidteilchen mittels röntgenstrahlen . Nachrichten van der Gedellschaft der Wissenschaften zu Gottigen 2, 98–100.

Segal, L., Creely, J.J., Martin, A.E., Conrad, C.M., 1959. An empirical method for estimating the degree of crystallinity of native cellulose using the X-ray diffractometer. Text. Res. J. 29, 786–794. https://doi.org/10.1177/004051755902901003

Segato, F., Damásio, A.R.L., Gonc, T. a, Lucas, R.C. De, 2012. High-yield secretion of multiple client proteins in Aspergillus. Enzyme Microb. Technol. 51, 100–106.

Segato, F., Dias, B., Berto, G.L., de Oliveira, D.M., De Souza, F.H.M., Citadini, A.P., Murakami, M.T., Damásio, A.R.L., Squina, F.M., Polikarpov, I., 2017. Cloning, heterologous expression and biochemical characterization of a non-specific endoglucanase family 12 from Aspergillus terreus NIH2624. Biochim. Biophys. Acta - Proteins Proteomics 1865, 395–403. https://doi.org/10.1016/j.bbapap.2017.01.003

Shackford, L.D., 2003. A comparison of pulping and bleaching of kraft softwood and eucalyptus pulps. 36th Int. Pulp Pap. Congr. Exhib.

Shatkin, J.A., Wegner, T.H., Bilek, E.M., Cowie, J., 2014. Market projections of cellulose nanomaterial-enabled products - part 1: Applications. Tappi J. 13, 57–69.

Shinoda, R., Saito, T., Okita, Y., Isogai, A., 2012. Relationship between length and degree of polymerization of TEMPO-oxidized cellulose nanofibrils. Biomacromolecules 13, 842–849. https://doi.org/10.1021/bm2017542

Siqueira, G.A., Dias, I.K.R., Arantes, V., 2019. Exploring the action of endoglucanases on bleached eucalyptus kraft pulp as potential catalyst for isolation of cellulose nanocrystals. Int. J. Biol. Macromol. 133, 1249–1259. https://doi.org/10.1016/j.ijbiomac.2019.04.162

Siró, I., Plackett, D., 2010. Microfibrillated cellulose and new nanocomposite materials: A review. Cellulose 17, 459–494. https://doi.org/10.1007/s10570-010-9405-y

Sixta, H., 2006. Handbook of Pulp. Wiley-VCH Verlag, Weinheim.

Sjöholm, E., Gustafsson, K., Berthold, F., Colmsjö, A., 2000. Influence of the

carbohydrate composition on the molecular weight distribution of kraft pulps. Carbohydr. Polym. 41, 1–7. https://doi.org/10.1016/S0144-8617(99)00066-1

Sluiter, A., Hames, B., Ruiz, R., Scarlata, C., Sluiter, J., Templeton, D., Nrel, D.C., 2012. Determination of Structural Carbohydrates and Lignin in Biomass.

Spence, K.L., Venditti, R. a., Rojas, O.J., Habibi, Y., Pawlak, J.J., 2011. A comparative study of energy consumption and physical properties of microfibrillated cellulose produced by different processing methods. Cellulose 18, 1097–1111. https://doi.org/10.1007/s10570-011-9533-z

Spence, K.L., Venditti, R.A., Habibi, Y., 2010a. Aspects of raw materials and processing conditions on the production and utilization of microfibrillated cellulose. TAPPI Int. Conf. Nanotechnol. For. Prod. Ind.

Spence, K.L., Venditti, R.A., Rojas, O.J., Habibi, Y., Pawlak, J.J., 2010b. The effect of chemical composition on microfibrillar cellulose films from wood pulps: Water interactions and physical properties for packaging applications. Cellulose 17, 835–848. https://doi.org/10.1007/s10570-010-9424-8

Stelte, W., Sanadi, A.R., 2009. Preparation and characterization of cellulose nanofibers from two commercial hardwood and softwood pulps. Ind. Eng. Chem. Res. 48, 11211–11219. https://doi.org/https://10.1021/ie9011672

Suchy, M., Linder, M.B., Tammelin, T., Campbell, J.M., Vuorinen, T., Kontturi, E., 2011. Quantitative assessment of the enzymatic degradation of amorphous cellulose by using a quartz crystal microbalance with dissipation monitoring. Langmuir 27, 8819–8828. https://doi.org/10.1021/la2014418

Sultanova, N., Kasarova, S., Nikolov, I., 2009. Dispersion properties of optical polymers. acta Phys. Pol. A 116, 585–587.

Syverud, K., Chinga-carrasco, G., Toledo, J., Toledo, P.G., 2011. A comparative study of Eucalyptus and Pinus radiata pulp fibres as raw materials for production of cellulose nanofibrils. Carbohydr. Polym. 84, 1033–1038. https://doi.org/https://10.1016/j.carbpol.2010.12.066

Szczesna-Antczak, M., Kazimierczak, J., Antczak, T., 2012. Nanotechnology - methods of manufacturing cellulose nanofibres. Fibres Text. East. Eur. 91, 8–12.

Tarrés, Q;, Saguer, E.., Pelach, M.A.., Alcala, M.., Aguilar-Delgado, M.., Mutjé, P.., 2016. The feasibility of incorporating cellulose micro / nanofibers in papermaking processes : the relevance of enzymatic hydrolysis. Cellulose 23, 1433–1445. https://doi.org/10.1007/s10570-016-0889-y

Tarrés, Q., Saguer, E., Pèlach, M.A., Alcalà, M., Delgado-Aguilar, M., Mutjè, P., 2016. The feasibility of incorporating cellulose micro/nanofibers in papermaking processes: the relevance of enzymatic hydrolysis. Cellulose 23, 1433–1445. https://doi.org/10.1007/s10570-016-0889-y

Tejado, A., Alam, N., Antal, M., 2012. Energy requirements for the disintegration of cellulose fibers into cellulose nanofibers. Cell. Mol. life Sci. 19, 831–842. https://doi.org/10.1007/s10570-012-9694-4

Tibolla, H., Pelissari, F.M., Menegalli, F.C., 2014. Cellulose nanofibers produced from banana peel by chemical and enzymatic treatment. LWT - Food Sci. Technol. 59, 1311–1318. https://doi.org/10.1016/j.lwt.2014.04.011

Tonoli, G.H.D., Teixeira, E.M., Corrêa, A.C., Marconcini, J.M., Caixeta, L.A., Pereira-da-silva, M.A., Mattoso, L.H.C., 2012. Cellulose micro / nanofibres from eucalyptus kraft pulp : preparation and properties. Carbohydr. Polym. 89, 80–88.

Turbak, A.F., Snyder, F.W., Sandberg, K.R., 1983. Microfibrillates cellulose -United States Patent 4,374,702.

Turon, X., Rojas, O.J., Deinhammer, R.S., 2008. Enzymatic kinetics of cellulose hydrolysis: A QCM-D study. Langmuir 24, 3880–3887. https://doi.org/10.1021/la7032753

Van Den Brink, J., De Vries, R.P., 2011. Fungal enzyme sets for plant polysaccharide degradation. Appl. Microbiol. Biotechnol. 91, 1477–1492. https://doi.org/10.1007/s00253-011-3473-2

Van Heiningen, A., 2006. Converting a kraft pulp mill into an integrated forest biorefinery. Pulp Pap. Canada 107, 38–43.

Viamajala, S., McMillan, J.D., Schell, D.J., Elander, R.T., 2009. Rheology of corn stover slurries at high solids concentrations - Effects of saccharification and particle size. Bioresour. Technol. 100, 925–934. https://doi.org/10.1016/j.biortech.2008.06.070

Vlasenko, E., Schülein, M., Cherry, J., Xu, F., 2010. Substrate specificity of family 5, 6, 7, 9, 12, and 45 endoglucanases. Bioresour. Technol. 101, 2405–2411. https://doi.org/10.1016/j.biortech.2009.11.057

Wakabayashi, M., Fujisawa, S., Saito, T., Isogai, A., 2020. Nanocellulose Film Properties Tunable by Controlling Degree of Fibrillation of TEMPO-Oxidized Cellulose. Front. Chem. 8, 1–9. https://doi.org/10.3389/fchem.2020.00037

Walker, C., 2012. Thinking small is leading to big changes. Paper360°. https://doi.org/10.1039/C0CS00108B.8

Wang, Q.Q., Zhu, J.Y., Gleisner, R., Kuster, T.A., Baxa, U., McNeil, S.E., 2012. Morphological development of cellulose fibrils of a bleached eucalyptus pulp by mechanical fibrillation. Cellulose 19, 1631–1643. https://doi.org/10.1007/s10570-012-9745-x

Wang, W., Mozuch, M.D., Sabo, R.C., Kersten, P., Zhu, J.Y., Jin, Y., 2015. Production of cellulose nanofibrils from bleached eucalyptus fibers by hyperthermostable endoglucanase treatment and subsequent microfluidization. Cellulose 22, 351–361. https://doi.org/10.1007/s10570-014-0465-2

Witono, J.R., Noordergraaf, I.W., Heeres, H.J., Janssen, L.P.B.M., 2014. Water absorption, retention and the swelling characteristics of cassava starch grafted with polyacrylic acid. Carbohydr. Polym. 103, 325–332. https://doi.org/10.1016/j.carbpol.2013.12.056

Yarbrough, J.M., Zhang, R., Mittal, A., Vander Wall, T., Bomble, Y.J., Decker, S.R., Himmel, M.E., Ciesielski, P.N., 2017. Multifunctional Cellulolytic Enzymes Outperform Processive Fungal Cellulases for Coproduction of Nanocellulose and Biofuels. ACS Nano 11, 3101–3109. https://doi.org/10.1021/acsnano.7b00086

Zhu, H., Helander, M., Moser, C., Ståhlkranz, A., Söderberg, D., Henriks-, G., 2012. A novel nano cellulose preparation method and size fraction by cross flow ultra-filtration. Curr. Org. Chem. 16, 1871–1875.

Zhu, H., Parvinian, S., Preston, C., Vaaland, O., Ruan, Z., Hu, L., 2013. Transparent nanopaper with tailored optical properties. Nanoscale 5, 3787–3792.

Zhu, J.Y., Sabo, R., Luo, X., 2011. Integrated production of nano-fibrillated cellulose and cellulosic biofuel (ethanol) by enzymatic fractionation of wood fibers. Green Chem. 13, 1339. https://doi.org/10.1039/c1gc15103g

Zimmermann, T., Bordeanu, N., Strub, E., 2010. Properties of nanofibrillated cellulose from different raw materials and its reinforcement potential. Carbohydr. Polym. 79, 1086–1093. https://doi.org/10.1016/j.carbpol.2009.10.045

Supplementary material I

Tables of complete ANOVA analysis

Analysis of Variance: Input Energy

Source	Degree of freedom	Sum of squares (Adj.)	Mean squares (Adj.)	*F*-Value	*p*-Value
Model	3	70,750	23,583	5,58	0,096
Linear	2	58,500	29,250	6,92	0,075
Enzyme Loading	1	56,250	56,250	13,31	0,036
Reaction Time	1	2,250	2,250	0,53	0,518
Interaction of 2 factors	1	12,250	12,250	2,90	0,187
Error	3	12,679	4,226		
Curvature	1	10,012	10,012	7,51	0,111
Pure Error	2	2,667	1,333		
Total	6	83,429			

Analysis of Variance: Particle Size

Source	Degree of freedom	Sum of squares (Adj.)	Mean squares (Adj.)	*F*-Value	*p*-Value
Model	3	0,1475	0,0492	0,00	1,000
Linear	2	0,1250	0,0625	0,00	0,995
Enzyme Loading	1	0,0025	0,0025	0,00	0,990
Reaction Time	1	0,1225	0,1225	0,01	0,929
Interaction of 2 factors	1	0,0225	0,0225	0,00	0,970
Error	3	39,2496	13,0832		
Curvature	1	34,8430	34,8430	15,81	0,058
Pure Error	2	4,4067	2,2033		
Total	6	39,3971			

Analysis of Variance: Viscosity

Source	Degree of freedom	Sum of squares (Adj.)	Mean squares (Adj.)	*F*-Value	*p*-Value
Model	3	42,7048	14,2349	16,92	0,022
Linear	2	38,9082	19,4541	23,13	0,015
Enzyme Loading	1	25,8725	25,8725	30,76	0,012
Reaction Time	1	13,0357	13,0357	15,50	0,029
Interaction of 2 factors	1	3,7967	3,7967	4,51	0,124
Error	3	2,5237	0,8412		
Curvature	1	0,4525	0,4525	0,44	0,577
Pure Error	2	2,0712	1,0356		
Total	6	45,2285			

Analysis of Variance: Shear Stress

Source	Degree of freedom	Sum of squares (Adj.)	Mean squares (Adj.)	*F*-Value	*p*-Value
Model	3	0,742543	0,247514	16,71	0,022
Linear	2	0,676237	0,338118	22,82	0,015
Enzyme Loading	1	0,448230	0,448230	30,26	0,012

Reaction Time	1	0,228006	0,228006	15,39	0,029
Interaction of 2 factors	1	0,066306	0,066306	4,48	0,125
Error	3	0,044441	0,014814		
Curvature	1	0,007985	0,007985	0,44	0,576
Pure Error	2	0,036456	0,018228		
Total	6	0,786984			

Analysis of Variance: Crystallinity index

Source	Degree of freedom	Sum of squares (Adj.)	Mean squares (Adj.)	*F*-Value	*p*-Value
Model	3	35,9192	11,9731	0,60	0,659
Linear	2	1,6892	0,8446	0,04	0,959
Enzyme Loading	1	0,3185	0,3185	0,02	0,908
Reaction Time	1	1,3707	1,3707	0,07	0,811
Interaction of 2 factors	1	34,2300	34,2300	1,71	0,282
Error	3	60,1403	20,0468		
Curvature	1	7,1012	7,1012	0,27	0,656
Pure Error	2	53,0391	26,5196		
Total	6	96,0595			

Supplementary material II

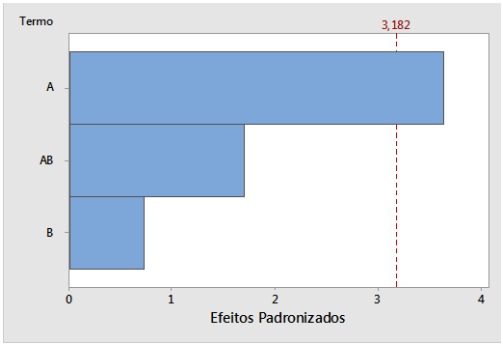

Pareto chart indicating the accumulative effect of the two factors (enzyme loading (A)and reaction time (B)) and their interaction (AB) in the input energy as response.

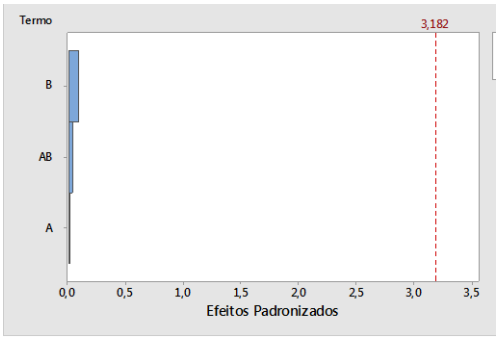

Pareto chart indicating the accumulative effect of the two factors (enzyme loading (A) and reaction time (B)) and their interaction (AB) in the particle size as response.

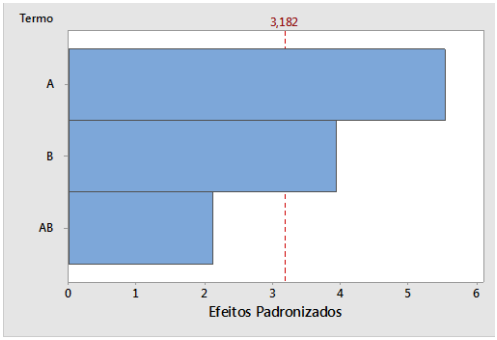

Pareto chart indicating the accumulative effect of the two factors (enzyme loading (A) and reaction time (B)) and their interaction (AB) in the viscosity as response.

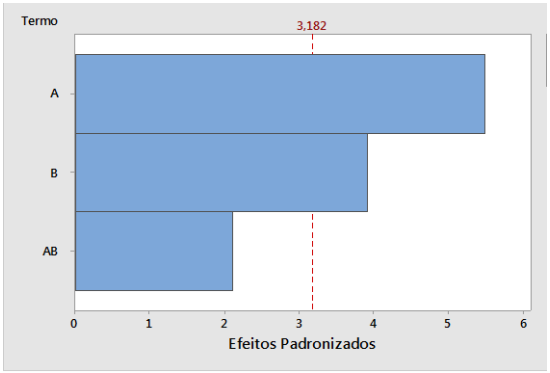

Pareto chart indicating the accumulative effect of the two factors (enzyme loading (A) and reaction time (B)) and their interaction (AB) in the shear stress as response.

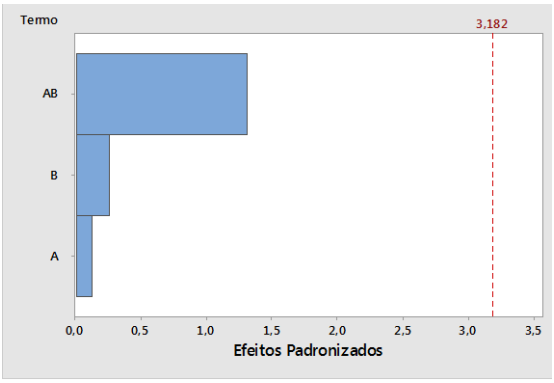

Pareto chart indicating the accumulative effect of the two factors (enzyme loading (A) and reaction time (B)) and their interaction (AB) in the crystallinity index as response.